# Field Theory of Interacting Crumpled Manifolds

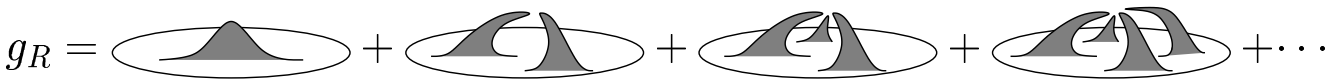

Dissertation zur Erlangung des Grades

**Doktor der Naturwissenschaften**

vorgelegt am

Fachbereich Physik der Universität Essen

von

Henryk A. Pinnow

Essen 2002

**Abstract**

The effect of a $\delta$-interaction on a polymerized membrane of arbitrary internal dimension $D$ has been studied. Depending on the dimensionality of membrane and embedding space, different physical scenarios are observed: The delocalization of a membrane from an attractive defect as well as steric repulsions. The difference of polymers from membranes is emphasized. For the latter, non-trivial contributions appear at the 2-loop level. Furthermore, a "massive scheme" inspired by calculations in fixed dimensions for scalar field theories has been exploited. Despite the fact that these calculations are only amenable numerically, it has been found that in the limit of $D \to 2$ each diagram can be evaluated *analytically*. This property extends in fact to any order in perturbation theory, allowing for a summation of all orders. An analytically continued expression for the effective coupling of membranes in the scaling limit of large sizes as compared to the microscopic cutoff is obtained. Finally, the construction of an expansion of the effective coupling about $D = 2$ is presented. Applications to the case of self-avoiding membranes are mentioned.

1. Gutachter: Dr. habil. K.J. Wiese

2. Gutachter: Prof. Dr. L. Schäfer

Tag der Disputation: 19. Juli 2002

# Contents

# 1 Introduction

## 1.1 Physics of fluctuating manifolds

Interacting lines and more generally manifolds play an important role in many areas of modern physics. Examples of lines are self-avoiding polymers [1], vortex-lines in super-conductors [2], directed polymers in a disordered environment, also equivalent to surface growth [3], diffusion of particles and many more. Generalizing results to membranes often poses severe problems, but also new insight into physics. Recently, a lot of work has been devoted to self-avoiding membranes (see [4] for a review).

From the point of view of statistical physics one major problem is to study the effect of interactions on the thermodynamical properties of extended fluctuating geometric objects. Generally, there are multi-particle attractive or repulsive interactions involved. One may divide these into two classes: Either (i) one may study the interaction of a single fluctuating object with itself as for instance the well known two-particle excluded volume interaction between any two monomers in a long chain polymer in a good solvent. There, the interaction leads to universal long-distance properties of chains as for example the anomalous scaling of the mean squared end-to-end distance. Or (ii), the interaction may act between different manifolds or between a single manifold and a fixed non-fluctuating object. It is then interesting to study how thermal fluctuations affect the depinning of the manifold from an attractive substrate as well as the steric repulsions from a wall.

Both cases have in common that they are fairly well understood as long as the fluctuating objects are one-dimensional [1,5–7]. Referring to the example mentioned above, the long-distance properties of self-avoiding polymers, which are always crumpled on large scales, can be analyzed with renormalization group techniques [8–10], either in the continuous Edwards Hamiltonian [11],

$$\mathcal{H}[\vec{r}] = \frac{1}{2} \int\limits_{x\in\mathcal{M}} \left(\nabla \vec{r}(x)\right)^2 + \frac{b_0}{2} \int\limits_{x\in\mathcal{M}} \int\limits_{y\in\mathcal{M}} \delta^d(\vec{r}(x) - \vec{r}(y)) \,, \tag{1.1}$$

or by mapping this model on a local $O(N)$ symmetric $\varphi^4$-theory in the limit of $N = 0$ components [12,6,1]. The critical exponents describing the long-distance properties are related to the critical exponents of the corresponding $N$-vector model at the critical point. What makes (1.1) a non-standard theory is that the interaction is nonlocal. The integration is over the internal volume of the manifold, that is, in the case of polymers along the chain.

Obtaining the corresponding results for membranes poses considerable challenges. The generalization of polymers to $2D$-surfaces are crystalline fixed-connectivity membranes as they appear for instance in the spectrin network of cell membranes. Considering "phantom" membranes, which can freely fold into itself, the existence of a bending rigidity induced phase transition separating a high rigidity, low temperature flat phase from a low rigidity, high temperature crumpled phase is well established [13–18]. This is in contrast to polymers, which are always crumpled on large scales. The scaling properties of the crumpled phase of phantom membranes are described by the $2D$ generalization of the free field part in (1.1). Taking self-avoidance into account, which is modeled in (1.1) through the short range two-body interaction, we expect more open manifolds than those predicted by the free theory, which will be expressed in a non-trivial radius of gyration exponent. The squared radius of gyration $R_g$ is defined as the mean squared distance of the manifold constituents from the center of mass. In the case of polymers

$R_g$ scales like the end-to-end distance. Much effort has been spent on calculating corrections to the radius of gyration exponent within an expansion in the deviation $\varepsilon$ from the critical space dimension [19,20]. These calculations can not be performed directly in $D = 2$, since the naive scaling dimension of the coupling in (1.1) equals

$$\varepsilon(D, d) := [b_0] = 2D - \frac{2 - D}{2} d \,, \tag{1.2}$$

where $d$ denotes the dimension of the embedding space, and is always finite as $D \to 2$. Equivalently, the critical embedding dimension defined through $\varepsilon(D, d_c(D)) = 0$ becomes $\infty$ in this limit. The reason is that the non-self-avoiding membrane densely fills out the embedding space, such that it always "sees" the interaction. A way to circumvent this problem is to set up the expansion about any point $(D < 0, d_c(D))$ and to extrapolate along an appropriate path in the $(D, d)$-plane to the physically interesting point $(D, d) = (2, 3)$ [4,21–26]. To second order in $\varepsilon$ one then finds a radius of gyration exponent of $\nu \approx 0.86$ [19,20] , which is a strong correction with respect to the only logarithmic dependence in the non-interacting theory, but nevertheless still indicates existence of a crumpled phase.
However, there is no unambiguous evidence for a crumpled phase in experiments [27–30]. Latest Monte-Carlo simulations on plaquette-models [31–34] starting from a discretization of the $2D$ generalized Hamiltonian (1.1) with system sizes of up to $\approx 17000$ plaquettes shows considerable evidence for a vanishing of the above mentioned crumpling transition in the presence of self-avoidance, such that even on large scales fixed-connectivity membranes stay always flat with a radius of gyration exponent of $\nu \approx 1$. This outcome might be reconciliated with the field theoretic calculation by going to higher loop orders.

The aim of this work is to develop techniques which allow to go beyond the two-loop result. We developed such techniques for a simplified model, which replaces the non-local interaction in (1.1) by an interaction with a single point in the embedding space and which is therefore related to case (ii). The corresponding physical situation we think of is the binding and unbinding of a long chain as e.g. a polymer or a membrane from a wall or the wetting of an interface. More precisely, we study the interaction of a single freely fluctuating manifold with another non-fluctuating, fixed object. Depending on whether the interaction is attractive or repulsive, one can distinguish two different scenarios: One may either observe a delocalization transition from an attractive substrate as in wetting phenomena or steric repulsions by a fluctuating manifold. Both cases have in common that excluded volume effects become important. The situation for polymers or a 1-dimensional interface is relatively simple: One knows that in this case polymers interacting with a defect or a wall (excluding or not half of the space) as well as

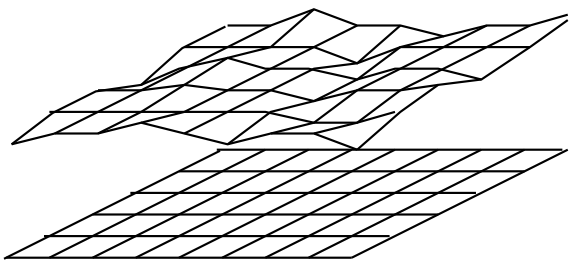

Figure 1.1: A fluctuating membrane interacting by excluded volume with a surface-like defect.

short-range critical wetting are in the same universality class [35–37]. For two-dimensional interfaces, the situation is more complicated, and a lot of effort has been spent to understand e.g. the delocalization transition [38–45]. Particularly, one is interested in critical wetting for the case of a short-ranged interaction potential. Then, it can not be approximated by a polynomial in the field $\vec{r}$ and the conventional field-theoretic approach known from $\phi^4-$theory fails. This led to a couple of different ansätze [39,40,42–44], among others the functional renormalization group approach of [43,44].

Here we follow a different route: We start by constructing a *systematic perturbative* renormalization group treatment of the delocalization transition as well as the universal repulsive force exerted by a membrane on a point, line or more generally hyper-plane like defect. We therefore introduce a flexible "phantom" manifold of internal dimension $0 \leq D \leq 2$. By introducing a $\delta$-potential in a subspace $\mathcal{E}$ of dimension $d'$, part of the embedding space $\mathbb{R}^{d+d'}$ (see fig. 1.1) we punish configurations crossing $\mathcal{E}$. Neglecting the effect of self-avoidance between distinct points within the fluctuating manifold, the free energy of a given configuration reads:

$$\mathcal{H}[\vec{r}] = \int_{x\in\mathcal{M}} \mathrm{d}^D x\, \frac{1}{2}(\nabla\vec{r}(x))^2 + g_0 \int_{x\in\mathcal{M}} \mathrm{d}^D x \int_{\vec{y}\in\mathcal{E}} \mathrm{d}^{d'}\vec{y}\ \delta^{d+d'}(\vec{r}(x)-\vec{y})\ , \tag{1.3}$$

where $\vec{r}(x)$ is the position of monomer $x \in \mathcal{M}$ in embedding space $\mathbb{R}^{d+d'}$, and $\mathcal{M}$ denotes the $D$-dimensional coordinate space of the manifold. In the case of a polymer this is simply the internal chain length. $g_0$ is the attractive or repulsive interaction, of dimension (in inverse length-units)

$$\varepsilon(D,d) := [g_0] = D - \frac{2-D}{2}d\ . \tag{1.4}$$

The interaction is naively relevant in the infrared for $\varepsilon$ positive, and irrelevant for $\varepsilon$ negative. In a perturbative treatment, $\varepsilon$ is the natural expansion parameter. The situation is similar to self-avoiding membranes and thus (1.3) has been studied as a "toy-model" for the analysis of the renormalizability of the more complicated interaction in the generalized Edwards model (1.1) for self-avoiding polymerized membranes [46–48]. It was shown to be renormalizable for arbitrary manifold dimensions $0<D<2$ [47,48]. This means that the large scale properties are universal, i.e. do neither depend on the regularization scheme used in these calculations, nor on the form of the contact interaction, as long as it is short-ranged. Universal quantities have thus been obtained to one-loop order. They are related, as we will be shown in section 2, to the correction to scaling exponent $\omega$, which as usually in critical phenomena contains deviations from the long-distance scaling behavior.

The aim of this work is two-fold: First, we present the necessary techniques to treat the model (1.3) beyond the leading order. We explicitly perform a two-loop calculation which gives the correction to scaling exponent $\omega$ at order $\varepsilon^2$. Specializing to membranes one finds that the 2-loop result naively diverges in the limit of $D \to 2$. This is a problem of the $\varepsilon$-expansion, since there, diagrams have to be evaluated at $\varepsilon(D, d_c(D)) = 0$, and taking $D \to 2$ implies $d_c(D) \to \infty$ causing the result to diverge. Following the above mentioned strategy which has been applied successfully to the calculation of the anomalous dimension of self-avoiding membranes we set up the expansion in $\varepsilon$ about some point $(D < 0, d_c(D))$ and extrapolate along some appropriate path to physically interesting points $(D, d)$. It will turn out that the result always depends strongly on the expansion point. Thus, the correction at the two-loop

level is ambiguous as long as one is only interested in the limit $D \to 2$. This motivated us to try a "massive scheme" in fixed dimension, i.e. at finite $\varepsilon$. It turns out that the limit $D \to 2$ can then be taken and is regular. Even more, the 2-loop diagram, which for $D < 2$ can only be calculated numerically, can now be evaluated *analytically*. This striking property even holds for higher orders, and we are able to give an explicit – quite simple – expression for the perturbation series. In a second step the whole series can be summed and the strong coupling limit analyzed. This is one of the very few cases where one can indeed obtain the *exact* relation between bare and renormalized coupling in the limit of $D \to 2$, and thus the *exact* $\beta$-function. This result does not depend on the explicit regularization and renormalization prescriptions, and is also obtained for a membrane of spherical or toroidal topology. Furthermore, it turns out that the behavior of the effective coupling, which is logarithmically diverging for large membrane sizes, together with the value of the correction-to-scaling exponent $\omega$, which is therefore forced to be zero, can not be extrapolated from any finite loop expansion. In a final step, we lay the foundations for an expansion about $D = 2$. In contrast to the leading order, the first order corrections already depend on the cut-off procedure. We studied one specific procedure already in [49], which turns out to reproduce results for polymers at leading order approximately, and even exactly in $d = 0$. In order to obtain exact results, we decided to set up the expansion in $2 - D$ on a manifold of toroidal internal topology; this corresponds to periodic boundary conditions. Our aim is to expand the exponent $\omega$ about $D = 2$ and this way to prove the smoothness of the limit $D \to 2$. This will be further discussed in the sections 6 and 7. The following introductory sections are a short exposé on tethered manifolds and the crumpling transition motivating Hamiltonians like (1.1) and (1.3). In section 2 we further discuss the model (1.3) and show, how the correction-to-scaling exponent $\omega$ is related to interesting physical observables, which might be also accessible to Monte-Carlo simulations.

## 1.2 Tethered surfaces and their realizations

Tethered surfaces are systems of particles (atoms or monomers) that are connected to form a regular two-dimensional array embedded in $d$-dimensional space [50] . Independently from the precise type of the $2D$ lattice as well as from the form of the bonding potential between the neighboring particles of the network, it is essential that the bonds between the adjacent atoms or monomers of the array can not be broken. This is in contrast to fluid membranes, where molecules making up the membrane can freely circulate within the surface. The distances between adjacent particles are subject to thermal fluctuations which are controlled by the next-nearest-neighbor bonding potentials. This is, too, in contrast to fluid membranes, whose particle density stays constant, while they undergo pronounced shape fluctuations. This property is the reason, why the question is still under debate whether the flat phase of fluid membranes becomes unstable with respect to thermal fluctuations or is rather stabilized, [51–55].
For tethered surfaces the situation is by far clearer: As long as no self-avoidance is taken into account, they are known to undergo a bending rigidity induced continuous phase transition separating a stable flat phase from a crumpled fractal phase. Due to the fixed connectivity tethered surfaces closely resemble linear polymers. The spatial conformation of a linear polymer can be described by a set of position vectors $\vec{r}(x)$, where $x$ is the internal index and $\vec{r}(x)$ the location in embedding space of the indexed monomer. Then, a natural generalization to $2D$ surfaces is made by use of a two-dimensional vector $\vec{x}$ as an index denoting the internal position of the

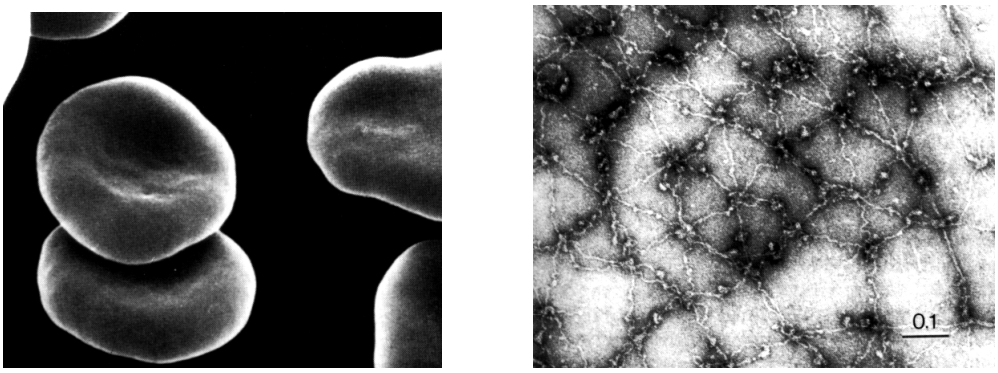


Figure 1.2: Extended view (right) of the crystalline spectrin/actin network which forms the cytoskeleton of the red blood cell membrane (left) .

atom. Such use of a fixed (flat) internal space and its clear separation from the external variable $\vec{r}$, on which the Hamiltonian of the system depends, enables an unambiguous definition of the statistical measure for the configurational space, thus avoiding problems regarding a proper measure as they are addressed in [54] in the case of fluid surfaces.

A naturally occurring physical example of tethered membranes are the cytoskeletons of cell membranes, which is essential to their stability as well as functionality. The simplest and most thoroughly studied example is the cytoskeleton of mammalian erythrocytes (red blood cells). The red blood cell cytoskeleton is a tethered network of triangular plaquettes formed primarily by the proteins spectrin and actin (see fig. (1.2) from [4,56,57]).
Inorganic realizations of crystalline membranes are graphitic oxide membranes, which are micron size sheets of solid carbon. They are formed by exfoliating carbon with a strong oxidizing agent [28–30]. Furthermore, metal dichalcogenides such as $MoS_2$ have also been observed to form rag-like sheets [27].

## 1.3 Landau theory of the crumpling transition

In this section let us discuss an order parameter theory of the crumpling transition [17]. Any $D$-dimensional manifold embedded in $d$- dimensional space can be parametrized by

$$\vec{r}: \ \vec{x} \in \mathbb{R}^D \ \longrightarrow \vec{r}(\vec{x}) \in \mathbb{R}^d \ , \tag{1.5}$$

where $\vec{r}(\vec{x})$ points to the position in embedding space of the manifold constituent labeled by $\vec{x}$. For $D = 1$, this represents a polymer, for $D = 2$ a membrane. Starting from a $D$- dimensional lattice with nearest neighbor interactions, a statistical description is developed by coarse graining this lattice so that the vector $\vec{x}$ becomes a continuous variable, which labels a "bloc" of lattice points. Translational invariance delimits the form of the free energy functional to depend only on the coarse grained tangent vectors $\vec{t}_\alpha = \partial\vec{r}(\vec{x})/\partial x_\alpha, \ \alpha = 1, \ldots, D$ and its derivatives. An expansion à la Ginzburg-Landau for small tangents then leads to an effective free energy [58]:

$$\mathcal{H}[\vec{r}] = \int \mathrm{d}^D x \ \left[ \frac{\kappa}{2} \left(\partial_\alpha \partial_\alpha \vec{r}\right)^2 + \frac{t}{2} \left(\partial_\alpha \vec{r}\right)^2 + u \left(\partial_\alpha \vec{r}\, \partial_\beta \vec{r}\right)^2 + \tilde{v} \left(\partial_\alpha \vec{r}\, \partial_\alpha \vec{r}\right)^2 \right] + \frac{b}{2} \int \mathrm{d}^D x \int \mathrm{d}^D y \, \delta^d(\vec{r}(\vec{x}) - \vec{r}(\vec{y})) \ . \tag{1.6}$$

The last term is a nonlocal excluded volume term, which represents the effects of self-avoidance at large length scales. Identifying the tangents $\vec{t}_\alpha$ with a set of order parameters $\phi_\alpha, \ \alpha = 1, \ldots, D$, an analogy with the normal $\phi^4$ theory becomes apparent. However, this analogy is only valid at the mean-field level.

At high temperatures one expects a crumpled phase, where $t$ is positive for entropic reasons, while the other terms are irrelevant on large scales. $\kappa$ denotes the bending rigidity, and the other elastic constants

$t, \ u$ and $\tilde{v}$ are related to the Lamé-coefficients of Landau elastic theory.

At low temperatures, the microscopic surface tangents tend to align in order to minimize the microscopic bending energy, driving the manifold to form a flat phase ($t < 0$). The manifold is stabilized by the anharmonic terms, provided that $u > 0$ and $v := \tilde{v} + u/D > 0$. There is a continuous transition between these phases when $t \equiv \alpha(T - T_c) = 0$. This can be seen within mean-field theory. In the absence of self-avoidance we make the ansatz

$$\vec{r}(\vec{x}) = \sum_{i=1}^{D} \xi x_i \vec{\mathbf{e}}_i \ , \tag{1.7}$$

where the sum is over two orthogonal cartesian unit vectors spanning a flat surface. Minimizing the corresponding mean-field effective potential,

$$V(\xi) = D\xi^2 \left( \frac{t}{2} + (u + \tilde{v}D)\xi^2 \right) \ , \tag{1.8}$$

leads to the following solution:

$$\xi^2 = \begin{cases} 0 \ , \ t \geq 0 \\ -\frac{t}{4(u+\tilde{v}D)} \ , \ t < 0 \end{cases}$$

Consequently, there is a flat phase for $t < 0$ and a crumpled phase for $t > 0$, separated by a crumpling transition at $t = 0$. Figure (1.3) shows a "phantom" membrane in typical states below, above and at the crumpling transition (Monte-Carlo samples from [59]).

## 1.4 Properties of the flat phase

Fluctuational states around the ordered state can be parametrized as

$$\vec{r}(\vec{x}) = \xi \left[ (x_\alpha + u_\alpha)\vec{\mathbf{e}}_\alpha + h_\beta \vec{\mathbf{e}}_\beta \right] \ , \tag{1.9}$$

where the summation over $\alpha$ is as in (1.7), while the $\vec{\mathbf{e}}_\beta$ are orthogonal to the latter. Specializing to membranes in $d = 3$ there is a single orthogonal space dimension. Inserting (1.9) into (1.6) leads to lowest non-trivial order to

$$\mathcal{H}[u, h] = \int \mathrm{d}^D x \ \left[ \frac{\kappa}{2} \left(\Delta h\right)^2 + \mu u_{ij}^2 + \frac{\lambda}{2} u_{kk}^2 \right] \ , \tag{1.10}$$

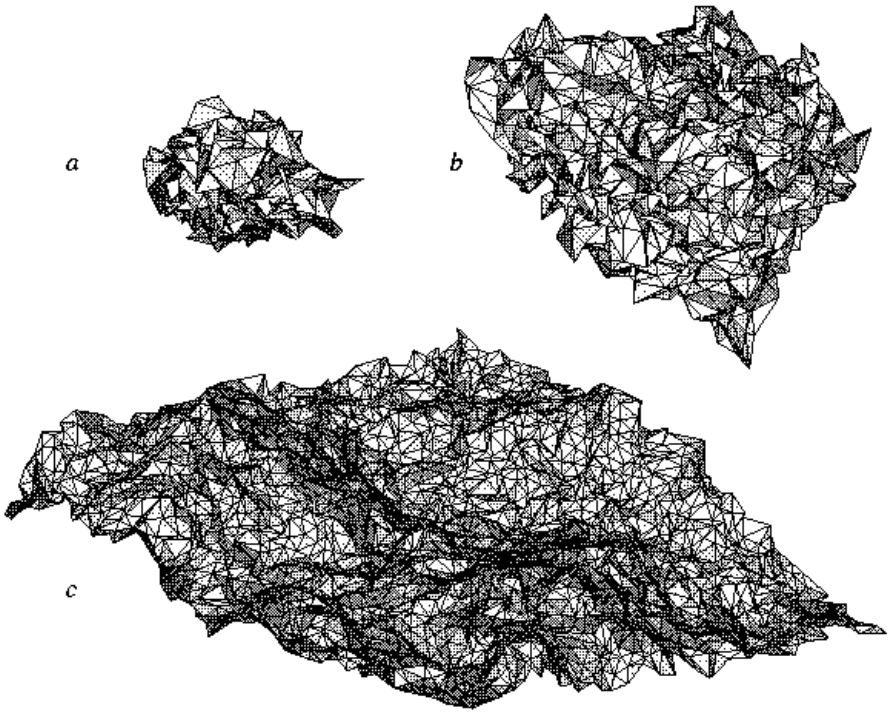


Figure 1.3: Crumpled phase (a), crumpling transition (b) and flat phase (c). No self-avoidance.

where $\mu = 4u\xi^4,\ \lambda = 8\tilde{v}\xi^4$ and $u_{ij} = \frac{1}{2}[\partial_i u_j + \partial_i u_j + \partial_i h_\beta\ \partial_j h_\beta]$ denotes the strain matrix. It was shown in [60] that the renormalized bending rigidity grows at large distances and stabilizes the stretched phase against undulations. For small wavevectors $\vec{\mathbf{q}}$ one finds an effective rigidity $\kappa_R$ with

$$\kappa_R(\mathbf{q}) \sim \sqrt{k_B T\ K_0}\ \mathbf{q}^{-1}\ , \qquad K_0 = \frac{4\mu(\mu+\lambda)}{2\mu+\lambda}\ . \tag{1.11}$$

Qualitatively, this is easily understood intuitively: Consider a low energy state of the nearly flat membrane, which is for instance a single low-wavevector undulation [1]. It does not necessitate any stretching of bonds between adjacent molecules. However, adding to the long-wavelength deformation with wavevector $\vec{\mathbf{q}}_1$ another short-wavelength deformation $\vec{\mathbf{q}}_2$ with $|\vec{\mathbf{q}}_1| \ll |\vec{\mathbf{q}}_2|$ and $\vec{\mathbf{q}}_1 \perp \vec{\mathbf{q}}_2$, this will induce a space varying gaussian curvature, which inevitably forces to locally stretch and squeeze bonds. Thus, the free energy of the short wavevector undulation is raised up with respect to the same undulation on the flat background. Correspondingly to (1.11), the normal-normal correlation function stays always finite:

$$\lim_{|x|\to\infty} \langle \vec{\mathbf{n}}(x)\vec{\mathbf{n}}(0)\rangle\ <\ \infty\ , \tag{1.12}$$

where $\vec{n}(x)$ denotes the local unit normal vector on the surface. Therefore, the membrane stays always oriented. The symmetry is broken, and the membrane is flat. This seems to be a violation of the Mermin-Wagner theorem: In fact, the fluctuations in the membrane give rise to

[1] Out-of-plane fluctuations called undulations are to be distinguished from internal phonon modes.

long-range interactions, to which the Mermin-Wagner theorem does not apply.

## 1.5 Properties of the crumpled phase

In the crumpled phase the free energy is governed by an entropic elasticity [15] such that (1.6) reduces to

$$\mathcal{H}_0[\vec{r}] = \frac{t}{2}\int \mathrm{d}^D x\ (\nabla\vec{r}(x))^2 + \text{irrel. terms}\ . \tag{1.13}$$

The spatial extend of the manifold is characterized by its radius of gyration, which is defined as

$$R_g^2 = \frac{1}{2N^2}\sum_{i,j}\left\langle(\vec{r}_i - \vec{r}_j)^2\right\rangle_{\mathcal{H}_0}\ . \tag{1.14}$$

In the case of polymers $N$ denotes the number of segments, while for $2D$ surfaces, correspondingly, it is the number of plaquettes. The radius of gyration is the mean squared distance of the surface constituents from the center of mass of the manifold. It scales with the linear size $L$ of the manifold like

$$R_g \sim L^\nu\ , \qquad 0 \le \nu \le 1 \tag{1.15}$$

and is related to the plaquette density correlation function, which is easily accessible experimentally by light scattering, small-angle $X$-ray scattering etc. [61].
For large manifolds $R_g$ scales like the two-point function

$$\frac{1}{2d}\left\langle(\vec{r}(\vec{x}) - \vec{r}(\vec{y}))\right\rangle_{\mathcal{H}_0} = \frac{|\vec{x}-\vec{y}|^{2-D}}{(2-D)S_D}\ , \tag{1.16}$$

where $a$ is a microscopic cutoff. One then finds:

$$R_g \sim \begin{cases} L^{\frac{2-D}{2}}\ , & D < 0 \\ \left(\ln\frac{L}{a}\right)^{1/2}\ , & D = 2 \end{cases}$$

Taking self-avoidance into account gives rise to corrections to the exponent $\nu$. This can be understood within the Flory approximation: It consists in replacing $\vec{r}(\vec{x})$ in (1.6) by the radius of gyration and derivatives with respect to $x_\alpha$ by $1/L$ as well as the integration over the internal volume by $L^D$, leading to

$$\mathcal{H} \simeq \kappa\, L^{D-4}R_g^2 + t\, L^{D-2}R_g^2 + (u + D\tilde{v})\, L^{D-4}R_g^4 + b\, L^{2D}R_g^{-d}\ . \tag{1.17}$$

The contribution from the bending rigidity $\kappa$ can always be neglected with respect to the terms proportional to $t$ and $u + D\tilde{v}$, respectively. Minimizing (1.17) provides:

$$R_g \sim \begin{cases} L\ , & \text{as } D \le d \text{ and } t < 0 \\ L^{\nu_{\text{Flory}}}\ , & \nu_{\text{Flory}} = \frac{2+D}{2+d}\ , \quad t > 0 \end{cases}$$

For polymers the Flory approximation makes predictions, which are sufficient for experiments. The prediction for membranes in $d = 3$, $\nu = \frac{4}{5}$, is close to what has been found in field theoretic calculations to two loops ($\nu \approx 0.86$).

# 2 Model and physical observables

## 2.1 The model

We start from the manifold Hamiltonian (1.3). We split the total embedding space $\mathbb{R}^{d+d'}$ into $\mathcal{E}$ and its orthogonal complement $\mathcal{E}_\perp$ of dimension $d$. Each $x \in \mathcal{V}$ points to a point $\vec{r}(x)=(\vec{r}_\perp(x), \vec{r}_\parallel(x))$, with $\vec{r}_\parallel(x) \in \mathcal{E}$ and $\vec{r}_\perp(x) \in \mathcal{E}_\perp$. The integration over the subspace $\mathcal{E}$ is then trivial and gives

$$\int_{\vec{y}\in\mathcal{E}} \delta^{d+d'}(\vec{r}(x)-\vec{y}) = \delta^d(\vec{r}_\perp(x)) \; . \tag{2.1}$$

In the partition function

$$\mathcal{Z}_{\rm total} = \int \mathcal{D}\,[\vec{r}]\; \exp(-\mathcal{H}\,[\vec{r}]) \tag{2.2}$$

the contributions from the parallel and orthogonal components of $\vec{r}(x)$ factorize as

$$\mathcal{Z}_{\rm total} = \mathcal{Z}_0 \times \mathcal{Z}(g_0) \tag{2.3}$$

with

$$\mathcal{Z}_0 = \int \mathcal{D}[\vec{r}_\parallel]\; \exp\left(-\frac{1}{2}(\nabla_\parallel \vec{r}(x))^2\right) \tag{2.4}$$

$$\mathcal{Z}(g_0) = \int \mathcal{D}[\vec{r}_\perp]\; \exp(-\mathcal{H}_\perp[\vec{r}_\perp]) \tag{2.5}$$

$$\mathcal{H}_\perp[\vec{r}_\perp] = \int_{\mathcal{M}} {\rm d}^D x \left(\frac{1}{2}(\nabla \vec{r}_\perp(x))^2 + g_0\; \delta^d(\vec{r}_\perp(x))\right) \; . \tag{2.6}$$

Since $\mathcal{Z}_0$ is trivial, we will only consider $\mathcal{H}_\perp[\vec{r}_\perp]$ and shall drop the subscript $_\perp$ for notational simplicity. We keep in mind that cases with $d < D$ make sense, for instance a polymerized (non-selfavoiding) membrane interacting with a wall is described by (2.6) setting $D = 2$ and $d = 1$.

Let us discuss (2.6) in more detail: The first term is the elastic energy of the manifold which is entropic in origin. We have scaled elasticity and temperature to unity. The second term models the interaction of the manifold with a single point at the origin in the external $d$-dimensional space, but we remind that the physical interpretation may well be that of a line or surface. The coupling constant $g_0$ may either be positive (repulsive interaction) or negative (attractive interaction). We now give the dimensional analysis. In coordinate-space units, the engineering dimensions are

$$\begin{gathered} \dim[x] = 1 \\ \nu := \dim[\vec{r}] = \frac{2-D}{2} \\ \varepsilon := \dim\left[\int_{\mathcal{M}} {\rm d}^D x\; \delta^d(\vec{r}(x))\right] = D - \nu d \\ g_0 \;\sim\; \mu^\varepsilon \\ \dim[\mu] \;=\; -1 \; , \end{gathered} \tag{2.7}$$

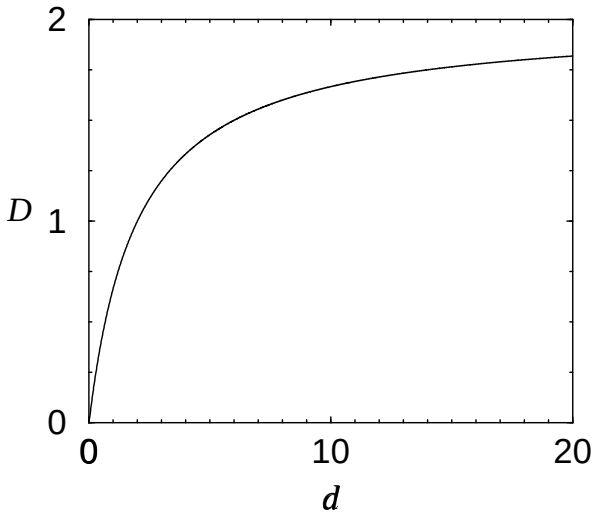


Figure 2.1: Critical line defined through $\varepsilon = 0 \Leftrightarrow d_c(D) = \frac{2D}{2-D}$. The interaction is relevant for points that lie above that line.

where

$$\mu \equiv \frac{1}{L} \tag{2.8}$$

is an inverse length scale. The interaction is naively relevant for $\varepsilon > 0$, i.e. $d < d_c$ with (see figure 2.1)

$$d_c = \frac{2D}{2-D} \, , \tag{2.9}$$

irrelevant for $\varepsilon < 0$ and marginal for $\varepsilon = 0$. It has been shown [47,48] that the model is renormalizable for $0 < D < 2$ and $\varepsilon \geq 0$. Results for negative $\varepsilon$ are obtained via analytical continuation. One can define the renormalized coupling $g$ as

$$g := \frac{\mathcal{N}}{\mathcal{V}_{\mathcal{M}}} \left[ \mathcal{Z}(0) - \mathcal{Z}(g_0) \right] L^{\varepsilon} \, , \tag{2.10}$$

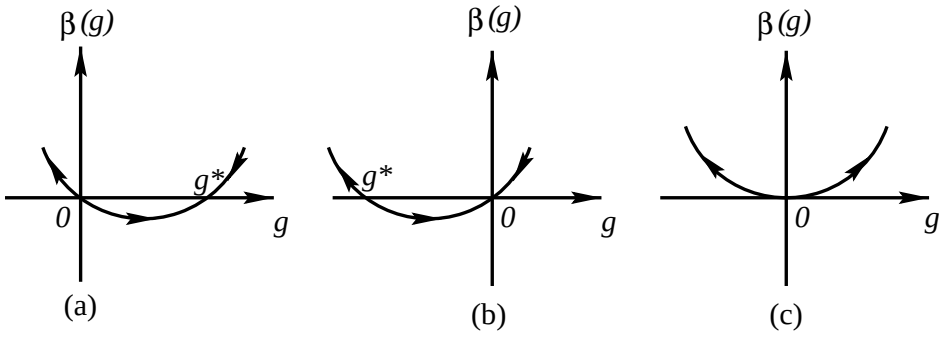


Figure 2.2: RG-function and flow for increasing manifold size $L$ for the dimensionless renormalized coupling $g$: (a) in the case $\varepsilon>0$, (b) in the case $\varepsilon<0$, (c) in the case $\varepsilon = 0$.

where the normalization $\mathcal{N}$ depends on the definition of the path-integral (but not on $L$) and is chosen such that

$$g = g_0 L^{\varepsilon} + O(g_0^2) \; . \tag{2.11}$$

Universal quantities are obtained at fixed-points of the $\beta$-function, which is defined as

$$\beta(g) := \mu \left. \frac{\partial g}{\partial \mu} \right|_{g_0} \; . \tag{2.12}$$

The $\beta$-function thus describes, how the effective coupling $g$ changes under scale transformations, while keeping the bare coupling $g_0$ fixed. Let us already anticipate the 1-loop result, which we derive later. It reads

$$\beta(g) = -\varepsilon g + \frac{1}{2} g^2 + O(g^3) \; , \tag{2.13}$$

where $g$ is the dimensionless renormalized coupling. Apart from the trivial solution, $g = 0$, the flow equation given by (2.12) and (2.13) has a non-trivial fixed point at the zero of the $\beta$-function

$$g^* = 2\varepsilon + O(\varepsilon^2) \; . \tag{2.14}$$

We shall show below that the scaling behavior is described by the slope of the RG-function at the fixed point, which is universal as a consequence of renormalizabilty. The long-distance behavior is then governed by the $\delta$-interaction as considered in our model (2.6), which is the most relevant operator at large scales. Let us now discuss possible physical situations (see fig. 2.2):

(a) $\varepsilon>0$: The RG-flow has an infrared stable fixed point at $g^* > 0$ and an IR-unstable fixed point at $g = 0$. The latter describes an unbinding transition whose critical properties are given by the non-interacting system, while the non-trivial IR stable fixed point determines the long-distance properties of the delocalized state, the long-range repulsive force exerted by the fluctuating manifold on the origin – which we remind may be a point, a line or a plane.

(b) $\varepsilon<0$: Now, the long-distance behavior is Gaussian, while the unbinding transition occurs at some finite value of the attractive potential, $g^*<0$, which corresponds to an infrared unstable fixed point of the $\beta$-function. Below $g^*$ the manifold stays always attracted.

(c) $\varepsilon = 0$: This is the marginal situation, where the transition takes place at $g^* = 0$; we expect logarithmic corrections to scaling.

Note that in the presence of an impenetrable wall constraining the configurational space strictly to half of the embedding space, the above considerations should still apply, when shifting the interaction strength appropriately. We shall discuss that in 2.4.

## 2.2 Repulsive force exerted by a membrane on a wall

Since we are mainly interested in the long-distance properties of membranes for which always $\varepsilon > 0$ (this is (a) on fig. 2.2), let us try to calculate the repulsive force exerted by the membrane

on the origin in the case that this point is strictly forbidden. We will derive a universal expression for this force [48]. We need the (not normalized) membrane density at position $\vec{r}$

$$\mathcal{Z}(\vec{r}, g_0) := \frac{1}{\mathcal{V}_\mathcal{M}} \int \mathcal{D}[\vec{r}] \int_\mathcal{M} \mathrm{d}^D x \; \delta^d(\vec{r}(x) - \vec{r}) \exp[-\mathcal{H}] \; . \tag{2.15}$$

Since the $\delta$-interaction also appears in $\mathcal{H}$, we can relate the density at the origin to the derivative of the partition function with respect to $g_0$:

$$\mathcal{Z}(\vec{0}, g_0) = -\left. \frac{1}{\mathcal{V}_\mathcal{M}} \frac{\partial}{\partial g_0} \right|_L \mathcal{Z}(g_0) = \left. \frac{1}{\mathcal{N}} \frac{\partial (g L^{-\varepsilon})}{\partial g_0} \right|_L \; , \tag{2.16}$$

where $g$ is the renormalized or effective coupling defined in (2.10). Since $\mathcal{Z}(\vec{0}, g_0)$ is dimensionless, it depends on the dimensionless combination $g_0 L^\varepsilon$ (and $\varepsilon$) only. Using $\mu = 1/L$, we obtain

$$\mathcal{N} \mathcal{Z}(\vec{0}, g_0) = L^{-\varepsilon} \left. \frac{\partial g}{\partial g_0} \right|_L \equiv -\frac{\beta(g)}{\varepsilon g_0 L^\varepsilon} \; . \tag{2.17}$$

For the further considerations, it is sufficient to know the behavior of the $\beta$-function close to the nontrivial zero. Expanding about $g{=}g^*$, we have

$$\beta(g) = (g - g^*)\omega(g^*) + O((g - g^*)^2) \; . \tag{2.18}$$

Combining (2.16), (2.17) and (2.18), we get

$$\left. \frac{\partial g}{\partial (g_0 L^\varepsilon)} \right|_L = -\frac{\beta(g)}{\varepsilon g_0 L^\varepsilon} = -\frac{(g - g^*)\omega(g^*)}{\varepsilon g_0 L^\varepsilon} \; . \tag{2.19}$$

The solution of this differential equation is

$$g - g^* \sim (g_0 L^\varepsilon)^{-\omega(g^*)/\varepsilon} + \ldots \quad . \tag{2.20}$$

Using (2.17), this implies the scaling law

$$\mathcal{Z}(\vec{0}, g_0) \sim (g_0^{1/\varepsilon} L)^{-\omega(g^*) - \varepsilon} \; . \tag{2.21}$$

We now use this result to derive a scaling law for $\mathcal{Z}(\vec{r}, g_0)$, with $\vec{r} \neq \vec{0}$. In addition to $g_0 L^\varepsilon$ (and $\varepsilon$), $\mathcal{Z}(\vec{r}, g_0)$ depends on $\vec{r}$; taking into account rotational symmetry and dimensionality, it depends on $\vec{r}$ only through the dimensionless combination $r/L^\nu$, with $r = |\vec{r}|$:

$$\mathcal{Z}(\vec{r}, g_0) = \mathcal{Z}(r/L^\nu, g_0 L^\varepsilon) \; . \tag{2.22}$$

For $\mathcal{Z}(\vec{r}, g_0)$, the most interesting limit is that of $g_0 \to \infty$. Physically, this corresponds to strictly forbidding monomers to be at the origin. Therefore it is clear that this limit is well-behaved, and

$$\mathcal{Z}_\infty(r/L^\nu) := \lim_{g_0 \to \infty} \mathcal{Z}(r/L^\nu, g_0 L^\varepsilon) \tag{2.23}$$

is finite. In order to be consistent with (2.21) it has to obey a power law in the scaling regime $r \ll L^\nu$

$$\mathcal{Z}_\infty(r/L^\nu) \sim (r/L^\nu)^\theta \; . \tag{2.24}$$

Comparing the $L$-dependence of $\mathcal{Z}_\infty(r/L^\nu)$ and $\mathcal{Z}(\vec{0}, g_0)$, we obtain the exponent identity

$$\theta = \frac{\varepsilon + \omega(g^*)}{\nu} \,. \tag{2.25}$$

Finally, from (2.24) we derive the repulsive force between the origin and the manifold

$$\vec{f}(\vec{r}) = \nabla_{\vec{r}} \ln \mathcal{Z}_\infty(|\vec{r}|/L^\nu) = \theta \frac{\vec{r}}{r^2} \,. \tag{2.26}$$

Note that to derive this result, $k_B T$ has been set to 1. Reestablishing the temperature-dependence, we find

$$\vec{f}(\vec{r}) = k_B T \theta \frac{\vec{r}}{r^2} \,. \tag{2.27}$$

Also note that this argument gives $\theta = 0$ at the Gaussian fixed point, which is necessary since for $g_0 = 0$ no force is exerted on the membrane.

## 2.3 Monomer density

Let us once again turn to the ensemble as defined in (2.16). The expectation value of the monomer density at the potential, $\langle n(0) \rangle$, where also the manifold is pinned, is obtained from

$$\langle n(0) \rangle = \frac{1}{\mathcal{Z}(\vec{0}, g_0)} \int \mathcal{D}[\vec{r}] \int_{\mathcal{V}_M} \delta^d(\vec{r}(x))\, \delta^d(\vec{r}(s))\, \mathrm{e}^{-\mathcal{H}[\vec{r}]} = -\frac{\partial}{\partial g_0} \ln Z(\vec{0}, g_0) \tag{2.28}$$

Since $g = \frac{\mathcal{N}}{\mathcal{V}_\mathcal{M}} [\mathcal{Z}(0) - \mathcal{Z}(g_0)] L^\varepsilon$ and $\frac{\partial}{\partial g_0} = L^\varepsilon \frac{\partial}{\partial z}$,

$$\langle n(0) \rangle = \frac{1}{g_0} \left( 1 + \frac{\omega(z)}{\varepsilon} \right) \,. \tag{2.29}$$

where $\omega(z) = -\varepsilon z (\partial\beta/\partial z)/\beta(z)$ and $\beta(z) = -\varepsilon z \partial g/\partial z$.
In particular, $\lim_{z\to\infty} \omega(z) = \omega(g^*) > 0$. The monomer density can be measured in a Monte-Carlo simulation and therefore offers a possibility also to check predictions for membranes $(D = 2)$. Let us point out that starting from the natural assumption that as long as $\varepsilon > 0$ the monomer density at the potential stays finite in the scaling limit of large manifolds one may directly deduce the existence of a strong coupling expansion of the effective coupling $g(z)$:

$$g(z) = g^* - s(\ln z) z^{-\omega/\varepsilon} + O(z^{-w}) \,, \tag{2.30}$$

where $s$ denotes some function that increases at most subexponentially and $w > \omega/\varepsilon > 0$.

## 2.4 Unbinding transition

Let us discuss the physical situation at the UV-stable fixed point in figure 2.2. The fixed point corresponds to a *delocalization transition* of the manifold, which is at vanishing coupling $g^*{=}0$ for $\varepsilon{>}0$ and at some finite attractive coupling $g^*{<}0$ for $\varepsilon{<}0$.
In the localized phase $g{<}g^*$, correlation functions such as $\langle [\vec{r}(x) - \vec{r}(y)]^2 \rangle$ and the associated

correlation length $\xi_{\|}$ (in the $D$-dimensional internal space) should be finite, as well as the radius of gyration $\xi_{\perp}$. Approaching the transition point these quantities diverge as [45]

$$\xi_{\|} \sim (g^*-g)^{-\nu_{\|}} \quad , \quad \xi_{\perp} \sim (g^*-g)^{-\nu_{\perp}} . \tag{2.31}$$

Since $\xi_{\perp} \sim \xi_{\|}^{\nu}$, the exponents $\nu_{\|}$ and $\nu_{\perp}$ are related through

$$\nu_{\perp} = \nu_{\|}\nu , \tag{2.32}$$

$\nu$ being the dimension of the field (2.7). To relate $\nu_{\|}$ to $\omega$, we first observe that $\xi_{\|}$ depends only on $g_0$ and the membrane size $L$, or its inverse $\mu = 1/L$. Writing $\xi_{\|}$ as a function of the renormalized coupling $g$ and the scale $\mu$, we thus have

$$\begin{aligned} 0 &= \mu\frac{\partial}{\partial\mu}\xi_{\|}(g,\mu) \\ &= \mu\frac{\partial}{\partial\mu}\left(\frac{1}{\mu}f(g)\right) \\ &= \frac{1}{\mu}\left(-f(g)+\beta(g)f'(g)\right) , \end{aligned} \tag{2.33}$$

where the dimension-full factor $1/\mu$ has been factored from the dependence on the dimensionless renormalized coupling $g$. Using that $\frac{\partial}{\partial g}\xi_{\|}(g) = \frac{1}{\mu}f'(g)$, this can be rewritten as

$$\begin{aligned} \xi_{\|}(g) &= \beta(g)\frac{\partial}{\partial g}\xi_{\|}(g) \\ &\approx \omega(g^*)(g-g^*)\frac{\partial}{\partial g}\xi_{\|}(g) . \end{aligned} \tag{2.34}$$

The solution to the above equation is

$$\xi_{\|} \sim |g-g^*|^{1/\omega(g^*)} . \tag{2.35}$$

This leads to the identification

$$\nu_{\|} = -\frac{1}{\omega(g^*)} , \qquad \nu_{\perp} = -\frac{\nu}{\omega(g^*)} . \tag{2.36}$$

Note that $\omega(g^*)<0$ at the transition. Specializing to $(D,d)=(1,1)$, we find

$$\nu_{\perp} = 1 \quad , \quad \nu_{\|} = 2 . \tag{2.37}$$

These exponents are also valid for the delocalization transition of a 1-dimensional interface from an attractive hard wall in 2-dimensional bulk space [39,45,37]. This can be understood as follows: The partition function of a fluctuating polymer interacting with a $\delta$-defect at the boundary of a hard wall can be written as

$$\mathcal{Z} = \frac{1}{2}\sum_{n=0}^{\infty}\mathcal{Z}_n\left(\frac{1}{2}\right)^n e^{-n\beta E} , \tag{2.38}$$

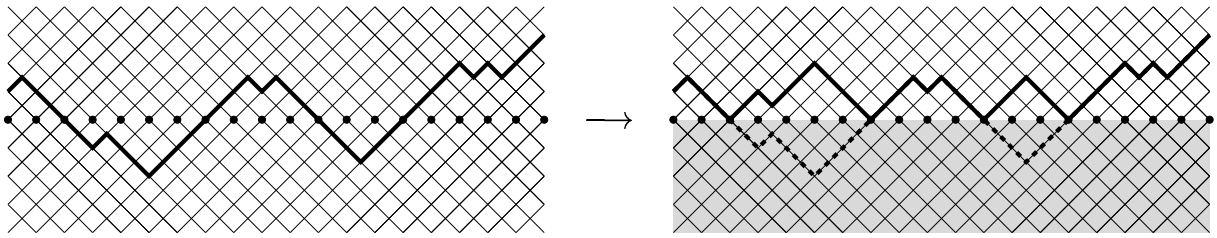

Figure 2.3: A polymer (here for simplicity directed) in interaction with a wall (thick dots). Left before and right after flapping up. The grey area is impenetrable.

where the sum runs over the number of contacts with the defect hyper-plane. $E$ denotes the contact energy, $\beta = (k_B T)^{-1}$ and $\mathcal{Z}_n$ is the constrained partition function of the free interface having exactly $n$ points of contact with the defect. The powers of $\frac{1}{2}$ only appear in the presence of an impenetrable defect and reflect the fact that all configurations in the presence of a hard wall can be obtained by flapping up those parts of the polymer which have penetrated the line (see figure 2.3). This accounts for a factor $\frac{1}{2}$ for each possible flap. Thus, the hard wall constraint translates into a shift in the binding energy according to

$$E_{\text{no wall}} \longrightarrow E_{\text{wall}} = E_{\text{no wall}} + k_B T \ \ln 2 \, . \tag{2.39}$$

The delocalization transition occurring for $(D, d)$=$(1, 1)$ at vanishing potential strength is shifted to an attractive interaction dependent on the temperature. Due to the correspondence (2.39) the exponents characterizing the transition remain unchanged.

# 3 Operator product expansion and one-loop result

The partition function of the model has been defined in (2.5). Analogously, we define the expectation value of an observable $\mathcal{O}(r)$ as (we denote $r$ for $\vec{r}$ from now on)

$$\langle \mathcal{O}(r) \rangle_{g_0} := \frac{\int \mathcal{D}[r] \ \exp(-\mathcal{H}[r])}{Z(g_0)} \ . \tag{3.1}$$

Most physical observables can be derived from expectation values of general $M$-point vertex operators like

$$\mathcal{O}(r) = \prod_{j=1}^{M} \mathrm{e}^{ip_j r(s_j)} \ . \tag{3.2}$$

Before we go on, let us make some changes in normalizations which will be helpful in the following. First, we rescale the field and the coupling constant according to [2]

$$r \longrightarrow (2-D)^{1/2} r \ , \quad g_0 \longrightarrow (2-D)^{d/2} g_0 \ . \tag{3.3}$$

Second, we change the integration over internal coordinates to

$$\int_x := \frac{1}{S_D} \int \mathrm{d}^D x \ , \quad S_D = 2\frac{\pi^{D/2}}{\Gamma(D/2)} \tag{3.4}$$

being the volume of the $D$-dimensional unit-sphere. Third, the normalization of the $\delta$-distribution is changed to

$$\tilde{\delta}^d(r(x)) := (4\pi)^{d/2} \delta(r(x)) = \int_k \mathrm{e}^{ikr(x)} \tag{3.5}$$

with

$$\int_k := \pi^{-d/2} \int \mathrm{d}^d k \ . \tag{3.6}$$

The advantage of these normalizations is that

$$\int_k \mathrm{e}^{-k^2} = 1 \ , \quad \int_x \Theta(|x| < 1) = 1 \ . \tag{3.7}$$

The model in the new normalizations now reads

$$\mathcal{H}[r] = \frac{1}{2-D} \int_x \frac{1}{2} \left(\nabla r(x)\right)^2 + g_0 \int_x \tilde{\delta}^d(r(x)) \ , \tag{3.8}$$

and (due to the factor of $1/(2-D)$ in the above definition) the two-point correlator is

$$C(x_i - x_j) := \frac{1}{2d} \left\langle [r(x_i) - r(x_j)]^2 \right\rangle_0 = |x_i - x_j|^{2\nu} \ . \tag{3.9}$$

[2] At this stage this is to be undertood only as a formal procedure, that simplifies calculations. All loop integrals are normed with respect to the one loop integral. The precise meaning in the limit $D \to 2$ is discussed in section (6.8).

We now proceed with the calculation of physical observables. As an explicit example, let us consider the perturbation expansion of the 1-point vertex operator

$$\mathcal{Z}^{(p)} := \mathcal{Z}(g_0)\langle \mathrm{e}^{ipr(s)}\rangle_{g_0} = \sum_{N=0}^{\infty} \frac{(-g_0)^N}{N!}\mathcal{Z}_N^{(p)}, \ , \tag{3.10}$$

where

$$\mathcal{Z}_N^{(p)} = \left\langle \mathrm{e}^{ipr(s)} \prod_{i=1}^{N} \int_{x_i} \tilde{\delta}^d(r(x_i)) \right\rangle_0 \ . \tag{3.11}$$

This can be written as

$$\mathcal{Z}_N^{(p)} = \prod_{i=1}^{N} \int_{x_i} \int_{k_i} \tilde{\delta}^d(p + \sum k_i) \times \left\langle \exp\left[ i(\sum_{i=1}^{N} k_i r(x_i) + pr(s)) \right] \right\rangle_0 \ , \tag{3.12}$$

where we have already integrated out a global translation of the field $r$. The Gaussian average is:

$$\left\langle \exp\left[ i(\sum_{i=1}^{N} k_i r(x_i) + pr(s)) \right] \right\rangle_0 = \exp\left[ \frac{1}{2} \sum_{i,j=0}^{N} k_i k_j C(x_i - x_j) \right] \ , \ k_0 = p \ . \tag{3.13}$$

The $\mathcal{Z}_N^{(p)}$ in (3.11) posses short distance singularities for $N \geq 2$. In order to analyze these singularities we will use the techniques of normal ordering and operator product expansion in the sequel. In our problem the procedure of normal ordering a vertex operator $\mathrm{e}^{ik_j r(x_j)}$ turns out to be quite simple: In any expectation value, we factorize out the contractions between the vertex operators. At one-loop order or equivalently at second order in (3.10) this means that

$$\mathrm{e}^{ik_1 r(x_1)} \mathrm{e}^{ik_2 r(x_2)} \ = :\mathrm{e}^{i(k_1 r(x_1) + k_2 r(x_2))}: \ \mathrm{e}^{k_1 k_2 C(x_1 - x_2)} \ . \tag{3.14}$$

This can be understood as a definition of the normal ordered product $:\mathrm{e}^{i(k_1 r(x_1) + k_2 r(x_2))}:$. Note, that equality in the above equation is meant in the sense of operators, that is when inserted into expectation values within the free theory.
Let us now turn to an explicit derivation of the OPE of two $\delta$-interactions, i.e. we study (3.14) for small distances $x_1 - x_2$. Since the short-distance singularities appear only in the internal contractions, the normal ordered product in the r.h.s. of (3.14) is regular for small distances $x_1 - x_2$ and thus can be expanded therein. We then project the resulting terms on the corresponding operators. For that purpose we make a change in the momentum variables according to

$$\begin{pmatrix} k_1 \\ k_2 \end{pmatrix} \longrightarrow \begin{pmatrix} \frac{k_1}{2} - k_2 \\ \frac{k_1}{2} + k_2 \end{pmatrix} \ . \tag{3.15}$$

In internal space we change coordinates to the center of mass system:

$$\bar{x} := \frac{1}{2}(x_1 + x_2) \ , \quad y := x_2 - x_1 \ . \tag{3.16}$$

Thus, the r.h.s. of (3.14) takes the form

$$
\begin{aligned}
&:\mathrm{e}^{i[(\frac{k_1}{2}-k_2)r(\bar{x}-y/2)+(\frac{k_1}{2}+k_2)r(\bar{x}+y/2)]}:\ \mathrm{e}^{(k_1^2/4-k_2^2)C(y)} \;=\\
&:\mathrm{e}^{ik_1 r(\bar{x})}\ \left(1+ik_2 y\nabla r(\bar{x})+ik_1\frac{1}{2!}\frac{y^\alpha y^\beta}{4}\nabla_\alpha\nabla_\beta r(\bar{x})-\frac{(k_2 y\nabla r(\bar{x}))^2}{2!}+\dots\right):\times\\
&\qquad\left(1+\frac{k_1^2}{4}C(y)+\dots\right)\ \mathrm{e}^{-k_2^2 C(y)}\ . \qquad (3.17)
\end{aligned}
$$

Integration over $k_1$, $k_2$ yields the OPE of $\tilde{\delta}^d(r(x_1))$ with $\tilde{\delta}^d(r(x_2))$:

$$
\begin{aligned}
\tilde{\delta}^d(r(\bar{x}-\frac{y}{2}))\tilde{\delta}^d(r(\bar{x}+\frac{y}{2})) = {}& y^{-\nu d}\tilde{\delta}^d(r(\bar{x}))-y^{-\nu d+2\nu}\frac{1}{4}\,\partial_r^2\tilde{\delta}^d(r(\bar{x}))\\
&-y^{-\nu d-2\nu+2}\frac{1}{4D}\tilde{\delta}^d(r(\bar{x}))(\nabla r(\bar{x}))^2\\
&-y^{-\nu d+2}\frac{1}{16D}(-\Delta_r)\tilde{\delta}^d(r(\bar{x}))(\nabla r(\bar{x}))^2\\
&+y^{-\nu d+2}\frac{1}{8D}\,\partial_{r_i}\tilde{\delta}^d(r(\bar{x}))\Delta r_i(\bar{x})+\dots\ . \qquad (3.18)
\end{aligned}
$$

Restricting ourselves to the most relevant next to leading operators for internal dimension $D$ smaller than, but close to 2, the operator product expansion reads:

$$
\tilde{\delta}^d(r(\bar{x}-\frac{y}{2}))\tilde{\delta}^d(r(\bar{x}+\frac{y}{2}))\ =\ y^{-\nu d}\tilde{\delta}^d(r(\bar{x}))+\sum_{n=1}^{\infty}y^{-\nu d+n(D-2)}\frac{(-\partial_r^2)^n\tilde{\delta}^d(r(\bar{x}))}{4^n n!}\ . \qquad (3.19)
$$

The OPE-coefficient in front of the leading operator, which is the $\delta$-interaction itself, carries the leading short distance singularity. In the following we introduce some diagrammatic notation. Denoting $\bullet\ :=\ \tilde{\delta}^d(r(x))$ we abbreviate the projection of two nearby $\delta$-interactions on the $\delta$-interaction itself as

$$
\big(\bullet\!\!\bullet\,\big|\bullet\big)\ =\ y^{-\nu d}\ . \qquad (3.20)
$$

We now analyze short-distance divergences of the perturbation expansion using the OPE in (3.18). Being interested in the leading scaling behavior, we drop all subdominant terms for $0<D<2$, such that we only need the leading OPE-coefficient (3.20). The integral over the relative distance in $\int_y(\bullet\!\!\bullet\,|\bullet)\,\bullet$ is logarithmically divergent for $\varepsilon{=}0$. In order to define a counter term we use dimensional regularization, i.e. we set $\varepsilon{>}0$. The integral is then UV-convergent, but IR-divergent. An IR regulator or equivalently a subtraction scale $\mu{=}L^{-1}$ has to be introduced to define the subtraction operation. Generally, we integrate over all distances bound by the inverse subtraction scale $L$. The OPE-coefficient in (3.20) then reduces to a number as

$$
\big\langle\bullet\!\!\bullet\,\big|\bullet\big\rangle_L:=\int_{|y|<L}\big(\bullet\!\!\bullet\,\big|\bullet\big)=L^{\varepsilon}f(\varepsilon,D)\ . \qquad (3.21)
$$

Let us use the scheme of minimal subtraction (MS). The internal dimension of the membrane is fixed and (3.21) is expanded in a Laurent-series in $\varepsilon$, starting here at order $\varepsilon^{-1}$. Denoting the term of order $\varepsilon^p$ in $\langle\ \ |\ \ \rangle_L|_{L=1}$ by $\langle\ \ |\ \ \rangle_{\varepsilon^p}$, the simple pole in (3.21) is

$$
\big\langle\bullet\!\!\bullet\,\big|\bullet\big\rangle_{\varepsilon^{-1}}=\frac{1}{\varepsilon}\ . \qquad (3.22)
$$

Of course, in this case, due to our normalizations, this is exact.
Let us rewrite the Hamiltonian in (2.6) in terms of the renormalized dimensionless coupling $g$. For perturbative calculations it is custom to write

$$g_0 = g Z_g \mu^{\varepsilon} \ , \tag{3.23}$$

where $Z_g$ is the renormalization factor, which is fixed by demanding that observables remain finite in the limit of $\varepsilon \to 0$. The Hamiltonian becomes

$$\mathcal{H}[r] = \frac{1}{2-D} \int_x \frac{1}{2} (\nabla r(x))^2 + \int_x g Z_g \mu^{\varepsilon} \, \tilde{\delta}^d(r(x)) \ . \tag{3.24}$$

We find to one-loop order

$$Z_g = 1 + \frac{g}{2} \Big\langle \bullet\!\!\bullet \Big| \bullet \Big\rangle_{\varepsilon^{-1}} + O(g^2) \ . \tag{3.25}$$

There is no field-renormalization since the elastic part has also to describe the manifold far away from the origin, for which the interaction term can be neglected. Formally, of course, this follows from the OPE. The renormalization group $\beta$-function is defined as

$$\beta(g) := \mu \frac{\mathrm{d}}{\mathrm{d}\mu}\bigg|_{g_0} g \ , \tag{3.26}$$

from what follows together with (3.23) that

$$\beta(g) = \frac{-\varepsilon g}{1 + g \frac{\partial}{\partial g} \ln Z_g} \ . \tag{3.27}$$

To one-loop order we obtain from (3.27) and (3.25) as anticipated earlier

$$\beta(g) = -\varepsilon g + \frac{g^2}{2} + O(g^3) \ . \tag{3.28}$$

The long-distance behavior of the theory is governed by the IR–stable fixed point of the RG–flow. Fixed points are zeros of the $\beta$–function:

$$\beta(g^*) = 0 \quad \Rightarrow \quad g^* = 0 \quad \text{or} \quad g^* = 2\varepsilon \ . \tag{3.29}$$

In section 2.2, we had defined the correction-to-scaling exponent $\omega$. It is obtained from the slope-function $\omega(g)$, defined as

$$\omega(g) := \frac{\mathrm{d}}{\mathrm{d}g} \beta(g) \ . \tag{3.30}$$

The correction to scaling exponent is $\omega(g)$ evaluated at the fixed points, and is found to be

$$\omega(g^*{=}0) = -\varepsilon \ , \qquad \omega(g^*{=}2\varepsilon) = \varepsilon \ . \tag{3.31}$$

Of course, this result is apart from the very existence of a fixed point rather trivial, since it is determined through the leading term of the $\beta$-function, which is always $-\varepsilon g$. In order to obtain any non-trivial information from the perturbation series it is thus necessary to go beyond the leading order.

# 4 Two-loop calculation in a MS-scheme

## 4.1 Operator product expansion

Let us now continue with the calculation at the two-loop order. At each order of perturbation theory there is only one new diagram. At two-loop order this comes from three coalescing $\delta$-interactions. Again, let us rewrite the product of the three vertex operators as its expectation value times the normal ordered product:

$$\begin{aligned} &\mathrm{e}^{ik_1 r(x_1)}\mathrm{e}^{ik_2 r(x_2)}\mathrm{e}^{ik_3 r(x_3)} \\ &= :\mathrm{e}^{i[k_1 r(x_1)+k_2 r(x_2)+k_3 r(x_3)]}:\ \mathrm{e}^{k_1 k_2 C(x_1-x_2)}\mathrm{e}^{k_1 k_3 C(x_1-x_3)}\mathrm{e}^{k_2 k_3 C(x_2-x_3)}\ . \end{aligned} \tag{4.1}$$

We use the following change of coordinates

$$\left.\begin{array}{l} \bar{x} := \frac{1}{3}(x_1+x_2+x_3) \\ a := x_2 - x_1 \\ b := x_3 - x_2 \\ c := x_1 - x_3 \end{array}\right\} \Leftrightarrow \left\{\begin{array}{l} x_1 = \bar{x} + \frac{1}{3}(c-a) \\ x_2 = \bar{x} + \frac{1}{3}(a-b) \\ x_3 = \bar{x} + \frac{1}{3}(b-c) \end{array}\right. , \ . \tag{4.2}$$

As at 1-loop order, $:\mathrm{e}^{i[k_1 r(x_1)+k_2 r(x_2)+k_3 r(x_3)]}:$ is free of divergences upon approaching the points $x_i$, whereas the UV-divergence comes from the factor $\mathrm{e}^{k_1 k_2 C(x_1-x_2)}\mathrm{e}^{k_1 k_3 C(x_1-x_3)}\mathrm{e}^{k_2 k_3 C(x_2-x_3)}$. The leading term is thus obtained upon setting $x_1 = x_2 = x_3 = \bar{x}$ in $:\mathrm{e}^{i[k_1 r(x_1)+k_2 r(x_2)+k_3 r(x_3)]}:$, dropping the gradient terms. Further shifting $k_1 \to k_1 - k_2 - k_3$, we obtain

$$\mathrm{e}^{ik_1 r(\bar{x})}\ \mathrm{e}^{(k_1-k_2-k_3)k_2 C(a)+k_2 k_3 C(b)+(k_1-k_2-k_3)k_3 C(c)}\ . \tag{4.3}$$

Integrating over $k_1$, $k_2$ and $k_3$ yields the final result

$$\tilde{\delta}^d(r(x_1))\tilde{\delta}^d(r(x_2))\tilde{\delta}^d(r(x_3)) = \left(\bigcirc\!\!\bullet\right)\tilde{\delta}^d(r(\bar{x})) + \left(\bigcirc\!\!\bullet''\right)(-\partial_r^2)\tilde{\delta}^d(r(\bar{x})) + \dots\ , \tag{4.4}$$

where the OPE–coefficients are given by

$$\begin{aligned} \left(\bigcirc\!\!\bullet\right) &= \left[C(a)C(c) - \frac{1}{4}(C(a)+C(c)-C(b))^2\right]^{-d/2} \\ &= \left[\frac{1}{4}(a^\nu+b^\nu+c^\nu)(b^\nu+c^\nu-a^\nu)(a^\nu+c^\nu-b^\nu)(a^\nu+b^\nu-c^\nu)\right]^{-d/2}\ , \end{aligned} \tag{4.5}$$

which contributes to the renormalization factor at two-loop order. The first subleading term is (denoting $\bullet'' := (-\partial_r^2)\tilde{\delta}^d(r(\bar{x}))$)

$$\left(\bigcirc\!\!\bullet''\right) = -\frac{1}{4}C(a)C(b)C(c)\left[\frac{1}{4}(a^\nu+b^\nu+c^\nu)(b^\nu+c^\nu-a^\nu)(a^\nu+c^\nu-b^\nu)(a^\nu+b^\nu-c^\nu)\right]^{-d/2-1} \tag{4.6}$$

### 4.2 Numerical calculation in $0 < D < 2$

Let us now turn to the explicit calculation of the second order contribution to the coupling constant renormalization. To two-loop order the renormalization group $Z_g$-factor for the coupling constant reads

$$Z_g = 1 + \frac{g}{2}\Big\langle \bullet\!\!\bullet \,\Big|\bullet\Big\rangle_{\varepsilon^{-1}} - \frac{g^2}{6}\left[\Big\langle \bullet\!\!\bullet\!\!\bullet \,\Big|\bullet\Big\rangle_{\varepsilon^{-2},\varepsilon^{-1}} - \frac{3}{2}\Big\langle \bullet\!\!\bullet \,\Big|\bullet\Big\rangle^2_{\varepsilon^{-1}}\right] + \frac{g^2}{4}\Big\langle \bullet\!\!\bullet \,\Big|\bullet\Big\rangle^2_{\varepsilon^{-1}} + O(g^3)\,. \tag{4.7}$$

Note that this $Z_g$-factor can either be obtained from (2.10) and (3.23) or by expanding the perturbative series and checking that divergent contributions proportional to $\tilde{\delta}(r(x))$ cancel.

The formula is arranged such that in the brackets the second order pole in $\varepsilon$ cancels. This is, because to leading order in $1/\varepsilon$, the two-loop diagram factorizes into two one-loop diagrams. The combinatorial factor of $3/2$ is composed of a factor of 3 for the number of possible subdivergences, and a factor of $1/2$ for the nested integration: The subdivergence in the distance say $a$ only appears in the sector (i.e. part of the domain of integration) in which $a$ is smallest.

Let us define:

$$I_2(D,L) := \Big\langle \bullet\!\!\bullet\!\!\bullet \,\Big|\bullet\Big\rangle_L - \frac{3}{2}\Big\langle \bullet\!\!\bullet \,\Big|\bullet\Big\rangle^2_L\,. \tag{4.8}$$

Let us already note that we will later calculate in a "massive" scheme in fixed dimension $d$. In order to use the results derived here, we keep $d$ arbitrary instead of setting $d = d_c$. We now want to derive an expression which can be integrated numerically. Since the bounds on the integrations in (4.8) are asymmetric (remind that in $\big\langle \bullet\!\!\bullet\!\!\bullet \,\big|\bullet\big\rangle_L$ all 3 distances $a$, $b$, and $c$ are bounded by $L$, whereas $\langle \bullet\!\!\bullet \,|\bullet\rangle^2_L$ is an integral with two bounds only) we treat both terms separately. We start with the first one, which can be written as

$$I_2^{\mathrm{M}}(D,L) = \int_{a,b,c} \Theta(a\le L)\Theta(b\le L)\Theta(c\le L)\Big(\bullet\!\!\bullet\!\!\bullet \,\Big|\bullet\Big)\,. \tag{4.9}$$

The divergence when integrating over the global scale is eliminated by noting that $L\frac{\partial}{\partial L} I_2(D,L) = 2\varepsilon\, I_2(D,L)$. There remains of course the sub-divergences, which will be subtracted later by the counter-term. Applying this procedure to (4.9), we obtain

$$2\varepsilon I_2^{\mathrm{M}}(D,L) = \int_{a,b,c} \Big[\delta(a-L)\Theta(b\le L)\Theta(c\le L) + \delta(c-L)\Theta(b\le L)\Theta(a\le L) + \delta(b-L)\Theta(a\le L)\Theta(c\le L)\Big]\Big(\bullet\!\!\bullet\!\!\bullet \,\Big|\bullet\Big)\,. \tag{4.10}$$

Since the integral is symmetric in $a$, $b$, and $c$, we can replace it by 3 times the first term. Introducing proper normalizations, an explicit representation for the measure and factoring out the explicit $L$-dependence, we obtain

$$2\varepsilon I_2^{\mathrm{M}}(D,L) = 3L^{2\varepsilon}\frac{S_{D-1}}{S_D}\int_{-\infty}^{\infty}\mathrm{d}c_{\parallel}\int_0^{\infty}\mathrm{d}c_{\perp}\, c_{\perp}^{D-2}\Theta(b\le 1)\Theta(c\le 1)\,\Big(\bullet\!\!\bullet\!\!\bullet \,\Big|\bullet\Big)\Big|_{a=1,b,c} \tag{4.11}$$

We also have to derive an expression for the counter-term. It can be written as

$$I_2^{\mathrm{C}}(D,L) = -\frac{3}{2}\int_a\int_c a^{-\nu d}c^{-\nu d}\,\Theta(a\le L)\Theta(c\le L)\,. \tag{4.12}$$

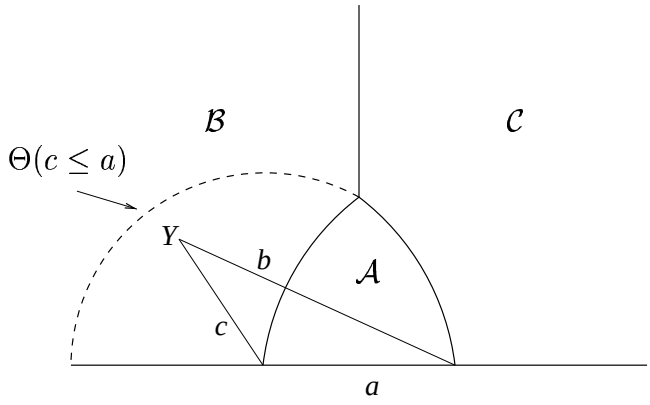


Figure 4.1: Area of integration (dashed) of the first integral in (4.13). The intersection with $\mathcal{B}$ is to be mapped onto $\mathcal{A}$

Using the same trick to derive w.r.t. the IR-regulator as above, we obtain

$$2\varepsilon I_2^{\rm C}(D,L) = -\frac{3}{2}L^{2\varepsilon}\int_{\mathcal{A},\mathcal{B},\mathcal{C}} a^{-\nu d}c^{-\nu d}\left[\delta(a-1)\Theta(c\leq a)+\delta(c-1)\Theta(a\leq c)\right] . \quad (4.13)$$

Using the technique of conformal mapping, which is presented in appendix E, both integrals above can be transformed into one having support in the single sector $\mathcal{A}$ defined through $b,c \leq a$, (where here $a$ is set to 1). Analogously, we define sectors $\mathcal{B}$ and $\mathcal{C}$, as the subset of domains where $b$ respectively $c$ is the longest distance. Note that the first term in (4.13) only has contributions from $\mathcal{A}$ and $\mathcal{B}$, while the second can be restricted to $\mathcal{A}$ and $\mathcal{C}$ after renaming $a$ into $b$ and $c$ into $a$.
Performing explicitly the mapping of both $\mathcal{B}$ and $\mathcal{C}$ onto $\mathcal{A}$ one obtains

$$\begin{aligned}\int_{\mathcal{B}}(a^{-\nu d}c^{-\nu d}\Theta(c\leq a))\Big|_{a=1} &= \int_{\mathcal{A}} b^{-\nu d-2\varepsilon}c^{-\nu d}\Theta(c\leq b)\\ \int_{\mathcal{C}}(a^{-\nu d}b^{-\nu d}\Theta(b\leq a))_{|a=1} &= \int_{\mathcal{A}} c^{-\nu d-2\varepsilon}b^{-\nu d}\Theta(b\leq c) .\end{aligned} \quad (4.14)$$

Combining the contributions from all sectors, we arrive at

$$2\varepsilon I_2^{\rm C}(D,L) = -\frac{3}{2}L^{2\varepsilon}\int_{\mathcal{A}}\left(b^{-\nu d}+c^{-\nu d}+b^{-\nu d}c^{-\nu d}\max(b,c)^{-2\varepsilon}\right) . \quad (4.15)$$

Combining (4.11) and (4.15), we obtain an expression for the complete diagram

$$\begin{aligned}2\varepsilon I_2(D,L) = 3L^{2\varepsilon}\frac{S_{D-1}}{S_D}\int_{-\infty}^{\infty}{\rm d}c_{||}\int_0^{\infty}{\rm d}c_{\perp}c_{\perp}^{D-2}\Theta(b\leq 1)\Theta(c\leq 1)\\ \times\Bigg\{\left[\frac{1}{4}(1+b^{\nu}+c^{\nu})(b^{\nu}+c^{\nu}-1)(1+c^{\nu}-b^{\nu})(1+b^{\nu}-c^{\nu})\right]^{-d/2}\\ -\frac{1}{2}\left[b^{-\nu d}+c^{-\nu d}+b^{-\nu d}c^{-\nu d}\max(b,c)^{-2\varepsilon}\right]\Bigg\} .\end{aligned} \quad (4.16)$$

This expression will also be used later in a massive scheme. Since here we are only interested

in the $\varepsilon$-expansion, we take the limit of $\varepsilon \to 0$ in the integrand. We have made the (non-trivial) check that the integrand remains a finite integrable function, which can be integrated numerically:

$$\begin{aligned} I_2(D,L) = 3\frac{L^{2\varepsilon}}{2\varepsilon}\frac{S_{D-1}}{S_D}\int_{-\infty}^{\infty}\mathrm{d}c_{\|}\int_0^{\infty}\mathrm{d}c_{\perp}c_{\perp}^{D-2}\Theta(b\le 1)\Theta(c\le 1) \\ \times\Bigg\{\left[\frac{1}{4}(1+b^{\nu}+c^{\nu})(b^{\nu}+c^{\nu}-1)(1+c^{\nu}-b^{\nu})(1+b^{\nu}-c^{\nu})\right]^{-d_c/2} \\ -\frac{1}{2}\left[b^{-\nu d_c}+c^{-\nu d_c}+b^{-\nu d_c}c^{-\nu d_c}\right]\Bigg\} \\ +O(\varepsilon^0)\,. \end{aligned} \tag{4.17}$$

Let us now proceed with the explicit numeric evaluation of (4.17). There are integrable singularities both in $c_{\|}$ and $c_{\perp}$. To disentangle them [26,20] we make a change of variables from Cartesian coordinates $(c_{\|}, c_{\perp})$ to radial and angular coordinates $(c, \alpha)$ according to

$$c_{\|} = c\cos(\alpha)\,, \qquad c_{\perp} = c\sin(\alpha)\,. \tag{4.18}$$

such that

$$\int_{-\infty}^{\infty}\mathrm{d}c_{\|}\int_0^{\infty}\mathrm{d}c_{\perp}c_{\perp}^{D-2} \longrightarrow \int_0^1 \mathrm{d}c\, c^{D-1}\int_0^{\pi/2}\mathrm{d}\alpha\,(\sin(\alpha))^{D-2}\,, \tag{4.19}$$

where the upper bounds of $\pi/2$ on $\alpha$ and 1 on $c$ is due to the bound of 1 on $b$ and $c$. We can further restrict integration to the half-sector with $c < b$. In this sector, there remain singularities for small $\alpha$ and small $c$. The reader is invited to verify that they are eliminated by a second change of variables

$$\begin{aligned} \alpha &= \frac{\pi}{2}\beta^{\frac{1}{D-1}} \\ c &= \tilde{c}^{\frac{1}{2-D}}\,. \end{aligned}$$

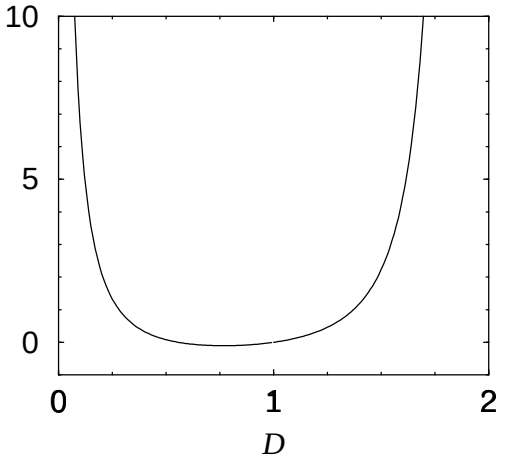


| D | | D | | D | |
|---|---|---|---|---|---|
| 0.1 | 6.71 | 0.8 | -0.102 | 1.5 | 2.24 |
| 0.2 | 2.11 | 0.9 | -0.0712 | 1.6 | 4.45 |
| 0.3 | 0.847 | 1.0 | 0 | 1.7 | 10.4 |
| 0.4 | 0.325 | 1.1 | 0.123 | 1.8 | 36.7 |
| 0.5 | 0.0807 | 1.2 | 0.321 | 1.9 | 658 |
| 0.6 | -0.0415 | 1.3 | 0.644 | 2.0 | $\infty$ |
| 0.7 | -0.0949 | 1.4 | 1.20 | | |

Figure 4.2: Numerically obtained results for the two-loop diagram in the MS-scheme. Some values are tabulated.

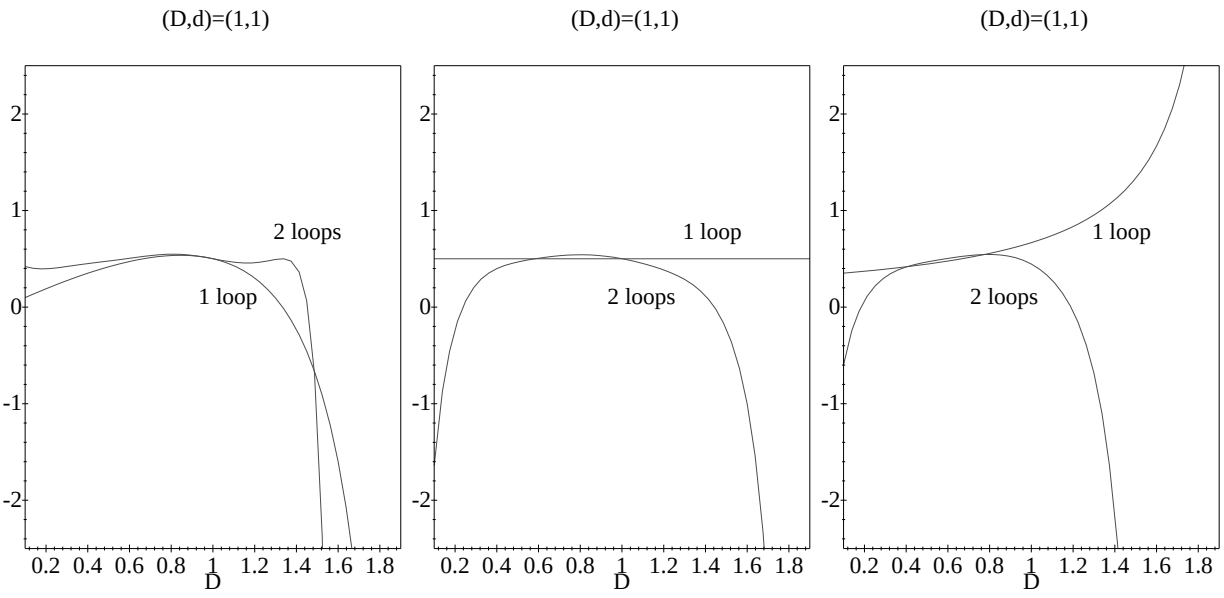


Figure 4.3: Correction to scaling exponent $\omega$ for $(D{=}1, d{=}1)$ with different extrapolation parameters $(D,d),(D,\varepsilon(D,d)),(D,D_c(d))$ (from left to right). The abscissa labels the corresponding internal dimension $D_0$ of the departure point on the critical line $\varepsilon(D_0,d_0){=}0$.

The above method works for $D > 1$ only. For $D < 1$, one has to analytically continue the integration over $c_\perp$ in (4.11). This can be done by partial integration, since the integrand does not explicitly depend on $c_\perp$ but on $c = \sqrt{c_\perp^2 + c_\parallel^2}$. To have no boundary terms, one should partially integrate before mapping everything onto the sector $\mathcal{A}$. We have explicitly checked consistency with the earlier used measure for $1{<}D{<}2$. Note finally, that in the special case of $D = 1$ in (4.17) the integration measure becomes a distribution reducing the integration measure to a line along $c_\parallel$.

The diagram is shown on figure (4.2). It grows as $D^{-1}$ for $D \to 0$ and exponentially for $D \to 2$:

$$I_2(D) \sim \left(\frac{3}{4}\right)^{-d_c/2} \sim \left(\frac{3}{4}\right)^{-D/(2-D)} . \tag{4.20}$$

In the case of polymers $D{=}1$ it vanishes. The reason is that the diagrams factorize, and thus the 1-loop result is correct to all orders when working in an appropriate scheme. (See e.g. [4].)

## 4.3 RG-function and extrapolation

From (3.27) the renormalization $\beta$-function in second order of perturbation theory reads

$$\beta(g) = -\varepsilon g + \frac{g^2}{2} - \frac{g^3}{3} I_2(D) + O(g^4) . \tag{4.21}$$

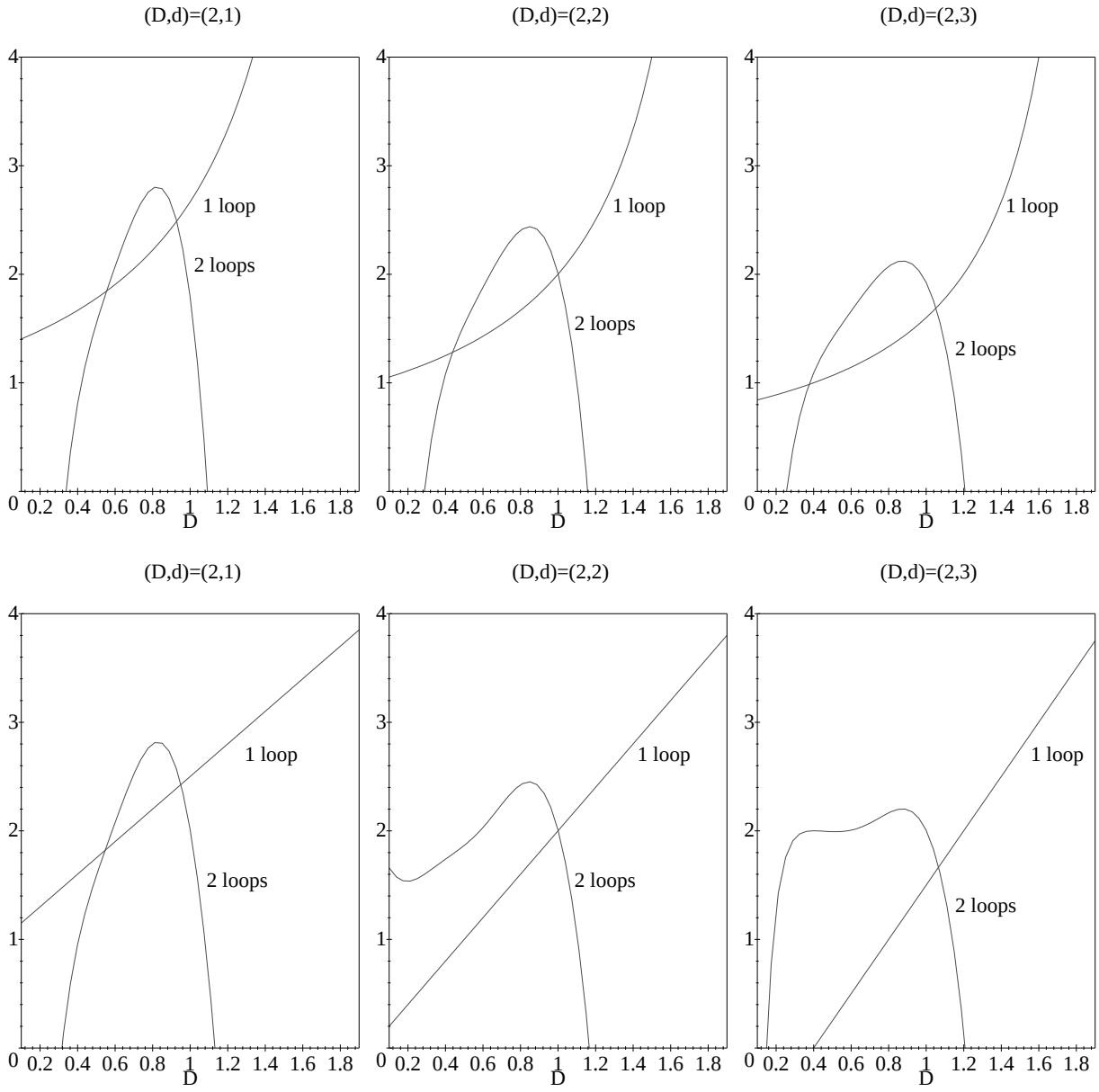


| $(x,y)\,;(D,d)$ | (1,1) | (2,1) | (2,2) | (2,3) |
|---|---|---|---|---|
| $(D,Dc)$ , max | 0.55 | 2.80 | 2.43 | 2.10 |
| $(D,d)$ , max | 0.55 | 2.80 | 2.43 | 2.20 |
| $(D,\varepsilon)$ , max | 0.55 | | | |

Figure 4.4: Correction to scaling exponent $\omega$ for different extrapolation points $(D,d)$: Extrapolation parameters are $(D, D_c(d))$ (top) and $(D,d)$ (bottom). The abscissa labels the corresponding internal dimension $D_0$ of the departure point on the critical line $\varepsilon(D_0,d_0)=0$. Furthermore, the two-loop values with minimal sensitivity with respect to the departure point are tabulated.

The long-distance behavior of the theory is governed by the IR–stable fixed point of the RG–flow. Fixed points are given by zeros of the $\beta$–function:

$$\beta(g^*) = 0 \qquad \Rightarrow \quad g^* = 0 \quad \vee \quad -\varepsilon + \frac{g^*}{2} - \frac{g^{*2}}{3} I_2(D) + O(g^{*3}) = 0 \,. \tag{4.22}$$

The physically interesting nontrivial fixed point is the one that is next to zero. In an $\varepsilon$–expansion it reads:

$$g^* = 2\varepsilon + \frac{8}{3} I_2(D)\varepsilon^2 + O(\varepsilon^3) \,. \tag{4.23}$$

The correction to scaling exponent $\omega$ at this fixed point is found in an $\varepsilon$-expansion to be

$$\omega(g^*) = \varepsilon - \frac{4}{3} I_2(D)\varepsilon^2 + O(\varepsilon^3) \,. \tag{4.24}$$

The question now arises of how to calculate $\omega$ for a given physical situation. The general strategy that we follow in the MS-scheme is that we make use of the freedom to choose any point on the critical line (2.2) around which to start our expansion [25,26]. To expand towards some physically interesting point $(D, d)$ we furthermore dispose of the freedom to follow any path starting on the curve $\varepsilon$=0. Since our expansion (4.24) is exact in $D$ but only of second order in $\varepsilon$, we can equally well expand it to second order in $D$ around any point on the critical curve. Now we can change our extrapolation path through an invertible transformation $(x, y) = (x(D, d), y(D, d))$. One expresses $D$ and $\varepsilon$ as functions of $x$ and $y$ and reexpands $\omega$ to second order in $x$ and $y$ around the point $(x_0, y_0) = (x_0(D_0, d_c(D_0)), y_0(D_0, d_c(D_0)))$, where we recall that $d_c(D)$ is defined such that $\varepsilon(D, d_c(D)) = 0$. The aim is to find an optimal choice of variables $(x, y)$. The guidelines for such a choice have been discussed in [20], where this procedure has been successfully applied to extrapolate results for the anomalous dimension of self-avoiding membranes. As a general rule, we "trust" most a result that is the least sensitive to the starting point of the extrapolation. Therefore, we would like to find a plateau for some suitable chosen variables $(x, y)$. This procedure works well for polymers, or more generally for membranes with inner dimension close to 1. However it turns out that for membranes it works much less well than in the self-avoiding case: we could not find a plateau, but at best an extremum.

Some extrapolations are shown in the following figures (4.3, 4.4). We start with polymers interacting with a $\delta$-wall corresponding to the point $(D, d) = (1, 1)$. (Note that for $d < 2$ the interaction becomes relevant for polymers.) This can be seen on fig. 4.3. The values obtained from the plateaus appearing at the two-loop level ($\omega \approx 0.55$) are quite close to the exact value $\omega = 1/2$, known from the fact that the result in $D = 1$ at one-loop is exact. From the latter it follows that it is best to use $(D, \varepsilon)$ as extrapolation parameters and to stay in $D = 1$.

Let us now turn to the results obtained for $\omega$ extrapolated to points $D = 2$ (fig. 4.13): The extrapolated value depends strongly on the starting-point on the critical line. We can identify a least sensitive value, which lies below $D = 1$, reflecting the $D$-dependence of the two-loop diagram. We obtain identical results for different extrapolation paths. Note, that if we fix $d = 1$ and perform an $\varepsilon$-expansion in $D$ as is commonly done [62], then, this corresponds to starting from $D_c(d{=}1) = 2/3 < 1$. The $d$-dependence of the extrapolated values is recovered in the massive scheme, which we discuss in the next section.

# 5 Calculation in fixed dimension: The massive scheme

## 5.1 Phantom manifolds

An alternative scheme to an $\varepsilon$-expansion is a calculation in fixed dimension. This way we hope to circumvent the difficulty that we faced when calculating the two-loop diagram in the previous section in the limit of $D \to 2$: Since the diagram behaves like $\left(\frac{4}{3}\right)^{d/2}$, it becomes large when the dimension of the embedding space is large. When working in an $\varepsilon$-expansion, $d$ and $D$ are related by $\varepsilon = D - d(2-D)/2$ and sending $\varepsilon \to 0$ before $D \to 2$ imposes that $d \to \infty$. Thus one would like to work at finite $d$, thus finite $\varepsilon$. The diagrams are UV-convergent for $d < d_c$. They are cut-off in the infrared by a finite membrane size. Alternatively, we can use a "soft" IR cut-off, that is we introduce a chemical potential $\tau$ into the Hamiltonian and sum over all manifold sizes. For polymers $(D = 1)$ this scheme corresponds to a "massive scheme" in an $O(N)$-symmetric, scalar $\phi^4$-theory as can be seen via a de Gennes Laplace transformation on the $N = 0$ component limit. (The correlator in momentum-space reads $\frac{1}{k^2+t}$) In the following we keep a hard IR regulator and calculate the two-loop diagram in fixed dimension. We use the analytical expression given in (4.16). For the numerical integration in $1 < D < 2$ we proceed as before. The result for different embedding dimensions $d$ is shown graphically on figure 5.1, where also some explicit values in the limit of $D = 2$ are given. Note, that the exact factorization-property in the limit of $D = 1$ is only valid in the MS-scheme or in a massive scheme with suitable soft cut-off as mentioned above. However, even the method is not tailored to capture that feature, the obtained value $\omega = 0.6$ in the case of $(D, d) = (1, 1)$ is not too far from the exact value $1/2$. We expect that higher order terms would again reproduce the exact value of $\omega = 1/2$. Also note that results for membranes ($D = 2$) are close to those from the $\varepsilon$-expansion, especially for small $d$.

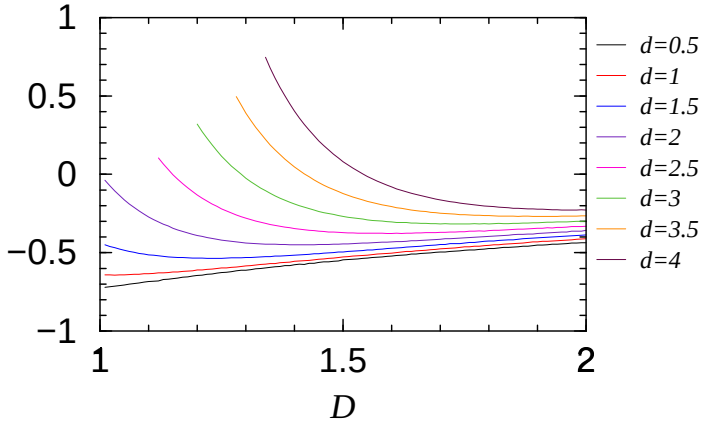


| $d$ | $I_{2\|_{D=2}}$ |
|---|---|
| 0.5 | -0.437 |
| 1 | -0.410 |
| 1.5 | -0.386 |
| 2 | -0.358 |
| 2.5 | -0.331 |
| 3 | -0.299 |
| 3.5 | -0.265 |
| 4 | -0.229 |

Figure 5.1: 2-loop diagram in fixed dimension for embedding dimensions $d$=0.5 to $d$=4 (from bottom to top). The curves are only shown for values of $D$ such that $\varepsilon \geq 0$.

## 5.2 Self-avoiding membranes

Up to now we were considering a $D$-dimensional polymerized "phantom" membrane interacting with a point-like impurity in $d$-dimensional embedding space modeled through a $\delta$-potential.

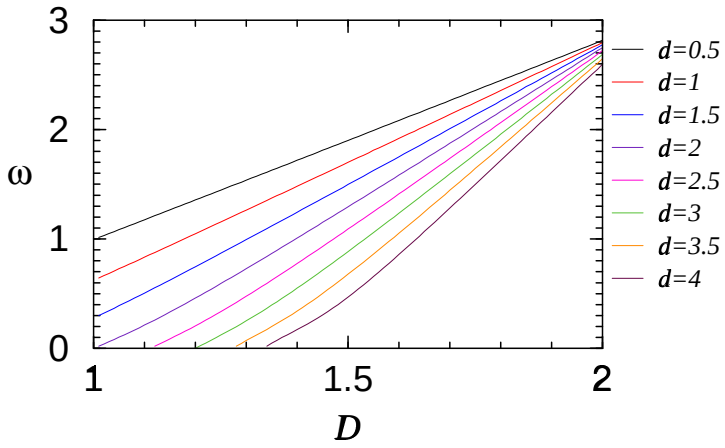


| $d$ | $\omega_{\vert_{D=2}}$ |
|---|---|
| 0.5 | 2.82 |
| 1 | 2.80 |
| 1.5 | 2.77 |
| 2 | 2.75 |
| 2.5 | 2.72 |
| 3 | 2.69 |
| 3.5 | 2.65 |
| 4 | 2.60 |

Figure 5.2: Correction to scaling exponent $\omega$ for embedding dimension $d$=0.5 to $d$=4 (from top to bottom). $\varepsilon$ is restricted to $\varepsilon \geq 0$; otherwise one has to work with an explicit UV-cutoff.

The infinite fractal dimension of the free manifold was causing problems, and since all operators of the type $(-\Delta_r)^n \delta(r),\ n \geq 0$, attain the same relevance in $D = 2$, it is not clear whether the model will break down. Physically, the problem is much better defined for self-avoiding membranes. From field-theoretical calculations, which have recently been refined up to two-loop [19,20], we know that two-dimensional self-avoiding manifolds embedded in three dimensional space have an anomalous dimension of $\nu^* \approx 0.85$. We now try to overcome the problem of an infinite Hausdorff-dimension by a crude simplification: We approximate the self-avoiding manifold by a Gaussian theory with the same scaling dimension, that is a Hamiltonian of the type [47]

$$\mathcal{H}[r] = \frac{1}{k-D} \int_x \frac{1}{2}\, r(x) (-\Delta_x)^{k/2} r(x)\ , \tag{5.1}$$

where

$$r:\ x \in \mathbb{R}^D \longrightarrow r(x) \in \mathbb{R}^d$$

as before providing the two-point correlator in our normalizations:

$$C(x,y) = |x-y|^{k-D}\ . \tag{5.2}$$

The scaling dimension is

$$\nu = \frac{k-D}{2}\ . \tag{5.3}$$

We recover (3.9) by setting $k = 2$, but the model can be continued analytically to any real value of $k$, with $k \geq 2$. Setting

$$k^* = 2\nu^* + D \tag{5.4}$$

we get a Gaussian manifold with identical scaling dimension as obtained for self-avoiding crumpled membranes at two-loop. The critical embedding dimension of the interaction then reads

$$d_c = \frac{2D}{k^*-D} = \frac{D}{\nu^*}\ , \tag{5.5}$$

that is the interacting is relevant in $d<d_c$. For membranes $d_c = \frac{2}{0.85} \approx 2.4$. All operators of the type $(-\Delta_r^n \delta^d(r))$ are at least naively irrelevant for $n > 0$, as

$$[(-\Delta_r^n \delta^d(r))] = -\nu^*(d+2n) \tag{5.6}$$

and the corresponding coupling has in inverse length units the dimension

$$[g_0^{(n)}] = D - \nu^*(d+2n) < 0\,, \qquad n > 0\,. \tag{5.7}$$

We may repeat the calculation in the massive scheme setting the free scaling dimension $\nu^*{=}0.85$ and $(D,d){=}(2,1)$. The result is shown in table (5.2).
Let us stress that this method can not be turned into a systematic expansion, since perturbation theory neglects all effects of the non-Gaussian nature of the nontrivial crumpled state. We only know that for $d \to \infty$ the Gaussian variational approximation for the Hamiltonian, i.e. (5.1) becomes exact [63–65].

| | I | $\omega(g^*)$ | $\theta(g^*)$ |
|---|---|---|---|
| 1-loop | 1.000 | 1.15 | 2.71 |
| 2-loop | -0.379 | 1.49 | 3.10 |

Table 5.1: Two-loop results for self-avoiding membranes $(D{=}2)$ approximated through a Gaussian theory having identical scaling dimension $\nu^*{=}0.85$. Results are shown for the corresponding diagram, the correction to scaling exponent $\omega$ and the contact exponent $\theta$.

# 6 Summation of the perturbation series in the limit $D = 2$

In the last section we introduced a "massive" scheme allowing to perform the renormalization procedure in fixed dimension. As can be seen in figures 5.1 and 5.2, the limit $D \to 2$ can be taken in the 2-loop diagram and is smooth. Surprisingly, this limit can be calculated analytically: Setting $\nu = 0$ in (4.16), the integrand becomes constant, and thus trivial to calculate. This is a striking property. Even more, if we slightly modify the regularization prescription, this property holds to *all loop orders* in perturbation theory. Below, we will give an analytic expression for the complete perturbation series, which allows for analyzing the strong coupling limit. Furthermore, we show how corrections in $(2 - D)$ can be incorporated. We will see that only the latter depend on the explicit cut-off procedure, a point which will be further clarified below.
In the following– since we perform calculations on a torus – we slightly modify the rescaling of the field and the bare coupling:

$$r \to r(S_D(2-D))^{1/2}\,, \quad g_0 \to g_0(S_D(2-D))^{d/2}\,. \tag{6.1}$$

Our aim is to evaluate the perturbation series of the effective coupling, which reads:

$$g = \frac{g_0 L^\varepsilon}{\mathcal{V}_\mathcal{M}} \sum_{N=0}^{\infty} \frac{(-g_0)^N}{(N+1)!} \left\langle \prod_{i=1}^{N+1} \int_{x_i} \delta^d(r(x_i)) \right\rangle_0 \,. \tag{6.2}$$

The two-point function gets a factor $(S_D(2-D))^{d/2}$ due to the rescaling (6.1). All other factors $(S_D(2-D))^{d/2}$ will be dropped. We discuss this at the end of this section in 6.8.

## 6.1 $N$-loop order

In order to calculate the $N$–loop contribution to the perturbation theory we need the SDE of $N+1$ contact interactions. The normal ordered product of the corresponding vertex operators reads

$$\mathrm{e}^{ik_1 r(x_1)} \mathrm{e}^{ik_2 r(x_2)} \cdot \ldots \cdot \mathrm{e}^{ik_{N+1} r(x_{N+1})} = :\mathrm{e}^{i(\sum_{n=1}^{N+1} k_n r(x_n))}: \prod_{i,j=1}^{N+1} \mathrm{e}^{\frac{1}{2} k_i k_j C(x_i - x_j)}\,. \tag{6.3}$$

We choose $x_{N+1}$ as root in the renormalization procedure (for the precise definition, see below) and therefore $k_{N+1}$ to integrate over in order to obtain the $\delta$-distribution (or its derivative), onto which to project. We thus shift

$$k_{N+1} \;\longrightarrow\; k_{N+1} - \sum_{j=1}^{N} k_j$$

and rewrite the quadratic form in (6.3) as

$$\frac{1}{2} \sum_{i,j=1}^{N+1} k_i k_j C(x_i - x_j) = \sum_{j=1}^{N} k_{N+1} k_j C(x_{N+1} - x_j) + \frac{1}{2} \sum_{i,j=1}^{N} k_i k_j C(x_i - x_j)$$

$$\longrightarrow \sum_{j=1}^{N} k_{N+1}k_j C(x_{N+1}-x_j) - \sum_{i,j=1}^{N} k_i k_j C(x_{N+1}-x_j) + \frac{1}{2}\sum_{i,j=1}^{N} k_i k_j C(x_i-x_j)$$
$$= \sum_{j=1}^{N} k_{N+1}k_j C(x_{N+1}-x_j) - \sum_{i,j=1}^{N} k_i k_j \frac{C(x_{N+1}-x_i) + C(x_{N+1}-x_j) - C(x_i-x_j)}{2} \,. \tag{6.4}$$

(6.3) then becomes (up to subdominant terms[3] involving spatial derivatives of $r$)

$$:\exp\left[ik_{N+1}r(x_{N+1})\right]: \times \exp\left[\sum_{j=1}^{N} k_{N+1}k_j C(x_{N+1}-x_j) - \sum_{i,j=1}^{N} k_i k_j \frac{C(x_{N+1}-x_i) + C(x_{N+1}-x_j) - C(x_i-x_j)}{2}\right] \tag{6.5}$$

and the integration over $k_{N+1}$ produces the $\delta$-interaction and its derivatives; the latter come from the first term in (6.4). They are subdominant and thus will be dropped. We abbreviate the quadratic form in (6.4) as $(D_{ij})$, where the matrix elements are

$$D_{ij} = \frac{1}{2}\left[C(x_{N+1}-x_i) + C(x_{N+1}-x_j) - C(x_i-x_j)\right] \,, \quad i \neq j \,,$$
$$D_{ii} = C(x_{N+1}-x_i) \,. \tag{6.6}$$

Integrating out the momenta $k_1, \ldots k_N$ yields the operator product expansion of $N+1$ contact interactions as

$$\tilde{\delta}^d(r(x_1))\,\tilde{\delta}^d(r(x_2)) \ldots \tilde{\delta}^d(r(x_{N+1})) = \left[\det(D_{ij})\right]^{-d/2}\tilde{\delta}^d(r(x_{N+1})) + \text{subdominant operators} \,. \tag{6.7}$$

### 6.2 The limit $D \to 2$ and $(2-D)$-expansion on the torus

Whereas (6.7) is still completely general, we now want to study the limit $D \to 2$ as well as perturbations above it. We start by remarking that the propagator $C(x)$ may be rewritten as

$$C(x) = \mathbb{C}^{(0)}(x) + (2-D)\mathbb{C}(x) \,, \tag{6.8}$$

where $\mathbb{C}^{(0)}(x)$ denotes the limit $D \to 2$ of $C(x)$. Accordingly, we define matrices $\mathfrak{D}^{(0)}$ and $\mathfrak{D}$, such that

$$D_{ij} = \mathfrak{D}^{(0)}_{ij} + (2-D)\mathfrak{D}_{ij} \,, \tag{6.9}$$

where

$$\mathfrak{D}^{(0)}_{ij} = \frac{1}{2} \,, \qquad i \neq j$$
$$\mathfrak{D}^{(0)}_{ii} = 1 \tag{6.10}$$

[3]Here we argue in terms of an OPE. Note that in order to make these arguments rigorous, one should ask of whether these terms affect the effective action at *constant* background-field. This is not the case, since then $\nabla r = 0$.

and

$$\mathfrak{D}_{ij} = \frac{\mu^{-2\nu}}{2}(\mathbb{C}|(x_{N+1}-x_i)\mu| + \mathbb{C}|(x_{N+1}-x_j)\mu| - \mathbb{C}|(x_i-x_j)\mu|) \;, \qquad i \neq j$$
$$\mathfrak{D}_{ii} = \mu^{-2\nu}\mathbb{C}|(x_{N+1}-x_i)\mu| \;, \tag{6.11}$$

$\mu = 1/L$. Note, that we obtained (6.10) from the limit $D \to 2$ in (6.6), and we used for $C(x)$ the infinite $D$-space propagator $C(x) = |x|^{2-D}$. However, the constance in the limit $D \to 2$ for noncoinciding points stays conserved, even if we are considering closed manifolds. Thus, (6.9) together with (6.10) always stay valid as well as the following considerations:
Due to (6.9),

$$\begin{aligned} \det(D) &= \exp[\mathrm{Tr}\ln(D_{ij})] \\ &= \det(\mathfrak{D}^{(0)}) \cdot \exp[\mathrm{Tr}\ln[\mathbf{1} + (2-D)[\mathfrak{D}^{(0)}]^{-1}\tilde{D}]] \;, \end{aligned} \tag{6.12}$$

where $[\mathfrak{D}^{(0)}]^{-1}$ denotes the inverse matrix to $\mathfrak{D}^{(0)}$. Denoting

$$M := [\mathfrak{D}^{(0)}]^{-1}\mathfrak{D} \;, \tag{6.13}$$

let us expand the OPE-coefficient in (6.7) up to fourth order in $2-D$. Expanding first the logarithm,

$$\ln[\mathbf{1} + (2-D)M] = (2-D)M - \frac{(2-D)^2}{2}M^2 + \frac{(2-D)^3}{3}M^3 - \frac{(2-D)^4}{4}M^4 + O((2-D)^5)$$

and inserting into (6.12) one arrives at

$$\begin{aligned} &[\det(D)]^{-d/2} = [\det(\mathfrak{D}^{(0)})]^{-d/2}\left[1 - \frac{d}{2}\left[(2-D)\mathrm{Tr}M\right.\right. \\ &\left. -\frac{(2-D)^2}{2}\mathrm{Tr}M^2 + \frac{(2-D)^3}{2}\mathrm{Tr}M^3 - \frac{(2-D)^4}{4}\mathrm{Tr}M^4\right] \\ &+\frac{d^2}{8}\left[(2-D)^2\mathrm{Tr}^2M - (2-D)^3\mathrm{Tr}M\ \mathrm{Tr}M^2 + (2-D)^4\left[\frac{1}{4}\mathrm{Tr}^2M^2 + \frac{2}{3}\mathrm{Tr}M\ \mathrm{Tr}M^3\right]\right] \\ &\left.-\frac{d^3}{48}\left[(2-D)^3\mathrm{Tr}^3M - (2-D)^4\frac{3}{2}\mathrm{Tr}^2M\ \mathrm{Tr}M^2\right] + \frac{d^4}{384}(2-D)^4\mathrm{Tr}^4M\right] + O((2-D)^5) \end{aligned} \tag{6.14}$$

To check the above result consider that

$$\ln(1+x) = x - \frac{x^2}{2} + \frac{x^3}{3} - \frac{x^4}{4} + \cdots$$

and

$$(ax + bx^2 + cx^3 + cx^4)^2 = a^2x^2 + 2abx^3 + (b^2 + 2ac)x^4 + \cdots$$

as well as

$$(ax + bx^2 + cx^3 + cx^4)^3 = a^3x^3 + 3a^2bx^4 \;.$$

The zeroth order is $[\det(\mathfrak{D}^{(0)})]^{-d/2}$. In order to proceed we need the latter and the inverse matrix $[\mathfrak{D}^{(0)}]^{-1}$. Let us first calculate the determinant. From (6.9) we have

$$\mathfrak{D}^{(0)} = \mu^{-2\nu} \begin{pmatrix} 1 & \frac{1}{2} & \cdots & \frac{1}{2} \\ \frac{1}{2} & 1 & \ddots & \vdots \\ \vdots & \ddots & \ddots & \frac{1}{2} \\ \frac{1}{2} & \cdots & \frac{1}{2} & 1 \end{pmatrix} = \frac{\mu^{-2\nu}}{2} \left( \begin{pmatrix} 1 & \ldots & 0 \\ \vdots & \ddots & \vdots \\ 0 & \vdots & 1 \end{pmatrix} + \begin{pmatrix} 1 & \ldots & 1 \\ \vdots & \ddots & \vdots \\ 1 & \ldots & 1 \end{pmatrix} \right) = \frac{\mu^{-2\nu}}{2} (\mathbf{1} + N\mathbf{P}) \, ,$$

$$\mathbf{P} = \frac{1}{N} \begin{pmatrix} 1 & \ldots & 1 \\ \vdots & \ddots & \vdots \\ 1 & \ldots & 1 \end{pmatrix} \tag{6.15}$$

being the projector onto $(1, 1, \ldots, 1)$. Denoting by dim Im(**P**) the dimension of the space onto which $\mathbf{P}$ projects one has the general formula:

$$\det(\mathbf{1} + a\mathbf{P}) = (1 + a)^{\text{dim Im(}\mathbf{P}\text{)}} \, .$$

Since here dim Im(**P**) $= 1$, we find

$$\det(\mathfrak{D}^{(0)}) = \mu^{-2\nu N} \, \frac{1 + N}{2^N} \, . \tag{6.16}$$

The inverse matrix of $(\mathbf{1} + N\mathbf{P})$ can be inferred from the ansatz

$$(\mathbf{1} + N\mathbf{P})(\mathbf{1} + b\mathbf{P}) = \mathbf{1} \, .$$

Since $\mathbf{P}$ is a projector $\mathbf{P}^2 = \mathbf{P}$ and this implies

$$(N + b + Nb) \, \mathbf{P} = \mathbf{0} \, .$$

Therefore, $b = -N/(N + 1)$ and

$$[\mathfrak{D}^{(0)}]^{-1} = 2 \left( \mathbf{1} - \frac{N}{N + 1} \mathbf{P} \right) \mu^{2\nu} \, . \tag{6.17}$$

To obtain the first order contribution in $(2-D)$ from eq. (6.12) we only need $M = [\mathfrak{D}^{(0)}]^{-1} \mathfrak{D}$, which reads

$$(M_{ij}) = \left( [\mathfrak{D}^{(0)}]^{-1} \mathfrak{D} \right)_{ij} = \left( 2\mathfrak{D}_{ij} - \frac{2}{1 + N} \sum_{k=1}^{N} \mathfrak{D}_{ik} \right) \mu^{2\nu} \, . \tag{6.18}$$

The trace of (6.18) can easily be performed, with the result

$$\mathrm{Tr} M = \left( \frac{2N}{1 + N} \sum_{i=1}^{N} \mathfrak{D}_{ii} - \frac{2}{1 + N} \sum_{i=1}^{N} \sum_{k=1}^{N} (1 - \delta_{ik}) \mathfrak{D}_{ik} \right) \mu^{2\nu} \, . \tag{6.19}$$

In each order of perturbation theory we have to integrate the expression (6.7) over internal distances. These integrals have to be regularized in the infrared through an appropriate IR

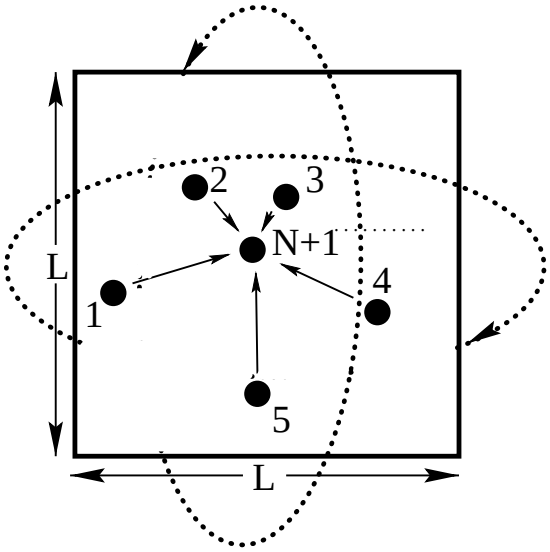


Figure 6.1: Regularization scheme for the $N$-loop diagrams on manifolds with toroidal topology (periodic boundary conditions). Here: $D = 2$

cut-off. In the preceding sections we have cut off the integrals such that all relative distances between internal points were smaller than $L = 1/\mu$. Here, we are considering a finite manifold of toroidal topology. In order to be consistent we need modify the regularization prescription (3.21): Specializing to a squared piece of membrane all components of internal $D$-dimensional vectors $\vec{x}_i$ are running from 0 to $L$. Accordingly, all components of the difference vectors $\vec{x}_i - \vec{x}_{N+1}$, where $\vec{x}_{N+1}$ is a fixed, but arbitrarily chosen point, the root of the subtraction prescription, are bounded by $L$. Implicitly, all other distances are restricted through $L$ as well (see fig. 6.1). Of course, on the torus the correlator has to be modified.

To simplify the calculations, we further introduce the following notation:

$$\overline{f(x_{i_1}, \ldots, x_{i_k})} := \int_{x_1} \cdots \int_{x_N} f(x_{i_1}, \ldots, x_{i_k}) \tag{6.20}$$

with normalization

$$\int_x := \int \mathrm{d}^D x \prod_{j=1}^{D} \theta(x^j < 1) \,, \tag{6.21}$$

which is chosen such that the overbar can be thought of as an averaging procedure, and especially

$$\overline{1} = 1 \tag{6.22}$$

Thanks to our regularization prescription the integral of (6.19) over internal points can be replaced by $\mu^{-ND}$ (for the integration measure $L^{ND}$) times

$$\begin{aligned} \overline{\mathrm{Tr}M} = & \frac{2N^2}{1+N} \, \overline{\mathbb{C}(x_{N+1} - x_i)} \\ & - \left( \frac{2N(N-1)}{1+N} \right) \left( \overline{\mathbb{C}(x_{N+1} - x_i)} - \frac{1}{2} \, \overline{\mathbb{C}(x_i - x_j)} \right) \end{aligned}$$

$$= \frac{2N}{1+N}\,\overline{\mathbb{C}(x_{N+1}-x_i)} + \frac{N(N-1)}{1+N}\,\overline{\mathbb{C}(x_i-x_j)}\;,\;. \tag{6.23}$$

Due to the internal symmetry of closed manifolds the expression above can be further simplified, since

$$\overline{\mathbb{C}(x_{N+1}-x_i)} = \overline{\mathbb{C}(x_i-x_j)} \equiv \overline{\mathbb{C}(x)}\;. \tag{6.24}$$

Introducing a diagrammatic notation


$$:= \overline{\mathbb{C}(x)}\;, \tag{6.25}$$

the $N$-loop integral reads up to first order in $2-D$

$$\int (\det D)^{-d/2} = \mu^{-N\varepsilon}\left(\frac{1+N}{2^N}\right)^{-d/2} \times \left[1 - \frac{d}{2}(2-D)\left(N\;\right.\right.$$

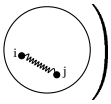


$$\left.\left. + O((2-D)^2)\right]\right. \tag{6.26}$$

For the further analysis we will not only need (6.23), but also the terms appearing to second order in $2-D$ in (6.14). We derived expressions like (6.23) for $\mathrm{Tr}^2 M$ and $\mathrm{Tr}M^2$ with *Mathematica®*. The *Mathematica®*–program will be presented and discussed in the appendix. It is based on the fact that all terms to appear in the expansion (6.14) are of the form $\mathrm{Tr}^n M^m$ or products of the latter and therefore can be written as $\mathrm{P}(N)/(N+1)^k$, where $n, m, k \in \mathbf{N}$ and $\mathrm{P}(N)$ is some polynomial in $N$. It will turn out soon that it is convenient to expand the polynomial $\mathrm{P}(N)$ in terms of the following base:

$$\{1, N, N(N-1), N(N-1)(N-2), \ldots, \prod_{j=0}^{k}(N-j), \ldots\}\;. \tag{6.27}$$

We obtain:

$$\overline{\mathrm{Tr}M^2} = \frac{-2N(N-1) - N(N-1)(N-2)}{1+N}\,\overline{\mathbb{C}(x)}^2 + \frac{2N + 3N(N-1) + N(N-1)(N-2)}{1+N}\,\overline{\mathbb{C}^2(x)}\;, \tag{6.28}$$

and

$$\overline{\mathrm{Tr}^2 M} = \frac{4N(N-1) + N(N-1)(N-2)}{1+N}\,\overline{\mathbb{C}(x)}^2 + \frac{2N}{1+N}\,\overline{\mathbb{C}^2(x)}\;. \tag{6.29}$$

Diagrammatically, the averages can be rewritten as


$$:= \overline{\mathbb{C}(x)}^2\;, \tag{6.30}$$

and


$$:= \overline{\mathbb{C}^2(x)}\;. \tag{6.31}$$

Like in the case of the first order diagram (6.28) and (6.29) are highly simplified as compared to an open manifold. The averages over both any open chain of two propagators like in (6.30)

and any closed loop of two propagators like in (6.31) are independent from the position of the root $x_{N+1}$. Diagrammatically, this symmetry can be written as

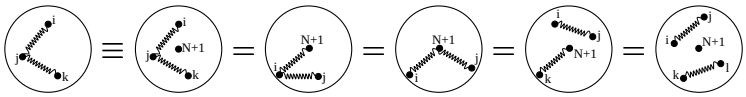

(6.32)

and

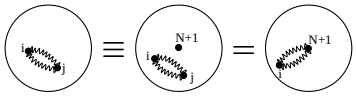

(6.33)

Combining (6.14), (6.23), (6.28) and (6.29) the $N$–loop integral reads up to the second order in $2-D$:

$$\int (\det D)^{-d/2} = \mu^{-N\varepsilon} \left(\frac{1+N}{2^N}\right)^{-d/2} \times \Bigg[1 - \frac{d}{2}(2-D)\left(N \;\; \right)$$

$$+ \frac{d}{4}(2-D)^2 \left(\frac{-2N(N-1) - N(N-1)(N-2)}{1+N} \;\; + \frac{2N + 3N(N-1) + N(N-1)(N-2)}{1+N} \;\; \right)$$

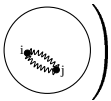

$$+ \frac{d^2}{8}(2-D)^2 \left(\frac{4N(N-1) + N(N-1)(N-2)}{1+N} \;\; + \frac{2N}{1+N} \;\; \right)$$

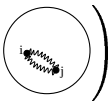

$$+O((2-D)^3)\Bigg] \,. \tag{6.34}$$

Then, we finally obtain for the renormalized coupling $g$ up to the second order in[4] $2-D$:

$$g = g_0 \mu^{-\varepsilon} \left(1 + \sum_{N=1}^{\infty} \frac{(-g_0\, 2^{d/2} \mu^{-\varepsilon})^N}{(N+1)!(1+N)^{d/2}} \left[1 - (2-D)\frac{d}{2}\left(N \;\; \right)\right.\right. +$$

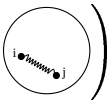

$$+ \frac{d}{4}(2-D)^2 \left(\frac{-2N(N-1) - N(N-1)(N-2)}{1+N} \;\; + \frac{2N + 3N(N-1) + N(N-1)(N-2)}{1+N} \;\; \right)$$

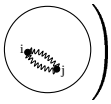

$$+ \frac{d^2}{8}(2-D)^2 \left(\frac{4N(N-1) + N(N-1)(N-2)}{1+N} \;\; + \frac{2N}{1+N} \;\; \right)$$

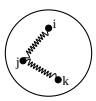

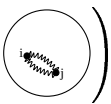

$$\left.\left. +O(2-D)^3\Bigg] \right)\right. \tag{6.35}$$

This can also be written as

$$g 2^{d/2} = -\sum_{N=0}^{\infty} \frac{(-g_0 2^{d/2} \mu^{-\varepsilon})^{N+1}}{N!\,(N+1)^{d/2+1}} + (2-D)\frac{d}{2} \sum_{N=0}^{\infty} \frac{(-g_0 2^{d/2} \mu^{-\varepsilon})^{N+1} N}{N!\,(N+1)^{d/2+1}}$$

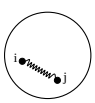

$$-(2-D)^2 \frac{d}{4} \sum_{N=0}^{\infty} \frac{(-g_0 2^{d/2} \mu^{-\varepsilon})^{N+1})(-2N(N-1) - N(N-1)(N-2))}{N!\,(N+1)^{d/2+2}}$$

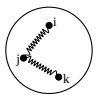

[4]The expression in parenthesis is the inverse renormalization $Z_g$-factor which relates the bare coupling $g_0$ to the renormalized coupling $g$ according to $g Z_g \mu^{\varepsilon} = g_0$.

$$
\begin{aligned}
&-(2-D)^2\frac{d}{4}\sum_{N=0}^{\infty}\frac{(-g_0 2^{d/2}\mu^{-\varepsilon})^{N+1})(2N+3N(N-1)+N(N-1)(N-2))}{N!\,(N+1)^{d/2+2}}\ \text{  }\\
&-(2-D)^2\frac{d^2}{8}\sum_{N=0}^{\infty}\frac{(-g_0 2^{d/2}\mu^{-\varepsilon})^{N+1})(4N(N-1)+N(N-1)(N-2))}{N!\,(N+1)^{d/2+2}}\ \text{  }\\
&-(2-D)^2\frac{d^2}{8}\sum_{N=0}^{\infty}\frac{(-g_0 2^{d/2}\mu^{-\varepsilon})^{N+1})(2N)}{N!\,(N+1)^{d/2+2}}\ \text{  }\qquad+O(2-D)^3
\end{aligned}
\tag{6.36}
$$

Absorbing a factor of $2^{d/2}$ both in $g$ and $g_0$ and defining the dimensionless coupling $z := g_0\mu^{-\varepsilon}$, we obtain the final result

$$
\begin{aligned}
g = {}& z\sum_{N=0}^{\infty}\frac{(-z)^N}{N!\,(N+1)^{d/2+1}}+(2-D)\frac{d}{2}\,z^2\sum_{N=0}^{\infty}\frac{(-z)^N}{N!\,(N+2)^{d/2+1}}\ \text{  }\\
&-(2-D)^2\frac{d}{4}\left(2z^3\sum_{N=0}^{\infty}\frac{(-z)^N}{N!\,(N+3)^{d/2+2}}-z^4\sum_{N=0}^{\infty}\frac{(-z)^N}{N!\,(N+4)^{d/2+2}}\right)\ \text{  }\\
&-(2-D)^2\frac{d}{4}\left(2z^2\sum_{N=0}^{\infty}\frac{(-z)^N}{N!\,(N+2)^{d/2+2}}-3z^3\sum_{N=0}^{\infty}\frac{(-z)^N}{N!\,(N+3)^{d/2+2}}+z^4\sum_{N=0}^{\infty}\frac{(-z)^N}{N!\,(N+4)^{d/2+2}}\right)\ \text{  }\\
&-(2-D)^2\frac{d^2}{8}\left(-4z^3\sum_{N=0}^{\infty}\frac{(-z)^N}{N!\,(N+3)^{d/2+2}}+z^4\sum_{N=0}^{\infty}\frac{(-z)^N}{N!\,(N+4)^{d/2+2}}\right)\ \text{  }\\
&-(2-D)^2\frac{d^2}{8}\left(2z^2\sum_{N=0}^{\infty}\frac{(-z)^N}{N!\,(N+2)^{d/2+2}}\right)\ \text{  }\qquad+O(2-D)^3\,.
\end{aligned}
\tag{6.37}
$$

This formula is the starting point for further analysis in the subsequent sections.

### 6.3 Asymptotic behavior of the series

In the following we are interested in the limit of large $z$ (strong repulsion), which also is the scaling behavior of infinitely large membranes. We therefore need an analytical expression for sums like (6.37) in the limit of large $z$. An example is the leading order expression

$$
g = z\sum_{N=0}^{\infty}\frac{(-z)^N}{N!\,(N+1)^{d/2+1}}\,. \tag{6.38}
$$

For the following analysis we need an integral representation of the above series. We claim that for all $k, d > 0$

$$
\sum_{N=0}^{\infty}\frac{(-z)^N}{N!(k+N)^{d/2}} = \frac{1}{\Gamma(\frac{d}{2})}\int_0^{\infty}\mathrm{d}r\; r^{d/2-1}\exp[-z\,\mathrm{e}^{-r}-kr]\,. \tag{6.39}
$$

This can be proven as follows:

$$
\begin{aligned}
\frac{1}{\Gamma(\frac{d}{2})}\int_0^{\infty}\mathrm{d}r\; r^{d/2-1}\exp[-z\,\mathrm{e}^{-r}-kr] &= \frac{1}{\Gamma(\frac{d}{2})}\sum_{N=0}^{\infty}\frac{(-z)^N}{N!}\int_0^{\infty}\mathrm{d}r\; r^{d/2-1}\mathrm{e}^{-(N+k)r}\\
&= \frac{1}{\Gamma(\frac{d}{2})}\sum_{N=0}^{\infty}\frac{(-z)^N}{N!}\frac{\Gamma(\frac{d}{2})}{(N+k)^{d/2}}\,.
\end{aligned}
$$

This integral-representation is not the most practical for our purpose. It is better to set $r \to s := \mathrm{e}^{-r}$ which yields

$$\sum_{N=0}^{\infty} \frac{(-z)^N}{N!(k+N)^{d/2}} = \frac{1}{\Gamma(\frac{d}{2})} \int_0^1 \mathrm{d}s\, s^{k-1} (-\ln s)^{d/2-1} \mathrm{e}^{-sz} \,. \tag{6.40}$$

This formula is already very useful for some purposes. It is still advantageous to make a second variable-transformation $s \to y := sz$, yielding

$$\sum_{N=0}^{\infty} \frac{(-z)^N}{N!(k+N)^{d/2}} = \frac{(\ln z)^{d/2-1}}{\Gamma(\frac{d}{2}) z^k} \int_0^z \mathrm{d}y\, y^{k-1} \left(1 - \frac{\ln y}{\ln z}\right)^{d/2-1} \mathrm{e}^{-y} \,. \tag{6.41}$$

Finally we remark that we usually have the following combination

$$f_k^d(z) := z^k \sum_{N=0}^{\infty} \frac{(-z)^N}{N!(k+N)^{d/2}} = \frac{(\ln z)^{d/2-1}}{\Gamma(\frac{d}{2})} \int_0^z \mathrm{d}y\, y^{k-1} \left(1 - \frac{\ln y}{\ln z}\right)^{d/2-1} \mathrm{e}^{-y} \,. \tag{6.42}$$

It satisfies the following simple recursion relation, which is helpful to calculate the $\beta$-function:

$$z \frac{\mathrm{d}}{\mathrm{d}z} f_k^d(z) = f_k^{d-2}(z) \,. \tag{6.43}$$

The derivative above can also be rewritten as

$$z \frac{\mathrm{d}}{\mathrm{d}z} f_k^d(z) = k f_k^d(z) - f_{k+1}^d(z) \,, \tag{6.44}$$

such that one obtains a useful formula in order to isolate the dominant behavior for large $z$:

$$f_{k+1}^d(z) = k f_k^d(z) - f_k^{d-2}(z) \tag{6.45}$$

From (6.39) $f_k(z) > 0$ for all $k, d > 0$ and the behavior for large $z$ is obtained by expanding $\left(1 - \frac{\ln y}{\ln z}\right)^{d/2-1}$ for small $\frac{1}{\ln z}$

$$\begin{aligned} f_k^d(z) = \frac{(\ln z)^{d/2-1}}{\Gamma(\frac{d}{2})} \Bigg[ & \int_0^\infty \mathrm{d}y\, y^{k-1} \mathrm{e}^{-y} \\ & - \frac{1}{\ln z} \left(\frac{d}{2} - 1\right) \int_0^\infty \mathrm{d}y\, y^{k-1} \ln y\, \mathrm{e}^{-y} \\ & + O\left(\frac{1}{(\ln z)^2}\right) \Bigg] \\ + O(\mathrm{e}^{-z}) \qquad & . \end{aligned} \tag{6.46}$$

The result is

$$f_k^d(z) = \frac{(\ln z)^{d/2-1} \Gamma(k)}{\Gamma(\frac{d}{2})} \left(1 - \frac{1}{\ln z} \frac{d-2}{2} \frac{\Gamma'(k)}{\Gamma(k)} + \dots\right) \,. \tag{6.47}$$

For later reference, we note a list of useful formulas ($\gamma = 0.577216\ldots$ is the Euler-constant)

$$f_1^d(z) = \frac{(\ln z)^{d/2-1}}{\Gamma(\frac{d}{2})} + \frac{\gamma(\ln z)^{d/2-2}}{\Gamma(\frac{d-2}{2})} + \frac{(6\gamma^2+\pi^2)(\ln z)^{d/2-3}}{12\Gamma(\frac{d-4}{2})} + \ldots \tag{6.48}$$

$$f_2^d(z) = \frac{(\ln z)^{d/2-1}}{\Gamma(\frac{d}{2})} + \frac{(\gamma-1)(\ln z)^{d/2-2}}{\Gamma(\frac{d-2}{2})} + \frac{(6\gamma(\gamma-2)+\pi^2)(\ln z)^{d/2-3}}{12\Gamma(\frac{d-4}{2})} + \ldots \tag{6.49}$$

$$f_3^d(z) = \frac{2(\ln z)^{d/2-1}}{\Gamma(\frac{d}{2})} + \frac{(2\gamma-3)(\ln z)^{d/2-2}}{\Gamma(\frac{d-2}{2})} + \frac{(6\gamma^2-18\gamma+6+\pi^2)(\ln z)^{d/2-3}}{6\Gamma(\frac{d-4}{2})} + \ldots . \tag{6.50}$$

Note that with the above notations, the relation (6.37) expressing $g$ as a function of $z$ becomes

$$\begin{aligned} g(z) = {} & f_1^{d+2}(z) + (2-D)\frac{d}{2} f_2^{d+2}(z) \quad \text{(i–j)} \\ & -(2-D)^2\frac{d}{4}\left[\left(2f_3^{d+4}(z) - f_4^{d+4}(z)\right) \text{(i–j, j–k)} + \left(2f_2^{d+4}(z) - 3f_3^{d+4}(z)\right) \text{(i–j)}\right] \\ & -(2-D)\frac{d^2}{8}\left[\left(-4f_3^{d+4}(z) + f_4^{d+4}(z)\right) \text{(i–j, j–k)} + \left(2f_2^{d+4}(z)\right) \text{(i–j)}\right] \quad + O(2-D)^3 . \end{aligned} \tag{6.51}$$

Making several times use of the relation (6.45), which can be rationalized with the help of an algebraic manipulation program (see *Mathematica*®–program in the appendix), the last equation can be cast into a form, that makes the leading behavior for large $z$ obvious at each order of the expansion in $2-D$. Let us return to the notation of (6.24) and let us define a "connected" correlation function $\mathbb{C}_c(x)$ as

$$\mathbb{C}_c(x) := \mathbb{C}(x) - \overline{\mathbb{C}(x)} . \tag{6.52}$$

Skipping the argument of the correlation function to be averaged, the notation simplifies to

$$\overline{\mathbb{C}(x)} \equiv \overline{\mathbb{C}} \qquad \text{a.s.f.,} \tag{6.53}$$

and we have

$$\overline{\mathbb{C}_c^2} = \overline{\mathbb{C}^2 - 2\overline{\mathbb{C}}\mathbb{C} + \overline{\mathbb{C}}^2} = \overline{\mathbb{C}^2} - \overline{\mathbb{C}}^2 , \tag{6.54}$$

such that (6.51) becomes

$$\begin{aligned} g(z) = {} & f_1^{d+2}(z) + (2-D)\frac{d}{2}\overline{\mathbb{C}}\, f_2^{d+2}(z) \\ & -(2-D)^2\frac{d}{4}\left[2\overline{\mathbb{C}_c^2}\, f_1^{d+4}(z) + (\overline{\mathbb{C}}^2 - 4\overline{\mathbb{C}_c^2})\, f_1^{d+2}(z) + (2\overline{\mathbb{C}_c^2} - \overline{\mathbb{C}}^2)\, f_1^{d}(z) - \overline{\mathbb{C}_c^2}\, f_1^{d-2}(z)\right] \\ & -(2-D)^2\frac{d^2}{8}\left[2\overline{\mathbb{C}_c^2}\, f_1^{d+4}(z) - (2\overline{\mathbb{C}_c^2} + \overline{\mathbb{C}}^2)\, f_1^{d+2}(z) + 2\overline{\mathbb{C}}^2\, f_1^{d}(z) - \overline{\mathbb{C}}^2\, f_1^{d-2}(z)\right] \\ & + O(2-D)^3 . \end{aligned} \tag{6.55}$$

Note, that the leading behavior for large values of $z$ has been absorbed into the terms ahead, respectively. That is, at second order in $2-D$, the leading behavior is isolated in $f_1^{d+4}(z)$. In (6.55) it turns out that the diagrams to be calculated are $\overline{\mathbb{C}}$ and $\overline{\mathbb{C}_c^2}$. On the torus this corresponds to the evaluation of two discrete sums as will be reported in the appendix. We find:

$$\overline{\mathbb{C}} = S_D \sum_{k\neq 0} \frac{1}{\vec{k}^2} - \frac{1}{2\pi(2-D)} = -1.4967(6) + S_D \cdot 0.3422(1)(2-D) \; + \; O(2-D)^2 \quad (6.56)$$

and

$$\overline{\mathbb{C}_c^2} = S_D^2 \sum_{k\neq 0} \frac{1}{\vec{k}^4} = 0.043(1) \; + \; O(2-D)\,. \quad (6.57)$$

$\vec{k}$ is $D$-dimensional with components $k_i = 2\pi/L\; n_i$, and the indices $n_i$ are running from $-\infty$ to $\infty$, $n_i = 0$ being excluded from the summation.

In the next two sections we shall present two formalisms which give results for $\omega$ at second order. It will turn out that the results catch qualitatively correctly the cross-over to $D = 1$; however they differ in the numerical values. This problem has already been reported in [49], where the same procedure has been applied to open manifolds. There, we suspected this to be a reflection of the fact that the $(2-D)$-expansion were not systematic due to an inconsistent regularization prescription. Now working with closed manifolds of finite size, regularization problems do not arise. Although the expansion on a torus considerably simplifies at second order as compared to an open manifold ((6.32), (6.33)), however there remain series problems with these schemes. They can be attributed to the fact that at second and higher order in $2-D$ the $\beta$–function does not show up a finite limit for $z \to \infty$, as it should at the fixed point ($\lim_{z\to\infty} \beta(z) = 0$). This problem, however, is no surprise. We expect the $\beta$-function to decay for large values of $z$ up to some scaling function like a powerlaw:

$$\beta(z) \sim z^{-\omega/\varepsilon}\,. \quad (6.58)$$

The dominant exponent containing the correction-to-scaling exponent $\omega$ will have some expansion in $2-D$. Therefore, an expansion of the $\beta$-function in powers of $2-D$ will provide some alternating series involving at each order powers of logarithms of $z$. Since the expansion of $\beta(z)$ is alternating in $2-D$ as we consider the leading behavior, there arises a zero at some finite $\ln z^* \sim (2-D)^{-2}$. The scheme to be presented first is trying to circumvent the problem of a diverging (truncated) $\beta$–function by treating the zero as a fixed point. Within the second scheme to be presented thereafter, we first invert the series for the renormalized coupling providing the bare coupling as a function of the latter. This also allows for expressing the $\beta$-function in terms of the renormalized coupling.
Unfortunately, it turns out that within the $2-D$–expansion both schemes do not provide a systematic way to gain information about the correction-to-scaling exponent $\omega$ at the fixed point.

## 6.4 The RG-functions in the bare coupling

The renormalization group $\beta$-function is defined as

$$\beta(g) := \mu \frac{\mathrm{d}}{\mathrm{d}\mu}\bigg|_0 g\,. \quad (6.59)$$

Since it is hard to invert the function $g(z)$, it is advantageous to study $\beta$ as function of the bare coupling $z$

$$\beta(g) \equiv \beta(z) = -\varepsilon z \frac{\mathrm{d}}{\mathrm{d}z} g \,. \tag{6.60}$$

Taking to each order only those terms into account, which carry the dominant behavior for large values of $z$, up to second order in $2-D$, we find from (6.51) using (6.43)

$$\beta(z) = -\varepsilon \left[ f_1^d(z) + (2-D)\frac{d}{2}\,\overline{\mathbb{C}}\, f_2^d(z) - (2-D)^2 \frac{d}{2}\left(1+\frac{d}{2}\right)\,\overline{\mathbb{C}_c^2}\, f_1^{d+2} + \ldots \right] . \tag{6.61}$$

Inserting the asymptotic expansions from the last section, this becomes

$$\beta(z) = -\frac{\varepsilon}{\Gamma(\frac{d}{2})} \left[ (\ln z)^{d/2-1} \left(1 + (2-D)\frac{d}{2}\,\overline{\mathbb{C}}\right) - (2-D)^2 \left(1+\frac{d}{2}\right)\,\overline{\mathbb{C}_c^2}\,(\ln z)^{d/2} + \ldots \right] , \tag{6.62}$$

where omitted terms have either one more power of $(2-D)$ or $1/\ln z$. As shown in section 2, universal properties are given by the correction to scaling exponent $\omega$, reading

$$\omega(z) := \frac{\mathrm{d}\beta(g)}{\mathrm{d}g} = \frac{\mathrm{d}\beta(z)}{\mathrm{d}z}\frac{1}{\frac{\mathrm{d}g}{\mathrm{d}z}} = -\frac{\varepsilon z}{\beta(z)}\frac{\mathrm{d}\beta(z)}{\mathrm{d}z} \,. \tag{6.63}$$

Let us first study $D = 2$. $\beta(z)$ and $\omega(z)$ are plotted on figure 6.2. We see that for $d < 2$ the $\beta$-function becomes 0 for $z \to \infty$. For $d > 2$, $\beta(z)$ has no zero, but the flow of $g$ is still to infinity. In both cases $\omega$ is given by $\omega = \lim_{z\to\infty} \omega(z)$. Taking only the leading term in the $(2-D)$-expansion of $\beta(z)$, $\omega(z)$ is given by

$$\omega(z) = -\varepsilon \frac{z\frac{\mathrm{d}}{\mathrm{d}z} f_1^d(z)}{f_1^d(z)} \to \frac{d-2}{2\ln z} \to 0 \,. \tag{6.64}$$

From (6.62) it is clear, that to first order in $2-D$ we do not obtain any correction to the above result. So, let us also take into account the second order in $2-D$. Then the "fixed point" (a zero) for small enough $2-D$ of (6.62) is at the finite value

$$\ln z^* = \overline{\mathbb{C}_c^2}\,\frac{2}{2+d}\,\frac{1}{(2-D)^2} + \cdots \,. \tag{6.65}$$

Next, when trying to calculate $\omega(z)$, we face the following problem: Since we truncated the series for $g$ at order two in $2-D$, $\beta'(z)$ does not vanish at the fixed point, i.e. the zero of $\beta(z)$. This might lead to the conclusion that $\omega(z^*)$ is always $\infty$, an absurd result. However since this is a consequence of the truncation of the series, we follow the strategy also to expand the denominator of $\omega(z)$ in powers of $2-D$. From (6.61) and (6.63) we obtain:

$$\begin{aligned} \omega(z) = -\varepsilon \Bigg[ \frac{f_1^{d-2}(z)}{f_1^d(z)} &- (2-D)^2 \frac{d}{2}\left(1+\frac{d}{2}\right)\,\overline{\mathbb{C}_c^2}\,\frac{f_1^d(z)}{f_1^d(z)} \\ &+ (2-D)^2 \frac{d}{2}\left(1+\frac{d}{2}\right)\,\overline{\mathbb{C}_c^2}\,\frac{f_1^{d+2}(z) f_1^{d-2}(z)}{(f_1^d(z))^2} + \cdots \Bigg] . \end{aligned} \tag{6.66}$$

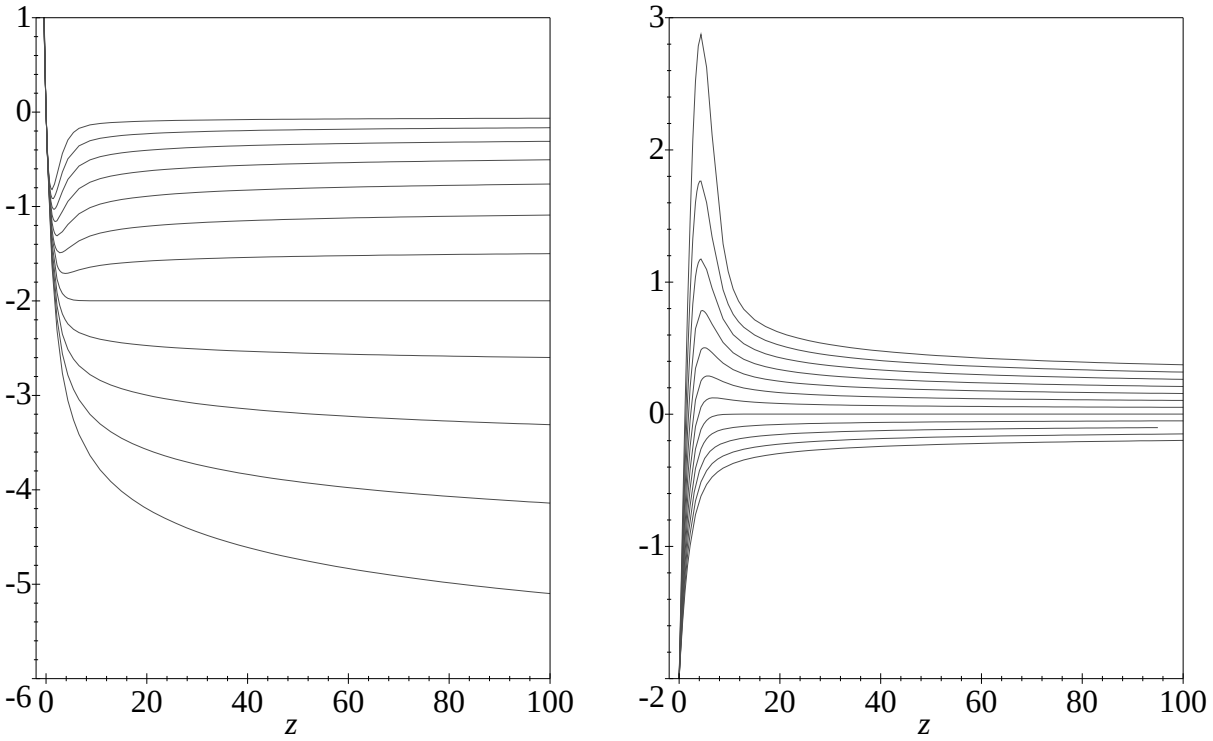


Figure 6.2: $\beta$-function (left) and $\omega$ (right) as functions of the dimensionless bare coupling $z$ for different dimensions $d$: $d = 0.25,\ 0.5,\ 0.75, \ldots,\ 3$ (from top to bottom, respectively). Note, that $\beta$ always has a fixed point at $z{=}0$ with $\omega(0){=}-\varepsilon$. Furthermore, there is a fixed point for $0{<}d{<}2$ at $z{=}\infty$ with $\omega(\infty){=}0$, the latter remaining true for $d{\geq}2$. In $d{=}2$ $\beta$ tends to $-\varepsilon$ as $z \to \infty$. Above, $\beta$ diverges.

Inserting the asymptotic series we find

$$\omega(z) = -\varepsilon \left[ \frac{d-2}{2} \frac{1}{\ln z} - (2-D)^2 \frac{d}{2} \left(1{+}\frac{d}{2}\right) \overline{\mathbb{C}_c^2} + (2-D)^2 \frac{d}{2} \left(1+\frac{d}{2}\right) \overline{\mathbb{C}_c^2} \, \frac{d-2}{d} + \cdots \right] . \tag{6.67}$$

Inserting the fixed point (6.65), we arrive at

$$\omega(z^*) = \varepsilon \left[ 2 + \frac{d}{2} - \frac{d^2}{4} \right] \overline{\mathbb{C}_c^2} \, (2-D)^2 \, . \tag{6.68}$$

This should be checked against the exact result in $D = 1$, which reads

$$\omega(D{=}1) = \varepsilon \, . \tag{6.69}$$

Due to the smallness of $\overline{\mathbb{C}_c^2}$ our resummation-procedure thus only reproduces qualitatively the behavior for finite $2 - D$.

Let us point out that the limit $D = 2$ has been analyzed in a completely consistent way within this scheme. Setting $D = 2$ in (6.67) the correction-to-scaling exponent is obtained from the limit $z \to \infty$ in (6.64). Therefore, we always find $\omega = 0$ (independently from $d > 0$) in $D = 2$. On the other hand, starting from an ansatz like (6.58) and expanding it in powers of $2 - D$, the lowest order coefficient of $\omega/\varepsilon$ is obtained from the constant lowest order term in $2 - D$ in the corresponding equation to (6.67). However, the ansatz (6.58) is oversimplified as will be discussed in section 7. In particular it does not cover the limit $D = 2$. Before further discussing the validity of the procedure, let us turn to the second scheme, namely the calculation in the renormalized coupling.

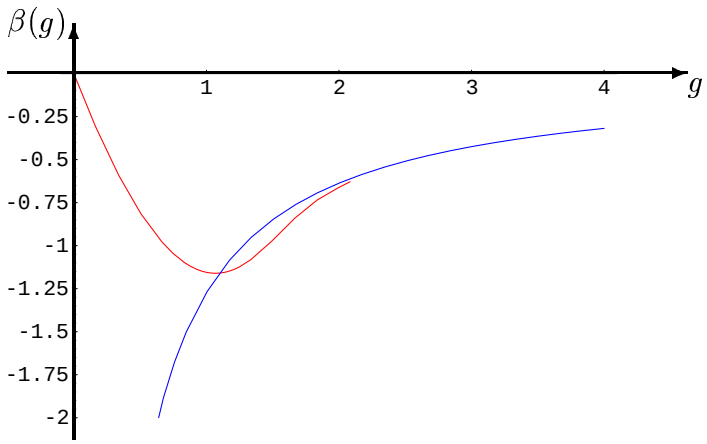


Figure 6.3: $\beta-$function in terms of the renormalized coupling $g$ truncated at order 160, Pade-resummed, and plotting only that part for which the truncated series converges. (This can e.g. be tested by taking away the last few terms of the series.) This is compared to the asymptotic behavior (6.72) (proportional to $1/g$ for large $g$). $d$ is set to 1, and we used the diagonal (80,80)-Pade approximant, which was find to converge best. (The non-resummed expression starts to diverge already at $g \approx 1.8$ at this order.)

## 6.5 Calculation in the renormalized coupling

We start from $g(z)$ given in (6.55). Taking to each order in $2-D$ only the dominant term for large $z$ into account this can be approximated by

$$g(z) = \frac{(\ln z)^{d/2}}{\Gamma(\frac{d}{2}+1)} \left[ 1 + (2-D)\frac{d}{2}\,\overline{\mathbb{C}} - (2-D)^2 \frac{d}{2}\,\overline{\mathbb{C}_c^2}\,\ln z \right] . \tag{6.70}$$

Using (6.70), we can write $\ln z$ as a function of $g$. To second order in $2-D$, this reads

$$\ln z = \tilde{g}^{2/d} \left( 1 - (2-D)\overline{\mathbb{C}} + (2-D)^2 \frac{d}{2}\overline{\mathbb{C}}^2 \right) + \tilde{g}^{4/d}(2-D)^2\,\overline{\mathbb{C}_c^2}\,,$$
$$\tilde{g} := g\,\Gamma(\tfrac{d}{2}+1)\,. \tag{6.71}$$

We now write the $\beta$-function in terms of $\tilde{g}$. Starting from (6.62) we obtain

$$\beta(\tilde{g}) = -\frac{\varepsilon}{\Gamma(\frac{d}{2})} \left[ \tilde{g}^{1-2/d} \left( 1 + (2-D)\,\overline{\mathbb{C}} + (2-D)^2\,\overline{\mathbb{C}}^2\,\frac{(d-4)(d-2)}{8} \right) - (2-D)^2\,2\overline{\mathbb{C}_c^2}\,\tilde{g} \right] . \tag{6.72}$$

Fixed points are at the zeros of the $\beta$-function. The non-trivial one is at

$$\tilde{g}^{*-2/d} = (2-D)^2\,2\overline{\mathbb{C}_c^2} + \cdots\,. \tag{6.73}$$

The correction to scaling exponent $\omega$ is simply obtained by evaluating the derivative of $\beta$ with respect to $g$ at the fixed point. In terms of $\tilde{g}$ this is

$$\omega(\tilde{g}) = \frac{\mathrm{d}\beta(g)}{\mathrm{d}g} = \frac{\mathrm{d}\beta(\tilde{g})}{\mathrm{d}\tilde{g}}\frac{\mathrm{d}\tilde{g}}{\mathrm{d}g} = \Gamma(\tfrac{d}{2}+1)\,\frac{\mathrm{d}\beta(\tilde{g})}{\mathrm{d}\tilde{g}}$$
$$= -\varepsilon\frac{\Gamma(\frac{d}{2}+1)}{\Gamma(\frac{d}{2})} \left[ \left(1-\frac{2}{d}\right) \tilde{g}^{-2/d} \left( 1 + (2-D)\,\overline{\mathbb{C}} + (2-D)^2\,\overline{\mathbb{C}}^2\,\frac{(d-4)(d-2)}{8} \right) - (2-D)^2\,2\overline{\mathbb{C}_c^2} \right] . \tag{6.74}$$

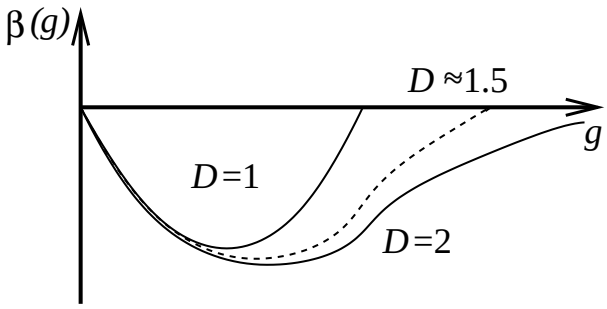


Figure 6.4: Qualitative behavior for the $\beta$-function in $D = 1$, $D = 2$ and result anticipated for $D \approx 1.5$.

Inserting the fixed point $\tilde{g}^*$ from (6.73) we find

$$\omega(\tilde{g}^*) = \varepsilon \; 2\overline{\mathbb{C}_c^2} \; (2 - D)^2 \; . \tag{6.75}$$

Again, this is only qualitatively correct as compared to the exact result $\omega(D{=}1) = \varepsilon$ in $D = 1$, and coincides with the result obtained from the previous scheme only in $d = 0$ and $d = 2$.
There is a series problem that has to be mentioned and that applies to the "bare scheme" from the previous subsection as well as to the calculation in renormalized coupling: In the "bare scheme" $\omega(z)$ is evaluated at the fixed point $\ln z^* \sim (2 - D)^{-2}$. However, each higher order power in $\ln z$ in (6.67) is coming up only with an extra power in $2 - D$, therefore providing arbitrarily diverging contributions in $2 - D$. The same applies to the second scheme, where $\omega(g)$ has an expansion in powers of $(2{-}D)g^{2/d}$ and the fixed point lies at $g^{*-2/d} \sim (2 - D)^2$.

Let us finally point out that in the limit $D = 2$ the true asymptotic behavior of the $\beta-$function in terms of the renormalized coupling $g$ is obtained from the completely summed series (6.38) leading to (6.72) for large $g$. Conversely, if one tries to invert (6.38) and truncates it taking only a finite number of orders into account, it is at least possible to reach the asymptotic regime – however, for large enough $g$ the truncated $\beta-$function wildly oscillates and thus strongly deviates from the true behavior. In figure (6.3) the Pade-resummed truncated $\beta-$function up to order $g^{160}$ in $d = 1$ is compared with the exact, asymptotic flow-function. One notices that the truncated $\beta$-function even though improved through a Pade-Resummation hardly gets into touch with the asymptotic regime. The same applies to the slope-function $\omega(g)$, which is not shown in fig. (6.3).

Note that the above arguments suggest quite intuitively the behavior of the exact $\beta$-function in $1 < D < 2$. Whereas for $D = 1$, the $\beta$-function is a parabola, and for $D = 2$ it decays like a power-law for large $g$ at least as long as $d < 2$, the $\beta$-function for values of $D$ between these two extremes should cut the axes $\beta(g) = 0$ at a finite value of $g$, which for $D \to 2$ wanders off to infinity, thus by continuity forcing the exponent $\omega$ to go to 0 for $D \to 2$.

## 6.6 The limit $d = 0$

Let us shortly consider the limit of vanishing bulk space dimension $d$, which is completely solvable for arbitrary internal dimensions $D$. However, the strong coupling limit of $g(z)$ is not analytic around $d = 0$. Starting from (6.38) and setting $d = 0$ one almost immediately obtains:

$$g(z) = 1 - \mathrm{e}^{-z} \; , \tag{6.76}$$

which can be inverted providing the bare coupling in terms of the renormalized coupling as

$$z = \ln(1-g)^{-1} \,. \tag{6.77}$$

Recalling the definition of the $\beta-$function (2.12) we find:

$$\beta(g) = \varepsilon(1-g)\ln(1-g) \tag{6.78}$$

with fixed points at

$$g^* = 0 \qquad \vee \qquad g^* = 1 \,. \tag{6.79}$$

Then, the correction-to-scaling exponent $\omega$ as well can be evaluated in terms of the renormalized coupling as

$$\omega(g) = \left.\frac{\mathrm{d}\beta(g)}{\mathrm{d}g}\right|_{g^*} = -\varepsilon \left.\left(1+\ln(1-g)\right)\right|_{g^*} \,, \tag{6.80}$$

such that one finds

$$\omega(g^*{=}0) = -\varepsilon \qquad \text{and} \qquad \omega(g^*{=}1) = +\infty \,. \tag{6.81}$$

Note that (6.76) is obtained from the leading order contribution in (6.55). All other terms do not contribute. The same result is found from the exact solution of the limit $D = 1$ setting $d = 0$ as is shown in the appendix (D.27).

## 6.7 Laplace-transformed picture

Let us finally point out that the correction to scaling exponent $\omega$ found at leading order remains unchanged in the Laplace-transformed picture introduced in section 5, that is we sum over all membrane-sizes weighted by a chemical potential $\tau$. The sum can easily be done, leading to an additional factor of $\Gamma(1+\frac{N\varepsilon}{D})$, which is $N!$ in the limit of $D \to 2$. (6.37) then has to be replaced by

$$g \;=\; -\sum_{N=1}^{\infty} \frac{(-z)^N}{N^{d/2}} \,, \tag{6.82}$$

which is a special function called polylogarithmic function

$$g \;=\; -\mathrm{Li}_{\frac{d}{2}}(-z) \,, \tag{6.83}$$

and accordingly from (6.60) the RG $\beta$-function reads

$$\beta(z) \;=\; \varepsilon \cdot \mathrm{Li}_{\frac{d}{2}-1}(-z) \tag{6.84}$$

while the correction to scaling exponent becomes (6.63)

$$\omega(z) \;=\; -\varepsilon \frac{\mathrm{Li}_{\frac{d-4}{2}}(-z)}{\mathrm{Li}_{\frac{d-2}{2}}(-z)} \,. \tag{6.85}$$

Indeed, we find the same fixed point behavior as before and $\lim_{z\to\infty}\omega(z) = 0$ for arbitrary $d{>}0$. This follows from the logarithmic divergence of $g(z)$ in the limit of strong coupling.

### 6.8 Discussion of the analytical continuation to $D = 2$.

Before we go on with the analysis of the expansion in powers of $2 - D$ let us discuss the analytical continuation to $D = 2$ in more detail. In particular we would like to discuss the proper treatment of the factor $(2 - D)^{d/2}$, which becomes singular in $D = 2$ and which appears to the $N$th power in the $N$th loop integral in the perturbation expansion of the effective coupling $g(z)$. It is due to the form of the two-point difference correlator, which reads in dimensions $0 < D < 2$:

$$C(x - y) := \frac{1}{2d} \left\langle |\vec{r}(\vec{x}) - \vec{r}(\vec{y})|^2 \right\rangle_{\mathcal{H}_0} = \frac{|x - y|^{2-D}}{(2 - D)S_D} , \tag{6.86}$$

where $S_D$ denotes the $D$-dimensional volume of the unitsphere.
Let us recall the expression for the perturbation series for the effective coupling in powers of the scaling variable $z := g_0 L^\varepsilon$:

$$g(z) = z \sum_{N=0}^{\infty} \frac{(-z)^N}{(N+1)!} \int_{x_1} \cdots \int_{x_N} (\det D_{ij})^{-d/2} , \tag{6.87}$$

where the internal linear size of the manifold has been scaled out of the integrations, which are left with the measure (6.21) on the torus. The quadratic form $D_{ij}$ is

$$D_{ij} = \frac{1}{2} \left[ C(x_{N+1} - x_i) + C(x_{N+1} - x_j) - C(x_i - x_j) \right] . \tag{6.88}$$

The arising of $N$ powers of $(2 - D)^{d/2}$ in the $N$th loop order is then clear.
Let us show how this factor can be absorbed into a rescaling of the bare coupling $z$. Substituting $r' = r(S_D(2 - D))^{1/2}$ in the functional integration, the free part of the Hamiltonian (2.6) gets a prefactor $(S_D(2 - D))^{-1}$ and, accordingly, the bare coupling is replaced with

$$z \to z(S_D(2 - D))^{d/2} \tag{6.89}$$

in order to leave the physics invariant. Then, the two-point function in the rescaled variables reads

$$C(x - y) = |x - y|^{2-D} . \tag{6.90}$$

Expressing the perturbation series (6.87) still in powers of the old coupling one has:

$$g(z) = (S_D(2-D))^{-d/2} \left( z(S_D(2-D))^{d/2} \sum_{N=0}^{\infty} \frac{(-z(S_D(2-D))^{d/2})^N}{(N+1)!} \int_{x_1} \cdots \int_{x_N} (\det D_{ij})^{-d/2} \right) \tag{6.91}$$

where, thanks to (6.90) the remaining integrand, $(\det D_{ij})^{-d/2}$, now has an expansion in powers of $2 - D$ as we discussed in the preceding subsections. The overall factor $(S_D(2-D))^{-d/2}$ is contributed from the Jacobian in the integration over the position of the center of mass. Actually, as compared to (6.87) in (6.91) nothing has changed. Summing up all loops at each order in $2 - D$ of the integrand, we arrive at (6.55):

$$(S_D(2-D))^{d/2} g(z) = f_1^{d+2}(z(S_D(2-D))^{d/2}) + (2-D)\frac{d}{2}\overline{\mathbb{C}}\, f_2^{d+2}(z(S_D(2-D))^{d/2}) + \dots . \tag{6.92}$$

Let us consider a reference membrane of linear internal size $L$ in $D = 2$: The expansion of the (dimensionfull) effective coupling of a manifold of linear internal size $L/(S_D(2-D))^{d/(2\varepsilon)}$ in $D < 2$ then reads:

$$L^{\varepsilon} g(z) = L^{\varepsilon}(f_1^{d+2}(z) + (2-D)\frac{d}{2}\overline{\mathbb{C}}\, f_2^{d+2}(z) + O(2-D)^2) \;, \tag{6.93}$$

where the singular scaling factor $(S_D(2-D))^{d/(2\varepsilon)}$ has canceled out.
In the limit $D = 2$ we are left with

$$g(z) = f_1^{d+2}(z) \;. \tag{6.94}$$

It is important to point out that performing the limit $D \to 2$ in this way corresponds to studying the scaling limit $a/L \ll 1$, where $a$ denotes a microscopic cutoff. Therefore, in addition to (6.94) we expect corrections to scaling for small membrane sizes. Equivalently, our statement is that after summing up the complete perturbation series in the limit $D = 2$ calculating each diagram with an explicit ultraviolet cutoff $a$ and the exact two point function, then, the long-distance behavior is expected to be independent from the cutoff $a$ in the scaling limit $a/L \ll 1$. It will coincide with the behavior that we obtained from the resummed, analytically continued diagrams after having sent $a$ to zero.
Let us finally emphasize that there is no alternative to forcing the membrane size to $\infty$ when approaching the limit $D = 2$. This is in contrast to what is done in the rescaling procedures in (3.3) and (6.1), which imply an infinite bare coupling $g_0$ in the limit $D = 2$. As discussed above the rescaling of the field contributes a Jacobian in the perturbation series of $g(z)$ from the integration over the position of the center of mass and can be only eliminated by forcing the size to $\infty$. The Jacobian has been dropped in the preceding sections, which is completely safe as long as one is only interested in the exponent $\omega$.
There is a simple way to anticipate the divergence of the fixed point in the limit $D \to 2$ and to justify that the analytical continuation of the exponent $\omega$ to $D = 2$ must become zero as we found it: The $\beta$-function at two loops reads (4.21)

$$\beta(g) = -\varepsilon g + \frac{g^2}{2} I_1(D) - \frac{g^3}{3} I_2(D) + O(g^4) \;, \tag{6.95}$$

where in contrast to (4.21) we have not made the value of the one loop integral, $I_1(D)$, explicit. Within the $\varepsilon$-expansion one finds a nontrivial fixed point at $g^*$ (4.23):

$$g^* = \frac{2\varepsilon}{I_1(D)} + \frac{8}{3}\frac{I_2(D)}{I_1^3(D)}\varepsilon^2 + O(\varepsilon^3) \;. \tag{6.96}$$

As we already discussed above each loop integral $I_N$ is coming up with $N$ powers of $(2-D)^{d/2}$, as long as we do not perform the rescaling procedure, such that the shift to infinity in the limit $D = 2$ of the fixed point $g^*$ can already be anticipated from (6.96). However calculating the correction -to-scaling exponent $\omega$, the $\varepsilon$-expansion reads (4.24):

$$\omega(g^*) = \varepsilon - \frac{4}{3}\frac{I_2(D)}{I_1^2(D)}\varepsilon^2 + O(\varepsilon^3) \;. \tag{6.97}$$

It turns out that all loop integrals appear only in a form, where they are normed with respect to the one loop integral. This way any singular factor from the one loop integral drops out. The reasoning above is not restricted to the $\varepsilon$-expansion. Even more, it has turned out that only within the calculations in fixed dimensions $(D, d)$ the remaining combinations $I_2(D)/I_1^2(D)$ have smooth expansions in $2 - D$, from what we may conclude that as long as one is interested in the analytical continuation of the exponent $\omega$ to $D = 2$ it is completely justified to norm all loop integrals with respect to the one loop integral. This is what the rescaling procedure does.

# 7 Higher order terms in the $(2-D)$- expansion on the torus

In this section we will render the analysis of the strong coupling behavior of the theory in $D$ slightly below 2 more systematic. For this purpose we will carry out the expansion in powers of $2-D$ up to the fourth order. This will allow for an insight into the general structure of the $2-D$-expansion. Next, we will give two different ansätze for the exact renormalized coupling $g(D,z)$ as a function of the internal dimension $D$ and show, how their free parameters get matched with the obtained expansion in $2-D$.
From the second order on, it is quite a tedious work to collect all terms to appear in the expansion. We accomplished this with the help of a *Mathematica*®-program, which we discuss in the appendix. However, we have only calculated the diagrams to appear up to the second order. To get an idea of the general form of the expansion we also needed the resummed terms to the third and fourth order, even if we do not have the explicit values of the corresponding diagrams available. Of course, our main purpose is to get information about the strong coupling behavior for finite $2-D$ close to zero.
First, let us list the diagrams to appear up to the fourth order:


$$= \overline{\mathbb{C}(x_i - x_j)}\,, \tag{7.1}$$

which contributes to first order in $2-D$. To second order one needs in addition


$$= \overline{\mathbb{C}^2(x_i - x_j)}\,. \tag{7.2}$$

To third order diagrams with new topology are


$$= \overline{\mathbb{C}^3(x_i - x_j)}\,,$$


$$= \overline{\mathbb{C}(x_i - x_j)\mathbb{C}(x_j - x_k)\mathbb{C}(x_i - x_k)}\,. \tag{7.3}$$

Finally, to fourth order we need:


$$= \overline{\mathbb{C}^4(x_i - x_j)}\,,$$


$$= \overline{\mathbb{C}^2(x_i - x_j)\mathbb{C}(x_k - x_j)\mathbb{C}(x_k - x_i)}\,,$$


$$= \overline{\mathbb{C}(x_i - x_j)\mathbb{C}(x_k - x_j)\mathbb{C}(x_l - x_k)\mathbb{C}(x_i - x_l)}\,. \tag{7.4}$$

We will express the resummed series in terms of averages over both the correlator $\mathbb{C}(x)$ (6.8) and the connected correlator $\mathbb{C}_c(x)$ (6.52). One can switch to one or the other representation depending on which might be the more convenient. Before stating the results let us remind the definition of the correlator $\mathbb{C}(x)$, which was

$$C(x) = \mathbb{C}^{(0)}(x) + (2-D)\mathbb{C}(x)\,, \tag{7.5}$$

where $\mathbb{C}^{(0)}(x)$ is the limit $D \to 2$ of the two-point correlator $C(x)$. In (6.52) we have already introduced a connected correlation function

$$\mathbb{C}_c(x) = \mathbb{C}(x) - \overline{\mathbb{C}}\,, \tag{7.6}$$

such that

$$\overline{\mathbb{C}_c^2} = \overline{\mathbb{C}^2} - \overline{\mathbb{C}}^2\,, \tag{7.7}$$

and the notation for the leading behavior of the renormalized coupling $g$ could be shortened (6.55). From the definition (7.6), we obtain other useful averages, which we will need at higher orders in $2 - D$. To third order we will need:

$$\overline{\mathbb{C}_c^3} = \overline{\mathbb{C}^3} - 3\overline{\mathbb{C}}\,\overline{\mathbb{C}^2} + 2\overline{\mathbb{C}}^3 \tag{7.8}$$

and

$$\begin{aligned}\overline{\mathbb{C}_c^{\triangle}} &= \overline{\mathbb{C}_c(x_i{-}x_j)\mathbb{C}_c(x_j{-}x_k)\mathbb{C}_c(x_k{-}x_i)} \\ &= \overline{\mathbb{C}(x_i{-}x_j)\mathbb{C}(x_j{-}x_k)\mathbb{C}(x_k{-}x_i)} + 3\overline{\mathbb{C}}^2\overline{\mathbb{C}(x_i{-}x_j)} - 3\overline{\mathbb{C}}\,\overline{\mathbb{C}(x_i{-}x_j)\mathbb{C}(x_j{-}x_k)} - \overline{\mathbb{C}}^3 \\ &= \overline{\mathbb{C}^{\triangle}} - \overline{\mathbb{C}}^3\,,\end{aligned} \tag{7.9}$$

where $x_i, x_j, x_k$ are distinct points, and the average is over their positions. In (7.9) we exploited the symmetry of the closed manifold as it is diagrammatically expressed in (6.32), and the definition of $\overline{\mathbb{C}^{\triangle}}$ is self-evident. Furthermore, we will need to fourth order in $2 - D$:

$$\overline{\mathbb{C}_c^4} = \overline{\mathbb{C}^4} + 12\overline{\mathbb{C}^2}\,\overline{\mathbb{C}}^2 - 4\overline{\mathbb{C}^3}\,\overline{\mathbb{C}} - 3\overline{\mathbb{C}}^4\,, \tag{7.10}$$

$$\begin{aligned}\overline{\mathbb{C}_c^{\diamond}} &= \overline{\mathbb{C}_c(x_i{-}x_j)\mathbb{C}_c(x_j{-}x_k)\mathbb{C}_c(x_k{-}x_l)\mathbb{C}_c(x_l{-}x_i)} \\ &= \overline{\mathbb{C}^{\diamond}} + 5\overline{\mathbb{C}}^4\end{aligned} \tag{7.11}$$

and

$$\begin{aligned}\overline{\mathbb{C}_c^{\diamond\!\!>}} &= \overline{\mathbb{C}_c^2(x_i{-}x_j)\mathbb{C}_c(x_i{-}x_k)\mathbb{C}_c(x_k{-}x_j)} \\ &= \overline{\mathbb{C}^{\diamond\!\!>}} - 2\overline{\mathbb{C}^{\triangle}}\,\overline{\mathbb{C}} - \overline{\mathbb{C}^2}\,\overline{\mathbb{C}}^2 + 2\overline{\mathbb{C}}^4\,.\end{aligned} \tag{7.12}$$

### 7.1 Resummed contributions to the expansion in $2-D$ up to the fourth order

In the following we will state all terms, which appear in the expansion of the renormalized coupling $g(z)$ up to the fourth order in $2-D$ according to (6.14). We have to calculate at order $N$ of perturbation theory:

$$\overline{\mathrm{Tr}M} = N\,\overline{\mathbb{C}} \tag{7.13}$$

Inserting this into the perturbation series and summing up the resulting terms to all orders in $N$ generates the following contributions in the $2-D$-expansion of the renormalized coupling:

$$\sum_{\text{loops}} (\det \mathfrak{D}^{(0)})^{-d/2} \frac{\overline{\mathrm{Tr}M}(-z)^{N+1}}{N!} = \overline{\mathbb{C}} f_1^{d+2}(z) - \overline{\mathbb{C}} f_1^{d}(z)\ , \tag{7.14}$$

which contributes to first order in $2-D$. To second order in $2-D$, we have:

$$\overline{\mathrm{Tr}M^2} = \frac{-2N(N-1) - N(N-1)(N-2)}{1+N}\,\overline{\mathbb{C}}^2 + \frac{2N + 3N(N-1) + N(N-1)(N-2)}{1+N}\,\overline{\mathbb{C}^2}\ , \tag{7.15}$$

providing

$$\sum_{\text{loops}} (\det \mathfrak{D}^{(0)})^{-d/2} \frac{\overline{\mathrm{Tr}M^2}(-z)^{N+1}}{N!} = (-2\overline{\mathbb{C}}^2 + 2\overline{\mathbb{C}^2}) f_1^{d+4}(z) + (5\overline{\mathbb{C}}^2 - 4\overline{\mathbb{C}^2}) f_1^{d+2} + (-4\overline{\mathbb{C}}^2 + 3\overline{\mathbb{C}^2}) f_1^{d}(z) - (-\overline{\mathbb{C}}^2 + \overline{\mathbb{C}^2}) f_1^{d-2}(z)\ , \tag{7.16}$$

and

$$\overline{\mathrm{Tr}^2 M} = \frac{4N(N-1) + N(N-1)(N-2)}{1+N}\,\overline{\mathbb{C}}^2 + \frac{2N}{1+N}\,\overline{\mathbb{C}^2}\ , \tag{7.17}$$

providing

$$\sum_{\text{loops}} (\det \mathfrak{D}^{(0)})^{-d/2} \frac{\overline{\mathrm{Tr}^2 M}(-z)^{N+1}}{N!} = (-2\overline{\mathbb{C}}^2 + 2\overline{\mathbb{C}^2}) f_1^{d+4}(z) + (\overline{\mathbb{C}}^2 - 2\overline{\mathbb{C}^2}) f_1^{d+2}(z) + 2\overline{\mathbb{C}}^2 f_1^{d}(z) - \overline{\mathbb{C}}^2 f_1^{d-2}(z)\ . \tag{7.18}$$

Let us rewrite this in terms of the connected correlator (7.7):

$$\sum_{\text{loops}} (\det \mathfrak{D}^{(0)})^{-d/2} \frac{\overline{\mathrm{Tr}M^2}(-z)^{N+1}}{N!} = 2\overline{\mathbb{C}_c^2}\ f_1^{d+4}(z) + (-4\overline{\mathbb{C}_c^2} + \overline{\mathbb{C}}^2) f_1^{d+2}(z) + (-\overline{\mathbb{C}}^2 + 3\overline{\mathbb{C}_c^2})\ f_1^{d}(z) - \overline{\mathbb{C}_c^2}\ f_1^{d-2}(z)\ , \tag{7.19}$$

$$\sum_{\text{loops}} (\det \mathfrak{D}^{(0)})^{-d/2} \frac{\overline{\mathrm{Tr}^2 M}(-z)^{N+1}}{N!} = 2\overline{\mathbb{C}_c^2}\ f_1^{d+4}(z) - (2\overline{\mathbb{C}_c^2} + \overline{\mathbb{C}}^2) f_1^{d+2}(z) + 2\overline{\mathbb{C}}^2\ f_1^{d}(z) - \overline{\mathbb{C}}^2\ f_1^{d-2}(z) \tag{7.20}$$

Let us now state the terms to appear at third order in $2-D$, which we derived with the help of a *Mathematica®* program ($N$ denotes the loop order.):

$$\begin{aligned}\sum_{\text{loops}}(\det\mathfrak{D}^{(0)})^{-d/2}\frac{\overline{\mathrm{Tr}M^3}(-z)^{N+1}}{N!} &= 4(6\overline{\mathbb{C}}^3-3\overline{\mathbb{C}\mathbb{C}^2}+\overline{\mathbb{C}^3}-4\overline{\mathbb{C}^\triangle})f_1^{d+4}(z)\\ &+(-62\overline{\mathbb{C}}^3+36\overline{\mathbb{C}\mathbb{C}^2}-10\overline{\mathbb{C}^3}+36\overline{\mathbb{C}^\triangle})f_1^{d+2}(z)\\ &+(63\overline{\mathbb{C}}^3-39\overline{\mathbb{C}\mathbb{C}^2}+9\overline{\mathbb{C}^3}-32\overline{\mathbb{C}^\triangle})f_1^{d}(z)\\ &+(-33\overline{\mathbb{C}}^3+18\overline{\mathbb{C}\mathbb{C}^2}-3\overline{\mathbb{C}^3}+17\overline{\mathbb{C}^\triangle})f_1^{d-2}(z)\\ &+(9\overline{\mathbb{C}}^3-3\overline{\mathbb{C}\mathbb{C}^2}-6\overline{\mathbb{C}^\triangle})f_1^{d-4}(z)+(-\overline{\mathbb{C}}^3+\overline{\mathbb{C}^\triangle})f_1^{d-6}(z)\end{aligned} \tag{7.21}$$

$$\begin{aligned}\sum_{\text{loops}}(\det\mathfrak{D}^{(0)})^{-d/2}\frac{\overline{\mathrm{Tr}M\ \mathrm{Tr}M^2}(-z)^{N+1}}{N!} &= 4(6\overline{\mathbb{C}}^3-3\overline{\mathbb{C}\mathbb{C}^2}+\overline{\mathbb{C}^3}-4\overline{\mathbb{C}^\triangle})f_1^{d+6}(z)\\ &+(-50\overline{\mathbb{C}}^3+26\overline{\mathbb{C}\mathbb{C}^2}-8\overline{\mathbb{C}^3}+32\overline{\mathbb{C}^\triangle})f_1^{d+4}(z)\\ &+(29\overline{\mathbb{C}}^3-16\overline{\mathbb{C}\mathbb{C}^2}+6\overline{\mathbb{C}^3}-20\overline{\mathbb{C}^\triangle})f_1^{d+2}(z)\\ &+(\overline{\mathbb{C}}^3-\overline{\mathbb{C}\mathbb{C}^2}-2\overline{\mathbb{C}^3}+4\overline{\mathbb{C}^\triangle})f_1^{d}(z)\\ &+(-5\overline{\mathbb{C}}^3+4\overline{\mathbb{C}\mathbb{C}^2})f_1^{d-2}(z)+(\overline{\mathbb{C}}^3-\overline{\mathbb{C}\mathbb{C}^2})f_1^{d-4}(z)\end{aligned} \tag{7.22}$$

$$\begin{aligned}\sum_{\text{loops}}(\det\mathfrak{D}^{(0)})^{-d/2}\frac{\overline{\mathrm{Tr}^3M}(-z)^{N+1}}{N!} &= 4(6\overline{\mathbb{C}}^3-3\overline{\mathbb{C}\mathbb{C}^2}+\overline{\mathbb{C}^3}-4\overline{\mathbb{C}^\triangle})f_1^{d+6}(z)\\ &+(-26\overline{\mathbb{C}}^3+6\overline{\mathbb{C}\mathbb{C}^2}-4\overline{\mathbb{C}^3}+24\overline{\mathbb{C}^\triangle})f_1^{d+4}(z)\\ &+(-3\overline{\mathbb{C}}^3+12\overline{\mathbb{C}\mathbb{C}^2}-8\overline{\mathbb{C}^\triangle})f_1^{d+2}(z)\\ &+3(\overline{\mathbb{C}}^3-2\overline{\mathbb{C}\mathbb{C}^2})f_1^{d}(z)\\ &+3\overline{\mathbb{C}}^3f_1^{d-2}(z)-\overline{\mathbb{C}}^3f_1^{d-4}(z)\end{aligned} \tag{7.23}$$

Again, let us rewrite this in terms of connected correlators:

$$\begin{aligned}\sum_{\text{loops}}(\det\mathfrak{D}^{(0)})^{-d/2}\frac{\overline{\mathrm{Tr}M^3}(-z)^{N+1}}{N!} &= 4(\overline{\mathbb{C}_c^3}-4\overline{\mathbb{C}_c^\triangle})f_1^{d+4}(z)\\ &+(-10\overline{\mathbb{C}_c^3}+36\overline{\mathbb{C}_c^\triangle}+6\overline{\mathbb{C}\mathbb{C}_c^2})f_1^{d+2}(z)\\ &+(9\overline{\mathbb{C}_c^3}-32\overline{\mathbb{C}_c^\triangle}-12\overline{\mathbb{C}\mathbb{C}_c^2}+\overline{\mathbb{C}}^3)f_1^{d}(z)\\ &+(3\overline{\mathbb{C}_c^3}-17\overline{\mathbb{C}_c^\triangle}-9\overline{\mathbb{C}\mathbb{C}_c^2}+\overline{\mathbb{C}}^3)f_1^{d-2}(z)\\ &-3(2\overline{\mathbb{C}_c^\triangle}+\overline{\mathbb{C}\mathbb{C}_c^2})f_1^{d-4}(z)+\overline{\mathbb{C}_c^\triangle}\ f_1^{d-6}(z)\ ,\end{aligned} \tag{7.24}$$

$$\sum_{\text{loops}} (\det \mathfrak{D}^{(0)})^{-d/2} \frac{\overline{\mathrm{Tr} M \ \mathrm{Tr} M^2}(-z)^{N+1}}{N!} = 4(\overline{\mathbb{C}_c^3} - 4\overline{\mathbb{C}_c^{\triangle}}) f_1^{d+6}(z)$$
$$+ (-8\overline{\mathbb{C}_c^3} + 32\overline{\mathbb{C}_c^{\triangle}} + 2\overline{\mathbb{C}\mathbb{C}_c^2}) f_1^{d+4}(z)$$
$$+ (6\overline{\mathbb{C}_c^3} - 20\overline{\mathbb{C}_c^{\triangle}} + 2\overline{\mathbb{C}\mathbb{C}_c^2} - 6\overline{\mathbb{C}}^3) f_1^{d+2}(z)$$
$$+ (-2\overline{\mathbb{C}_c^3} + 4\overline{\mathbb{C}_c^{\triangle}} - 7\overline{\mathbb{C}\mathbb{C}_c^2} + 2\overline{\mathbb{C}}^3) f_1^{d}(z)$$
$$- (\overline{\mathbb{C}}^3 - 4\overline{\mathbb{C}\mathbb{C}_c^2}) f_1^{d-2}(z) - \overline{\mathbb{C}\mathbb{C}_c^2}\, f_1^{d-4}(z)\,, \tag{7.25}$$

$$\sum_{\text{loops}} (\det \mathfrak{D}^{(0)})^{-d/2} \frac{\overline{\mathrm{Tr}^3 M}(-z)^{N+1}}{N!} = 4(\overline{\mathbb{C}_c^3} - 4\overline{\mathbb{C}_c^{\triangle}}) f_1^{d+6}(z)$$
$$+ (-4\overline{\mathbb{C}_c^3} + 24\overline{\mathbb{C}_c^{\triangle}} - 6\overline{\mathbb{C}\mathbb{C}_c^2}) f_1^{d+4}(z)$$
$$+ (-8\overline{\mathbb{C}_c^{\triangle}} + 12\overline{\mathbb{C}\mathbb{C}_c^2} + \overline{\mathbb{C}}^3) f_1^{d+2}(z)$$
$$- 3(\overline{\mathbb{C}}^3 + 2\overline{\mathbb{C}\mathbb{C}_c^2}) f_1^{d}(z)$$
$$+ 3\overline{\mathbb{C}}^3 f_1^{d-2}(z) - \overline{\mathbb{C}}^3 f_1^{d-4}(z)\,. \tag{7.26}$$

To fourth order in $2 - D$ we obtain:

$$\sum_{\text{loops}} (\det \mathfrak{D}^{(0)})^{-d/2} \frac{\overline{\mathrm{Tr} M^4}(-z)^{N+1}}{N!}$$
$$= 8(90\overline{\mathbb{C}}^4 - 36\overline{\mathbb{C}}^2\overline{\mathbb{C}^2} + 3\overline{\mathbb{C}^2}^2 + 4\overline{\mathbb{C}\mathbb{C}^3} - \overline{\mathbb{C}^4} + 24\overline{\mathbb{C}^{\diamond\!\!>}} - 36\overline{\mathbb{C}^{\diamond}} - 48\overline{\mathbb{C}\mathbb{C}^{\triangle}}) f_1^{d+8}(z)$$
$$+ 4(501\overline{\mathbb{C}}^4 - 222\overline{\mathbb{C}}^2\overline{\mathbb{C}^2} + 23\overline{\mathbb{C}^2}^2 + 28\overline{\mathbb{C}\mathbb{C}^3} - 6\overline{\mathbb{C}^4} + 128\overline{\mathbb{C}^{\diamond\!\!>}} - 180\overline{\mathbb{C}^{\diamond}} - 272\overline{\mathbb{C}\mathbb{C}^{\triangle}}) f_1^{d+6}(z)$$
$$- 4(561\overline{\mathbb{C}}^4 - 273\overline{\mathbb{C}}^2\overline{\mathbb{C}^2} + 31\overline{\mathbb{C}^2}^2 + 38\overline{\mathbb{C}\mathbb{C}^3} - 7\overline{\mathbb{C}^4} + 136\overline{\mathbb{C}^{\diamond\!\!>}} - 178\overline{\mathbb{C}^{\diamond}} - 308\overline{\mathbb{C}\mathbb{C}^{\triangle}}) f_1^{d+4}(z)$$
$$+ (1359\overline{\mathbb{C}}^4 - 696\overline{\mathbb{C}}^2\overline{\mathbb{C}^2} + 82\overline{\mathbb{C}^2}^2 + 100\overline{\mathbb{C}\mathbb{C}^3} - 16\overline{\mathbb{C}^4} + 304\overline{\mathbb{C}^{\diamond\!\!>}} - 396\overline{\mathbb{C}^{\diamond}} - 736\overline{\mathbb{C}\mathbb{C}^{\triangle}}) f_1^{d+2}(z)$$
$$+ (-500\overline{\mathbb{C}}^4 + 248\overline{\mathbb{C}}^2\overline{\mathbb{C}^2} - 36\overline{\mathbb{C}^2}^2 - 32\overline{\mathbb{C}\mathbb{C}^3} + 5\overline{\mathbb{C}^4} - 92\overline{\mathbb{C}^{\diamond\!\!>}} + 154\overline{\mathbb{C}^{\diamond}} + 252\overline{\mathbb{C}\mathbb{C}^{\triangle}}) f_1^{d}(z)$$
$$+ (116\overline{\mathbb{C}}^4 - 48\overline{\mathbb{C}}^2\overline{\mathbb{C}^2} + 12\overline{\mathbb{C}^2}^2 + 4\overline{\mathbb{C}\mathbb{C}^3} - \overline{\mathbb{C}^4} + 12\overline{\mathbb{C}^{\diamond\!\!>}} - 47\overline{\mathbb{C}^{\diamond}} - 48\overline{\mathbb{C}\mathbb{C}^{\triangle}}) f_1^{d-2}(z)$$
$$+ (-16\overline{\mathbb{C}}^4 + 4\overline{\mathbb{C}}^2\overline{\mathbb{C}^2} - 2\overline{\mathbb{C}^2}^2 + 10\overline{\mathbb{C}^{\diamond\!\!>}} + 4\overline{\mathbb{C}\mathbb{C}^{\triangle}}) f_1^{d-4}(z) + (\overline{\mathbb{C}}^4 - \overline{\mathbb{C}^{\diamond}}) f_1^{d-6}(z) \tag{7.27}$$

$$
\begin{aligned}
&\sum_{\text{loops}} (\det \mathfrak{D}^{(0)})^{-d/2} \frac{\overline{\mathrm{Tr}^2 M^2}(-z)^{N+1}}{N!} \\
&= 8(90\overline{\mathbb{C}}^4 - 36\overline{\mathbb{C}}^2\overline{\mathbb{C}^2} + 3\overline{\mathbb{C}^2}^2 + 4\overline{\mathbb{C}\mathbb{C}^3} - \overline{\mathbb{C}^4} + 24\overline{\mathbb{C}^{\triangleright}} - 36\overline{\mathbb{C}^{\diamond}} - 48\overline{\mathbb{C}\mathbb{C}^{\triangle}}) f_1^{d+8}(z) \\
&+ 4(501\overline{\mathbb{C}}^4 - 222\overline{\mathbb{C}}^2\overline{\mathbb{C}^2} + 23\overline{\mathbb{C}^2}^2 + 28\overline{\mathbb{C}\mathbb{C}^3} - 6\overline{\mathbb{C}^4} + 128\overline{\mathbb{C}^{\triangleright}} - 180\overline{\mathbb{C}^{\diamond}} - 272\overline{\mathbb{C}\mathbb{C}^{\triangle}}) f_1^{d+6}(z) \\
&- 4(537\overline{\mathbb{C}}^4 - 261\overline{\mathbb{C}}^2\overline{\mathbb{C}^2} + 28\overline{\mathbb{C}^2}^2 + 40\overline{\mathbb{C}\mathbb{C}^3} - 8\overline{\mathbb{C}^4} + 132\overline{\mathbb{C}^{\triangleright}} - 172\overline{\mathbb{C}^{\diamond}} - 296\overline{\mathbb{C}\mathbb{C}^{\triangle}}) f_1^{d+4}(z) \\
&+ (1111\overline{\mathbb{C}}^4 - 572\overline{\mathbb{C}}^2\overline{\mathbb{C}^2} + 44\overline{\mathbb{C}^2}^2 + 120\overline{\mathbb{C}\mathbb{C}^3} - 24\overline{\mathbb{C}^4} + 272\overline{\mathbb{C}^{\triangleright}} - 624\overline{\mathbb{C}\mathbb{C}^{\triangle}}) f_1^{d+2}(z) \\
&+ (260\overline{\mathbb{C}}^4 - 122\overline{\mathbb{C}}^2\overline{\mathbb{C}^2} - 10\overline{\mathbb{C}^2}^2 + 48\overline{\mathbb{C}\mathbb{C}^3} - 10\overline{\mathbb{C}^4} + 72\overline{\mathbb{C}^{\triangleright}} - 80\overline{\mathbb{C}^{\diamond}} - 160\overline{\mathbb{C}\mathbb{C}^{\triangle}}) f_1^{d}(z) \\
&+ (6\overline{\mathbb{C}}^4 + 18\overline{\mathbb{C}}^2\overline{\mathbb{C}^2} - 15\overline{\mathbb{C}^2}^2 + 8\overline{\mathbb{C}\mathbb{C}^3} - 2\overline{\mathbb{C}^4} + 8\overline{\mathbb{C}^{\triangleright}} - 8\overline{\mathbb{C}^{\diamond}} - 16\overline{\mathbb{C}\mathbb{C}^{\triangle}}) f_1^{d-2}(z) \\
&+ (8\overline{\mathbb{C}}^4 - 14\overline{\mathbb{C}}^2\overline{\mathbb{C}^2} + 6\overline{\mathbb{C}^2}^2) f_1^{d-4}(z) \\
&+ (-\overline{\mathbb{C}}^4 + 2\overline{\mathbb{C}}^2\overline{\mathbb{C}^2} - \overline{\mathbb{C}^2}^2) f_1^{d-6}(z)
\end{aligned}
\tag{7.28}
$$

$$
\begin{aligned}
&\sum_{\text{loops}} (\det \mathfrak{D}^{(0)})^{-d/2} \frac{\overline{\mathrm{Tr} M\ \mathrm{Tr} M^3}(-z)^{N+1}}{N!} \\
&= 8(90\overline{\mathbb{C}}^4 - 36\overline{\mathbb{C}}^2\overline{\mathbb{C}^2} + 3\overline{\mathbb{C}^2}^2 + 4\overline{\mathbb{C}\mathbb{C}^3} - \overline{\mathbb{C}^4} + 24\overline{\mathbb{C}^{\triangleright}} - 36\overline{\mathbb{C}^{\diamond}} - 48\overline{\mathbb{C}\mathbb{C}^{\triangle}}) f_1^{d+8}(z) \\
&+ 4(441\overline{\mathbb{C}}^4 - 186\overline{\mathbb{C}}^2\overline{\mathbb{C}^2} + 18\overline{\mathbb{C}^2}^2 + 22\overline{\mathbb{C}\mathbb{C}^3} - 5\overline{\mathbb{C}^4} + 114\overline{\mathbb{C}^{\triangleright}} - 168\overline{\mathbb{C}^{\diamond}} - 236\overline{\mathbb{C}\mathbb{C}^{\triangle}}) f_1^{d+6}(z) \\
&- 2(800\overline{\mathbb{C}}^4 - 351\overline{\mathbb{C}}^2\overline{\mathbb{C}^2} + 39\overline{\mathbb{C}^2}^2 + 41\overline{\mathbb{C}\mathbb{C}^3} - 9\overline{\mathbb{C}^4} + 204\overline{\mathbb{C}^{\triangleright}} - 294\overline{\mathbb{C}^{\diamond}} - 430\overline{\mathbb{C}\mathbb{C}^{\triangle}}) f_1^{d+4}(z) \\
&+ (661\overline{\mathbb{C}}^4 - 279\overline{\mathbb{C}}^2\overline{\mathbb{C}^2} + 36\overline{\mathbb{C}^2}^2 + 23\overline{\mathbb{C}\mathbb{C}^3} - 6\overline{\mathbb{C}^4} + 186\overline{\mathbb{C}^{\triangleright}} - 258\overline{\mathbb{C}^{\diamond}} - 364\overline{\mathbb{C}\mathbb{C}^{\triangle}}) f_1^{d+2}(z) \\
&+ (-90\overline{\mathbb{C}}^4 + 21\overline{\mathbb{C}}^2\overline{\mathbb{C}^2} - 6\overline{\mathbb{C}^2}^2 + 6\overline{\mathbb{C}\mathbb{C}^3} - 48\overline{\mathbb{C}^{\triangleright}} + 60\overline{\mathbb{C}^{\diamond}} + 59\overline{\mathbb{C}\mathbb{C}^{\triangle}}) f_1^{d}(z) \\
&+ (-24\overline{\mathbb{C}}^4 + 15\overline{\mathbb{C}}^2\overline{\mathbb{C}^2} - 3\overline{\mathbb{C}\mathbb{C}^3} + 6\overline{\mathbb{C}^{\triangleright}} - 6\overline{\mathbb{C}^{\diamond}} + 11\overline{\mathbb{C}\mathbb{C}^{\triangle}}) f_1^{d-2}(z) \\
&+ (10\overline{\mathbb{C}}^4 - 3\overline{\mathbb{C}}^2\overline{\mathbb{C}^2} - 7\overline{\mathbb{C}\mathbb{C}^{\triangle}}) f_1^{d-4}(z) + (-\overline{\mathbb{C}}^4 + \overline{\mathbb{C}\mathbb{C}^{\triangle}}) f_1^{d-6}(z)
\end{aligned}
\tag{7.29}
$$

$$
\begin{aligned}
&\sum_{\text{loops}} (\det \mathfrak{D}^{(0)})^{-d/2} \frac{\overline{\mathrm{Tr}^2 M\ \mathrm{Tr} M^2}(-z)^{N+1}}{N!} \\
&= 8(90\overline{\mathbb{C}}^4 - 36\overline{\mathbb{C}}^2\overline{\mathbb{C}^2} + 3\overline{\mathbb{C}^2}^2 + 4\overline{\mathbb{C}\mathbb{C}^3} - \overline{\mathbb{C}^4} + 24\overline{\mathbb{C}^{\triangleright}} - 36\overline{\mathbb{C}^{\diamond}} - 48\overline{\mathbb{C}\mathbb{C}^{\triangle}}) f_1^{d+8}(z) \\
&+ 4(381\overline{\mathbb{C}}^4 - 150\overline{\mathbb{C}}^2\overline{\mathbb{C}^2} + 13\overline{\mathbb{C}^2}^2 + 16\overline{\mathbb{C}\mathbb{C}^3} + 4\overline{\mathbb{C}^4} - 100\overline{\mathbb{C}^{\triangleright}} + 156\overline{\mathbb{C}^{\diamond}} - 200\overline{\mathbb{C}\mathbb{C}^{\triangle}}) f_1^{d+6}(z) \\
&+ 4(251\overline{\mathbb{C}}^4 - 90\overline{\mathbb{C}}^2\overline{\mathbb{C}^2} + 8\overline{\mathbb{C}^2}^2 + 8\overline{\mathbb{C}\mathbb{C}^3} - 3\overline{\mathbb{C}^4} + 70\overline{\mathbb{C}^{\triangleright}} - 116\overline{\mathbb{C}^{\diamond}} - 128\overline{\mathbb{C}\mathbb{C}^{\triangle}}) f_1^{d+4}(z) \\
&+ (159\overline{\mathbb{C}}^4 - 4\overline{\mathbb{C}}^2\overline{\mathbb{C}^2} - 4\overline{\mathbb{C}^2}^2 - 12\overline{\mathbb{C}\mathbb{C}^3} + 2\overline{\mathbb{C}^4} - 40\overline{\mathbb{C}^{\triangleright}} + 72\overline{\mathbb{C}^{\diamond}} - 72\overline{\mathbb{C}\mathbb{C}^{\triangle}}) f_1^{d+2}(z) \\
&+ (50\overline{\mathbb{C}}^4 - 53\overline{\mathbb{C}}^2\overline{\mathbb{C}^2} + 8\overline{\mathbb{C}^2}^2 + 16\overline{\mathbb{C}\mathbb{C}^3} - 8\overline{\mathbb{C}^{\triangleright}} + 16\overline{\mathbb{C}^{\diamond}} - 32\overline{\mathbb{C}\mathbb{C}^{\triangle}}) f_1^{d}(z) \\
&+ (-4\overline{\mathbb{C}}^4 + 5\overline{\mathbb{C}}^2\overline{\mathbb{C}^2} - 2\overline{\mathbb{C}^2}^2 - 4\overline{\mathbb{C}\mathbb{C}^3} + 8\overline{\mathbb{C}\mathbb{C}^{\triangle}}) f_1^{d-2}(z) \\
&+ (-6\overline{\mathbb{C}}^4 + 5\overline{\mathbb{C}}^2\overline{\mathbb{C}^2}) f_1^{d-4}(z) + (\overline{\mathbb{C}}^4 - \overline{\mathbb{C}}^2\overline{\mathbb{C}^2}) f_1^{d-6}(z)
\end{aligned}
\tag{7.30}
$$

$$
\begin{aligned}
&\sum_{\text{loops}} (\det \mathfrak{D}^{(0)})^{-d/2} \frac{\overline{\mathrm{Tr}^4 M}(-z)^{N+1}}{N!} \\
&= 8(90\overline{\mathbb{C}}^4 - 36\overline{\mathbb{C}}^2\overline{\mathbb{C}^2} + 3\overline{\mathbb{C}^2}^2 + 4\overline{\mathbb{C}\mathbb{C}^3} - \overline{\mathbb{C}^4} + 24\overline{\mathbb{C}^{\triangleright}} - 36\overline{\mathbb{C}^{\diamond}} - 48\overline{\mathbb{C}}\,\overline{\mathbb{C}^{\triangle}}) f_1^{d+8}(z) \\
&+ 4(261\overline{\mathbb{C}}^4 - 78\overline{\mathbb{C}}^2\overline{\mathbb{C}^2} + 3\overline{\mathbb{C}^2}^2 + 4\overline{\mathbb{C}\mathbb{C}^3} - 2\overline{\mathbb{C}^4} + 72\overline{\mathbb{C}^{\triangleright}} - 132\overline{\mathbb{C}^{\diamond}} - 128\overline{\mathbb{C}}\,\overline{\mathbb{C}^{\triangle}}) f_1^{d+6}(z) \\
&+ 4(61\overline{\mathbb{C}}^4 + 9\overline{\mathbb{C}}^2\overline{\mathbb{C}^2} - 6\overline{\mathbb{C}^2}^2 - 8\overline{\mathbb{C}\mathbb{C}^3} + 24\overline{\mathbb{C}^{\triangleright}} - 72\overline{\mathbb{C}^{\diamond}} - 8\overline{\mathbb{C}}\,\overline{\mathbb{C}^{\triangle}}) f_1^{d+4}(z) \\
&+ (-89\overline{\mathbb{C}}^4 + 36\overline{\mathbb{C}}^2\overline{\mathbb{C}^2} - 12\overline{\mathbb{C}^2}^2 - 16\overline{\mathbb{C}\mathbb{C}^3} - 48\overline{\mathbb{C}^{\diamond}} + 128\overline{\mathbb{C}}\,\overline{\mathbb{C}^{\triangle}}) f_1^{d+2}(z) \\
&+ (36\overline{\mathbb{C}}^2\overline{\mathbb{C}^2} - 32\overline{\mathbb{C}}\,\overline{\mathbb{C}^{\triangle}}) f_1^{d}(z) + (6\overline{\mathbb{C}}^4 - 12\overline{\mathbb{C}}^2\overline{\mathbb{C}^2}) f_1^{d-2}(z) \\
&+ 4\overline{\mathbb{C}}^4 f_1^{d-4}(z) - \overline{\mathbb{C}}^4 f_1^{d-6}(z)
\end{aligned}
\tag{7.31}
$$

Rewriting everything in terms of connected correlators we find:

$$
\begin{aligned}
&\sum_{\text{loops}} (\det \mathfrak{D}^{(0)})^{-d/2} \frac{\overline{\mathrm{Tr}^4 M}(-z)^{N+1}}{N!} \\
&= 8(222\overline{\mathbb{C}}^4 + 6\overline{\mathbb{C}}^2\overline{\mathbb{C}_c^2} + 3\overline{\mathbb{C}_c^2}^2 - \overline{\mathbb{C}_c^4} + 24\overline{\mathbb{C}_c^{\triangleright}} - 36\overline{\mathbb{C}_c^{\diamond}}) f_1^{d+8}(z) \\
&+ 4(804\overline{\mathbb{C}}^4 + 12\overline{\mathbb{C}}^2\overline{\mathbb{C}_c^2} + 3\overline{\mathbb{C}_c^2}^2 - 2\overline{\mathbb{C}_c^4} + 72\overline{\mathbb{C}_c^{\triangleright}} - 132\overline{\mathbb{C}_c^{\diamond}} - 4\overline{\mathbb{C}}\,\overline{\mathbb{C}_c^3} + 16\overline{\mathbb{C}}\,\overline{\mathbb{C}_c^{\triangle}}) f_1^{d+6}(z) \\
&- 4(432\overline{\mathbb{C}}^4 - 3\overline{\mathbb{C}}^2\overline{\mathbb{C}_c^2} - 6\overline{\mathbb{C}_c^2}^2 + 24\overline{\mathbb{C}_c^{\triangleright}} - 72\overline{\mathbb{C}_c^{\diamond}} - 8\overline{\mathbb{C}}\,\overline{\mathbb{C}_c^3} + 40\overline{\mathbb{C}}\,\overline{\mathbb{C}_c^{\triangle}}) f_1^{d+4}(z) \\
&+ (287\overline{\mathbb{C}}^4 - 36\overline{\mathbb{C}}^2\overline{\mathbb{C}_c^2} - 12\overline{\mathbb{C}_c^2}^2 - 48\overline{\mathbb{C}_c^{\diamond}} - 16\overline{\mathbb{C}}\,\overline{\mathbb{C}_c^3} + 128\overline{\mathbb{C}}\,\overline{\mathbb{C}_c^{\triangle}}) f_1^{d+2}(z) \\
&+ (4\overline{\mathbb{C}}^4 + 36\overline{\mathbb{C}}^2\overline{\mathbb{C}_c^2} - 32\overline{\mathbb{C}}\,\overline{\mathbb{C}_c^{\triangle}}) f_1^{d}(z) \\
&+ (-6\overline{\mathbb{C}}^4 - 2\overline{\mathbb{C}}^2\overline{\mathbb{C}_c^2}) f_1^{d-2}(z) + 4\overline{\mathbb{C}}^4 f_1^{d-4}(z) - \overline{\mathbb{C}}^4 f_1^{d-6}(z)
\end{aligned}
\tag{7.32}
$$

$$
\begin{aligned}
&\sum_{\text{loops}} (\det \mathfrak{D}^{(0)})^{-d/2} \frac{\overline{\mathrm{Tr} M^2\ \mathrm{Tr}^2 M}(-z)^{N+1}}{N!} \\
&= 8(222\overline{\mathbb{C}}^4 + 6\overline{\mathbb{C}}^2\overline{\mathbb{C}_c^2} + 3\overline{\mathbb{C}_c^2}^2 - \overline{\mathbb{C}_c^4} + 24\overline{\mathbb{C}_c^{\triangleright}} - 36\overline{\mathbb{C}_c^{\diamond}}) f_1^{d+8}(z) \\
&+ 4(960\overline{\mathbb{C}}^4 + 24\overline{\mathbb{C}}^2\overline{\mathbb{C}_c^2} + \overline{\mathbb{C}_c^2}^2 - 4\overline{\mathbb{C}_c^4} + 100\overline{\mathbb{C}_c^{\triangleright}} - 156\overline{\mathbb{C}_c^{\diamond}}) f_1^{d+6}(z) \\
&- 4(714\overline{\mathbb{C}}^4 + 20\overline{\mathbb{C}}^2\overline{\mathbb{C}_c^2} + 8\overline{\mathbb{C}_c^2}^2 - 3\overline{\mathbb{C}_c^4} + 70\overline{\mathbb{C}_c^{\triangleright}} - 116\overline{\mathbb{C}_c^{\diamond}} - 4\overline{\mathbb{C}}\,\overline{\mathbb{C}_c^3} + 12\overline{\mathbb{C}}\,\overline{\mathbb{C}_c^{\triangle}}) f_1^{d+4}(z) \\
&+ (889\overline{\mathbb{C}}^4 + 36\overline{\mathbb{C}}^2\overline{\mathbb{C}_c^2} - 2\overline{\mathbb{C}_c^2}^2 - 28\overline{\mathbb{C}}\,\overline{\mathbb{C}_c^3} - 4\overline{\mathbb{C}_c^4} + 80\overline{\mathbb{C}_c^{\triangleright}} - 144\overline{\mathbb{C}_c^{\diamond}} + 88\overline{\mathbb{C}}\,\overline{\mathbb{C}_c^{\triangle}}) f_1^{d+2}(z) \\
&+ (-99\overline{\mathbb{C}}^4 + 3\overline{\mathbb{C}}^2\overline{\mathbb{C}_c^2} + 8\overline{\mathbb{C}_c^2}^2 + 16\overline{\mathbb{C}}\,\overline{\mathbb{C}_c^3} - 8\overline{\mathbb{C}_c^{\triangleright}} + 16\overline{\mathbb{C}_c^{\diamond}} - 48\overline{\mathbb{C}}\,\overline{\mathbb{C}_c^{\triangle}}) f_1^{d}(z) \\
&+ (3\overline{\mathbb{C}}^4 - 11\overline{\mathbb{C}}^2\overline{\mathbb{C}_c^2} - 2\overline{\mathbb{C}_c^2}^2 - 4\overline{\mathbb{C}}\,\overline{\mathbb{C}_c^3} + 8\overline{\mathbb{C}}\,\overline{\mathbb{C}_c^{\triangle}}) f_1^{d-2}(z) \\
&+ (-\overline{\mathbb{C}}^4 - 5\overline{\mathbb{C}}^2\overline{\mathbb{C}_c^2}) f_1^{d-4}(z) - \overline{\mathbb{C}}^2\overline{\mathbb{C}_c^2} f_1^{d-6}(z)
\end{aligned}
\tag{7.33}
$$

$$
\begin{aligned}
&\sum_{\text{loops}} (\det \mathfrak{D}^{(0)})^{-d/2} \frac{\overline{\mathrm{Tr}^2 M^2}(-z)^{N+1}}{N!} \\
&= 8(222\overline{\mathbb{C}}^4 + 6\overline{\mathbb{C}}^2\overline{\mathbb{C}_c^2} + 3\overline{\mathbb{C}_c^2}^2 - \overline{\mathbb{C}_c^4} + 24\overline{\mathbb{C}_c^{\triangleright}} - 36\overline{\mathbb{C}_c^{\diamond}}) f_1^{d+8}(z) \\
&+ 4(1116\overline{\mathbb{C}}^4 + 36\overline{\mathbb{C}}^2\overline{\mathbb{C}_c^2} + 23\overline{\mathbb{C}_c^2}^2 - 6\overline{\mathbb{C}_c^4} + 128\overline{\mathbb{C}_c^{\triangleright}} - 180\overline{\mathbb{C}_c^{\diamond}} + 4\overline{\mathbb{C}}\,\overline{\mathbb{C}_c^3} - 16\overline{\mathbb{C}}\,\overline{\mathbb{C}_c^{\triangle}}) f_1^{d+6}(z) \\
&- 4(1080\overline{\mathbb{C}}^4 + 47\overline{\mathbb{C}}^2\overline{\mathbb{C}_c^2} + 28\overline{\mathbb{C}_c^2}^2 - 8\overline{\mathbb{C}_c^4} + 132\overline{\mathbb{C}_c^{\triangleright}} - 172\overline{\mathbb{C}_c^{\diamond}} + 8\overline{\mathbb{C}}\,\overline{\mathbb{C}_c^3} - 32\overline{\mathbb{C}}\,\overline{\mathbb{C}_c^{\triangle}}) f_1^{d+4}(z) \\
&+ (2111\overline{\mathbb{C}}^4 + 148\overline{\mathbb{C}}^2\overline{\mathbb{C}_c^2} + 44\overline{\mathbb{C}_c^2}^2 + 24\overline{\mathbb{C}}\,\overline{\mathbb{C}_c^3} - 24\overline{\mathbb{C}_c^4} + 272\overline{\mathbb{C}_c^{\triangleright}} - 328\overline{\mathbb{C}_c^{\diamond}} - 80\overline{\mathbb{C}}\,\overline{\mathbb{C}_c^{\triangle}}) f_1^{d+2}(z) \\
&+ (-538\overline{\mathbb{C}}^4 - 74\overline{\mathbb{C}}^2\overline{\mathbb{C}_c^2} + 10\overline{\mathbb{C}_c^2}^2 - 8\overline{\mathbb{C}}\,\overline{\mathbb{C}_c^3} + 10\overline{\mathbb{C}_c^4} - 72\overline{\mathbb{C}_c^{\triangleright}} + 80\overline{\mathbb{C}_c^{\diamond}} + 8\overline{\mathbb{C}}\,\overline{\mathbb{C}_c^{\triangle}}) f_1^{d}(z) \\
&+ (59\overline{\mathbb{C}}^4 + 20\overline{\mathbb{C}}^2\overline{\mathbb{C}_c^2} - 15\overline{\mathbb{C}_c^2}^2 - 2\overline{\mathbb{C}_c^4} + 8\overline{\mathbb{C}_c^{\triangleright}} - 8\overline{\mathbb{C}_c^{\diamond}}) f_1^{d-2}(z) \\
&+ (-2\overline{\mathbb{C}}^2\overline{\mathbb{C}_c^2} + 6\overline{\mathbb{C}_c^2}^2) f_1^{d-4}(z) - \overline{\mathbb{C}_c^2}^2 f_1^{d-6}(z)
\end{aligned}
\tag{7.34}
$$

$$
\begin{aligned}
&\sum_{\text{loops}} (\det \mathfrak{D}^{(0)})^{-d/2} \frac{\overline{\mathrm{Tr} M\ \mathrm{Tr} M^3}(-z)^{N+1}}{N!} \\
&= 8(222\overline{\mathbb{C}}^4 + 6\overline{\mathbb{C}}^2\overline{\mathbb{C}_c^2} + 3\overline{\mathbb{C}_c^2}^2 - \overline{\mathbb{C}_c^4} + 24\overline{\mathbb{C}_c^{\triangleright}} - 36\overline{\mathbb{C}_c^{\diamond}}) f_1^{d+8}(z) \\
&+ 4(1038\overline{\mathbb{C}}^4 + 30\overline{\mathbb{C}}^2\overline{\mathbb{C}_c^2} + 18\overline{\mathbb{C}_c^2}^2 - 5\overline{\mathbb{C}_c^4} + 114\overline{\mathbb{C}_c^{\triangleright}} - 168\overline{\mathbb{C}_c^{\diamond}} + 2\overline{\mathbb{C}}\,\overline{\mathbb{C}_c^3} - 8\overline{\mathbb{C}}\,\overline{\mathbb{C}_c^{\triangle}}) f_1^{d+6}(z) \\
&- 2(1818\overline{\mathbb{C}}^4 + 54\overline{\mathbb{C}}^2\overline{\mathbb{C}_c^2} + 39\overline{\mathbb{C}_c^2}^2 + \overline{\mathbb{C}}\,\overline{\mathbb{C}_c^3} - 9\overline{\mathbb{C}_c^4} + 204\overline{\mathbb{C}_c^{\triangleright}} - 294\overline{\mathbb{C}_c^{\diamond}} - 22\overline{\mathbb{C}}\,\overline{\mathbb{C}_c^{\triangle}}) f_1^{d+4}(z) \\
&+ (1583\overline{\mathbb{C}}^4 + 48\overline{\mathbb{C}}^2\overline{\mathbb{C}_c^2} + 36\overline{\mathbb{C}_c^2}^2 - \overline{\mathbb{C}}\,\overline{\mathbb{C}_c^3} - 6\overline{\mathbb{C}_c^4} + 186\overline{\mathbb{C}_c^{\triangleright}} - 258\overline{\mathbb{C}_c^{\diamond}} + 8\overline{\mathbb{C}}\,\overline{\mathbb{C}_c^{\triangle}}) f_1^{d+2}(z) \\
&+ (-358\overline{\mathbb{C}}^4 - 21\overline{\mathbb{C}}^2\overline{\mathbb{C}_c^2} - 6\overline{\mathbb{C}_c^2}^2 + 6\overline{\mathbb{C}}\,\overline{\mathbb{C}_c^3} - 48\overline{\mathbb{C}_c^{\triangleright}} + 60\overline{\mathbb{C}_c^{\diamond}} - 37\overline{\mathbb{C}}\,\overline{\mathbb{C}_c^{\triangle}}) f_1^{d}(z) \\
&+ (35\overline{\mathbb{C}}^4 + 12\overline{\mathbb{C}}^2\overline{\mathbb{C}_c^2} - 3\overline{\mathbb{C}}\,\overline{\mathbb{C}_c^3} + 6\overline{\mathbb{C}_c^{\triangleright}} - 6\overline{\mathbb{C}_c^{\diamond}} + 23\overline{\mathbb{C}}\,\overline{\mathbb{C}_c^{\triangle}}) f_1^{d-2}(z) \\
&+ (-3\overline{\mathbb{C}}^2 - 7\overline{\mathbb{C}}\,\overline{\mathbb{C}_c^{\triangle}}) f_1^{d-4}(z) + \overline{\mathbb{C}}\,\overline{\mathbb{C}_c^{\triangle}} f_1^{d-6}(z)
\end{aligned}
\tag{7.35}
$$

$$
\begin{aligned}
&\sum_{\text{loops}} (\det \mathfrak{D}^{(0)})^{-d/2} \frac{\overline{\mathrm{Tr} M^4}(-z)^{N+1}}{N!} \\
&= 8(222\overline{\mathbb{C}}^4 + 6\overline{\mathbb{C}}^2\overline{\mathbb{C}_c^2} + 3\overline{\mathbb{C}_c^2}^2 - \overline{\mathbb{C}_c^4} + 24\overline{\mathbb{C}_c^{\triangleright}} - 36\overline{\mathbb{C}_c^{\diamond}}) f_1^{d+8}(z) \\
&+ 4(1116\overline{\mathbb{C}}^4 + 36\overline{\mathbb{C}}^2\overline{\mathbb{C}_c^2} + 23\overline{\mathbb{C}_c^2}^2 - 6\overline{\mathbb{C}_c^4} + 128\overline{\mathbb{C}_c^{\triangleright}} - 180\overline{\mathbb{C}_c^{\diamond}} + 4\overline{\mathbb{C}}\,\overline{\mathbb{C}_c^3} - 16\overline{\mathbb{C}}\,\overline{\mathbb{C}_c^{\triangle}}) f_1^{d+6}(z) \\
&- 4(1110\overline{\mathbb{C}}^4 + 39\overline{\mathbb{C}}^2\overline{\mathbb{C}_c^2} + 31\overline{\mathbb{C}_c^2}^2 + 10\overline{\mathbb{C}}\,\overline{\mathbb{C}_c^3} - 7\overline{\mathbb{C}_c^4} + 136\overline{\mathbb{C}_c^{\triangleright}} - 178\overline{\mathbb{C}_c^{\diamond}} - 36\overline{\mathbb{C}}\,\overline{\mathbb{C}_c^{\triangle}}) f_1^{d+4}(z) \\
&+ (2473\overline{\mathbb{C}}^4 + 72\overline{\mathbb{C}}^2\overline{\mathbb{C}_c^2} + 82\overline{\mathbb{C}_c^2}^2 + 36\overline{\mathbb{C}}\,\overline{\mathbb{C}_c^3} - 16\overline{\mathbb{C}_c^4} + 304\overline{\mathbb{C}_c^{\triangleright}} - 396\overline{\mathbb{C}_c^{\diamond}} - 128\overline{\mathbb{C}}\,\overline{\mathbb{C}_c^{\triangle}}) f_1^{d+2}(z) \\
&+ (-955\overline{\mathbb{C}}^4 - 12\overline{\mathbb{C}}^2\overline{\mathbb{C}_c^2} - 36\overline{\mathbb{C}_c^2}^2 - 12\overline{\mathbb{C}}\,\overline{\mathbb{C}_c^3} + 5\overline{\mathbb{C}_c^4} - 92\overline{\mathbb{C}_c^{\triangleright}} + 154\overline{\mathbb{C}_c^{\diamond}} + 68\overline{\mathbb{C}}\,\overline{\mathbb{C}_c^{\triangle}}) f_1^{d}(z) \\
&+ (288\overline{\mathbb{C}}^4 + 12\overline{\mathbb{C}_c^2}^2 - \overline{\mathbb{C}_c^4} + 12\overline{\mathbb{C}_c^{\triangleright}} - 47\overline{\mathbb{C}_c^{\diamond}} - 24\overline{\mathbb{C}}\,\overline{\mathbb{C}_c^{\triangle}}) f_1^{d-2}(z) \\
&+ (-60\overline{\mathbb{C}}^4 - 2\overline{\mathbb{C}_c^2}^2 + 10\overline{\mathbb{C}_c^{\diamond}} + 4\overline{\mathbb{C}}\,\overline{\mathbb{C}_c^{\triangle}}) f_1^{d-4}(z) + (6\overline{\mathbb{C}}^4 - \overline{\mathbb{C}_c^{\diamond}}) f_1^{d-6}(z)
\end{aligned}
\tag{7.36}
$$

## 7.2 Renormalized coupling

Our purpose is to guess the exact form of the renormalized coupling $g(z)$ as a function of $2-D$ on a manifold of toroidal topology. The information that is of our disposal are the exact results in both $D=2$ (6.38) and $D=1$ (D.24) as well as the exact resummed series up to the fourth order in $2-D$.
From the structure of the expansion of $g(z)$ in powers of $2-D$ it is clear (see also discussion of the *Mathematica*®-program in the appendix) that to each order in $2-D$ $g(z)$ can be expressed in terms of $f_1^d s$ (6.45). Since

$$f_1^d(z) = \frac{z}{\Gamma(\frac{d}{2})} \int_0^\infty \mathrm{d}r\; r^{d/2-1} \exp[-z\mathrm{e}^{-r} - r] \;, \tag{7.37}$$

the exact $g(z)$ as a function of $2-D$ will be of the form:

$$g(z) \equiv g(D,z) = z \int_0^\infty \mathrm{d}r\; \tilde{g}(D,r) \exp[-z\mathrm{e}^{-r} - r] \;, \tag{7.38}$$

where $\tilde{g}(D,r)$ has some expansion in powers of $2-D$. To zeroth order corresponding to $D=2$ one has:

$$\tilde{g}(2,r) = \frac{r^{d/2}}{\Gamma(\frac{d}{2}+1)} \;. \tag{7.39}$$

Analyzing the series data from the preceding subsection reveals the following structure of the expansion of $\tilde{g}(D,z)$:

$$\tilde{g}(D,r) = r^{d/2} \left( \frac{1}{\Gamma(\frac{d}{2}+1)} + (2-D)\mathcal{P}(2-D,r) \right) \;, \tag{7.40}$$

where $\mathcal{P}(2-D,r)$ is analytic in $D=2$, such that

$$\mathcal{P}(2-D,r) = \sum_{n=0}^{\infty} \mathcal{P}_n(r)(2-D)^n \;, \tag{7.41}$$

and the $n$th order coefficient $\mathcal{P}_n(r)$ has a Laurent series in $r$:

$$\mathcal{P}_n(r) = \sum_{j=-n_{\max}}^{n} p_{n_j} r^j \;. \tag{7.42}$$

Note that powers $\alpha$ of $r$ on the level of $\tilde{g}$ (7.40) translate after integrating over $r$ (7.38) into powers $\alpha$ of $\log z$ (clarify 6.46). Therefore, positive powers of $r$ dominate the behavior for large $z$ (strong coupling).
Let us write down the terms of the expansion of $\tilde{g}(D,r)$ up to the third order in $2-D$ as one obtains them from the generated series contributions of the preceding subsection:

$$\tilde{g}(D,r) = r^{d/2} \left[ \frac{1}{\Gamma(\frac{d}{2}+1)} + (2-D)\frac{d}{2}\overline{\mathbb{C}} \left( \frac{1}{\Gamma(\frac{d}{2}+1)} - \frac{r^{-1}}{\Gamma(\frac{d}{2})} \right) \right.$$

$$
\begin{aligned}
&-(2-D)^2\left(\frac{d}{2}\left(1+\frac{d}{2}\right)\overline{\mathbb{C}_c^2}\frac{r}{\Gamma(\frac{d}{2}+2)}+\frac{\frac{d}{4}\left(\overline{\mathbb{C}}^2-4\overline{\mathbb{C}_c^2}\right)-\frac{d^2}{8}\left(2\overline{\mathbb{C}_c^2}+\overline{\mathbb{C}}^2\right)}{\Gamma(\frac{d}{2}+1)}\right.\\
&\left.+\frac{\left(\frac{d}{4}\left(-\overline{\mathbb{C}}^2+3\overline{\mathbb{C}_c^2}\right)-\frac{d^2}{8}\left(2\overline{\mathbb{C}}^2\right)\right)r^{-1}}{\Gamma(\frac{d}{2})}+\frac{\left(-\frac{d}{4}\overline{\mathbb{C}_c^2}+\frac{d^2}{8}\overline{\mathbb{C}}^2\right)r^{-2}}{\Gamma(\frac{d}{2}-1)}\right)\\
&+(2-D)^3\left(\frac{\left(\frac{d^2}{2}+\frac{d^3}{12}\right)\left(\overline{\mathbb{C}_c^3}-4\,\overline{\mathbb{C}_c^{\triangle}}\right)r^2}{\Gamma(\frac{d}{2}+3)}\right.\\
&+\frac{\left(d\left(\overline{\mathbb{C}_c^3}-4\,\overline{\mathbb{C}_c^{\triangle}}\right)+\frac{d^2}{8}\left(-8\,\overline{\mathbb{C}_c^3}+32\,\overline{\mathbb{C}_c^{\triangle}}+2\,\overline{\mathbb{C}\mathbb{C}_c^2}\right)+\frac{d^3}{48}\left(-4\,\overline{\mathbb{C}_c^3}+24\,\overline{\mathbb{C}_c^{\triangle}}-6\,\overline{\mathbb{C}\mathbb{C}_c^2}\right)\right)r}{\Gamma(\frac{d}{2}+2)}\\
&+\frac{\left(\frac{d}{4}\left(-10\,\overline{\mathbb{C}_c^3}+36\,\overline{\mathbb{C}_c^{\triangle}}+6\overline{\mathbb{C}\mathbb{C}_c^2}\right)+\frac{d^2}{8}\left(6\,\overline{\mathbb{C}_c^3}-20\,\overline{\mathbb{C}_c^{\triangle}}+2\,\overline{\mathbb{C}\mathbb{C}_c^2}-6\,\overline{\mathbb{C}}^3\right)+\frac{d^3}{48}\left(-8\,\overline{\mathbb{C}_c^{\triangle}}+12\,\overline{\mathbb{C}\mathbb{C}_c^2}+\overline{\mathbb{C}}^3\right)\right)}{\Gamma(\frac{d}{2}+1)}\\
&+\frac{\left(\frac{d}{4}\left(9\overline{\mathbb{C}_c^3}-32\overline{\mathbb{C}_c^{\triangle}}-12\overline{\mathbb{C}\mathbb{C}_c^2}+\overline{\mathbb{C}}^3\right)+\frac{d^2}{8}\left(-2\overline{\mathbb{C}_c^3}+4\overline{\mathbb{C}_c^{\triangle}}-7\overline{\mathbb{C}\mathbb{C}_c^2}+2\overline{\mathbb{C}}^3\right)-\frac{d^3}{16}\left(\overline{\mathbb{C}}^3+2\overline{\mathbb{C}\mathbb{C}_c^2}\right)\right)\,r^{-1}}{\Gamma(\frac{d}{2})}\\
&+\frac{\left(\frac{d}{4}\left(3\overline{\mathbb{C}_c^3}-17\overline{\mathbb{C}_c^{\triangle}}-9\overline{\mathbb{C}\mathbb{C}_c^2}+\overline{\mathbb{C}}^3\right)-\frac{d^2}{8}\left(\overline{\mathbb{C}}^3-4\overline{\mathbb{C}\mathbb{C}_c^2}\right)+\frac{d^3}{16}\,\overline{\mathbb{C}}^3\right)\,r^{-2}}{\Gamma(\frac{d}{2}-1)}\\
&\left.\left.+\frac{\left(-\frac{3d}{4}\left(2\overline{\mathbb{C}_c^{\triangle}}+\overline{\mathbb{C}\mathbb{C}_c^2}\right)-\frac{d^2}{8}\,\overline{\mathbb{C}\mathbb{C}_c^2}-\frac{d^3}{48}\,\overline{\mathbb{C}}^3\right)\,r^{-3}}{\Gamma(\frac{d}{2}-2)}+\frac{\frac{d}{4}\,\overline{\mathbb{C}_c^{\triangle}}\,r^{-4}}{\Gamma(\frac{d}{2}-3)}\right)\right]
\end{aligned}
\tag{7.43}
$$

Clearly, one discovers the form (7.40). Let us also state $\tilde{g}(D,r)$ up to the fourth order, but taking to each order only the dominant contribution into account:

$$
\begin{aligned}
\tilde{g}(D,r)=r^{d/2}\;\Bigg[&\frac{1}{\Gamma(\frac{d}{2}+1)}+(2-D)\frac{\left(\frac{d}{2}\right)}{\Gamma(\frac{d}{2}+1)}\overline{\mathbb{C}}-(2-D)^2\frac{\frac{d}{2}\left(1+\frac{d}{2}\right)}{\Gamma(\frac{d}{2}+2)}\,\overline{\mathbb{C}_c^2}\,r\\
&+(2-D)^3\frac{\left(\frac{d^2}{2}+\frac{d^3}{12}\right)\left(\overline{\mathbb{C}_c^3}-4\overline{\mathbb{C}_c^{\triangle}}\right)}{\Gamma(\frac{d}{2}+3)}r^2\\
&-(2-D)^4\frac{\left(d+\frac{3}{4}d^2+\frac{d^3}{4}+\frac{d^4}{48}\right)\left(222\overline{\mathbb{C}}^4+6\overline{\mathbb{C}}^2\overline{\mathbb{C}_c^2}+3\overline{\mathbb{C}_c^2}^2-\overline{\mathbb{C}_c^4}+24\overline{\mathbb{C}_c^{\triangleright}}-36\overline{\mathbb{C}_c^{\diamond}}\right)}{\Gamma(\frac{d}{2}+4)}r^3+\cdots\Bigg]
\end{aligned}
\tag{7.44}
$$

For completeness let us state the result of the $2-D$-expansion of the renormalized coupling up to the fourth order. This time performing the integration in (7.38), such that we obtain $g$ as a function of the bare coupling in terms of the functions $f_k^d(z)$, whose asymptotic behavior has been analyzed in (6.46). For this purpose and for the sake of more compactness we need introduce a new notation: Since all series contributions are of the form as stated in (B.1), we

introduce vectors $\mathbb{M}$ such that

$$\sum_{\text{loops}} (\det \mathfrak{D}^{(0)})^{-d/2} \overline{\frac{\prod_{i=1}^{l} (\mathrm{Tr} M^{n_i})^{m_i}}{N!}} (-z)^N \equiv \sum_{j=\min}^{\max} \mathbb{M}_{\binom{m_1\, m_2 \cdots m_l}{n_1\, n_2 \cdots n_l}} f_1^{d+2j}(z)$$
$$\equiv \mathbb{M}^j_{\left(\begin{smallmatrix} m_1\, m_2 \cdots m_l \\ n_1\, n_2 \cdots n_l \end{smallmatrix}\middle|\begin{smallmatrix} \max \\ \min \end{smallmatrix}\right)} f_1^{d+2j}(z) \ , \qquad (7.45)$$

where max and min are some integers, and summation over the double index $j$ is implicit. Inserting the results for the resummed series contributions into (6.14) we find for the renormalized coupling to the fourth order in $2-D$:

$$\begin{aligned} g(z) = {} & f_1^{d+2}(z) - (2-D)\,\frac{d}{2}\mathbb{M}^j_{\left(\begin{smallmatrix}1\\1\end{smallmatrix}\middle|\begin{smallmatrix}1\\0\end{smallmatrix}\right)} f_1^{d+2j}(z) + (2-D)^2 \left(\frac{d}{4}\mathbb{M}^j_{\left(\begin{smallmatrix}1\\2\end{smallmatrix}\middle|\begin{smallmatrix}2\\-1\end{smallmatrix}\right)} f_1^{d+2j}(z) + \frac{d^2}{8}\mathbb{M}^j_{\left(\begin{smallmatrix}2\\1\end{smallmatrix}\middle|\begin{smallmatrix}2\\-1\end{smallmatrix}\right)} f_1^{d+2j}(z)\right) \\ & - (2-D)^3 \left(\frac{d}{4}\mathbb{M}^j_{\left(\begin{smallmatrix}1\\3\end{smallmatrix}\middle|\begin{smallmatrix}2\\-3\end{smallmatrix}\right)} f_1^{d+2j}(z) + \frac{d^2}{8}\mathbb{M}^j_{\left(\begin{smallmatrix}1&1\\1&2\end{smallmatrix}\middle|\begin{smallmatrix}3\\-2\end{smallmatrix}\right)} f_1^{d+2j}(z) + \frac{d^3}{48}\mathbb{M}^j_{\left(\begin{smallmatrix}3\\1\end{smallmatrix}\middle|\begin{smallmatrix}3\\-2\end{smallmatrix}\right)} f_1^{d+2j}(z)\right) \\ & + (2-D)^4 \left(\frac{d}{8}\mathbb{M}^j_{\left(\begin{smallmatrix}4\\1\end{smallmatrix}\middle|\begin{smallmatrix}4\\-3\end{smallmatrix}\right)} f_1^{d+2j}(z) + \frac{d^2}{8}\left(\frac{1}{4}\mathbb{M}^j_{\left(\begin{smallmatrix}2\\2\end{smallmatrix}\middle|\begin{smallmatrix}4\\-3\end{smallmatrix}\right)} f_1^{d+2j}(z) + \frac{2}{3}\mathbb{M}^j_{\left(\begin{smallmatrix}1&1\\1&3\end{smallmatrix}\middle|\begin{smallmatrix}4\\-3\end{smallmatrix}\right)} f_1^{d+2j}(z)\right)\right. \\ & \left. + \frac{d^3}{32}\mathbb{M}^j_{\left(\begin{smallmatrix}2&1\\1&2\end{smallmatrix}\middle|\begin{smallmatrix}4\\-3\end{smallmatrix}\right)} f_1^{d+2j}(z) + \frac{d^4}{384}\mathbb{M}^j_{\left(\begin{smallmatrix}4\\1\end{smallmatrix}\middle|\begin{smallmatrix}4\\-3\end{smallmatrix}\right)} f_1^{d+2j}(z)\right) + O(2-D)^5 \end{aligned} \qquad (7.46)$$

The vector entries $\mathbb{M}^j$ are to be be taken from subsection 7.1.

### 7.3 Discussion of possible forms of $\tilde{g}(D,r)$

Before making a guess for the exact $\tilde{g}(r)$ and thus implicitly for $g(z)$, let us summarize the properties, to which $g(z)$ as a function of the internal dimension $D$ has to obey.

(I) In the limit $D=2$ $g(z)$ has to tend to the exact form as it is given by (6.38). Note, that in this limit $g(z)$ diverges logarithmically. There is no strong coupling expansion in $D=2$.

(II) A phantom polymer closed to form a ring corresponds to the limit $D=1$ of the toroidal manifold. This case has also been solved exactly. There are both weak- and strong coupling expansions available (D.23,D.34). In particular, $g(z)$ tends to a finite fixed point value as $z$ tends to $\infty$. In view of the logarithmic divergence in $D=2$ and the renormalizability of the theory for internal dimensions $0<D<2$ [47,48], we expect finiteness of $\lim_{z\to\infty} = g^*$ as soon as $2-D$ becomes positive. Then, we expect the existence of a strong coupling expansion starting with the fixed point value and a term, which encodes the correction to scaling behavior of the theory:

$$g(D,z) = g^*(D) + C_1(D,\ln z)\; z^{-\omega_1/\varepsilon} + C_2(D,\ln z)\; z^{-\omega_2/\varepsilon} + \cdots \ , \qquad (7.47)$$

$\omega_1, \omega_2, \omega_2 - \omega_1 > 0$ a.s.f.., and the scaling functions $C_i$ diverge at most subexponentially for large arguments. Powerlaw behavior in the strong coupling limit necessitates the resummation

of the series expansion (7.43) to turn into some exponentially growing function $\tilde{g}(D,r)$. This can be seen as follows:

$$\begin{aligned} f^2_{1+\frac{\omega}{\varepsilon}}(z) &= z^{1+\frac{\omega}{\varepsilon}} \int_0^\infty \mathrm{d}r\ \exp[-z\,\mathrm{e}^{-r} - (1+\omega/\varepsilon)r] = \Gamma(1+\frac{\omega}{\varepsilon}) + O(\mathrm{e}^{-z}) \\ \Rightarrow z^{-\omega/\varepsilon} &= \frac{z}{\Gamma(1+\frac{\omega}{\varepsilon})} \int_0^\infty \mathrm{d}r\ \exp[-z\,\mathrm{e}^{-r} - (1+\omega/\varepsilon)r] + O(\mathrm{e}^{-z}) \\ &= \frac{z}{\Gamma(1+\frac{\omega}{\varepsilon})} \sum_{n=0}^\infty \int_0^\infty \mathrm{d}r\ \frac{(-\omega/\varepsilon\, r)^n}{n!} \exp[-z\,\mathrm{e}^{-r} - r] + O(\mathrm{e}^{-z}) \\ &= \frac{1}{\Gamma(1+\frac{\omega}{\varepsilon})} \sum_{n=0}^\infty \frac{(-\omega/\varepsilon)^n}{n!} f_1^{2(n+1)}(z) + O(\mathrm{e}^{-z})\,, \end{aligned} \tag{7.48}$$

where it is to be understood that $\omega$ is expanded in powers of $2-D$.
Let us now postulate a possible form of $\tilde{g}(D,r)$ obeying to the demanded properties (I) and (II):

$$\tilde{g}(D,r) = \mathcal{C}\left(\frac{1-\mathrm{e}^{-\frac{\omega}{\varepsilon} r \mathcal{S}(2-D,r)}}{\omega/\varepsilon}\right)^{d/2}\,, \tag{7.49}$$

where $\mathcal{S}$ is analytic in $D=2$ such that

$$\mathcal{S}(2-D,r) = \sum_{n=0}^\infty \mathcal{S}_n(r)(2-D)^n \tag{7.50}$$

and to each order in $2-D$, there is a Laurent series of the $\mathcal{S}_n(r)$ of the form

$$\mathcal{S}_n(r) = \sum_{j=-\infty}^0 s_{n_j}\, r^j\,. \tag{7.51}$$

Furthermore, $\omega/\varepsilon$ has some expansion in powers of $2-D$:

$$\omega/\varepsilon = \omega_n(2-D)^n + O(2-D)^{n+1}\,. \tag{7.52}$$

Let us once again stress that powers in $r$ at the level of $\tilde{g}(r)$ translate into powers in $\log z$, while exponential growth in $r$ is providing powerlaw behavior for large $z$. Therefore, (7.49) obeys to the demanded properties (I) and (II). Note in particular, that setting $\mathcal{S}=1$ and integrating over $r$ according to (7.37) the expression in parentheses resembles to

$$\log z = \lim_{D\to 2} \frac{1-z^{-(2-D)}}{2-D}\,. \tag{7.53}$$

The r.h.s. expression above grows logarithmically in the limit $D=2$ and shows up a fixed point together with a strong coupling expansion as soon as $2-D>0$.
Let us expand (7.34) in powers of $2-D$ taking only the leading term of $\omega/\varepsilon$ into account:

$$\tilde{g}(D,r) = \mathcal{C}\left(r\ \mathcal{S}(2-D,r) - \frac{\omega_n(2-D)^n r^2}{2!}\mathcal{S}^2(2-D,r) + \cdots\right)^{d/2} \tag{7.54}$$

Inserting the expansion of $\mathcal{S}(2-D,r)$,

$$\mathcal{S}(2-D,r) = \mathcal{S}_0(r) + (2-D)\mathcal{S}_1(r) + O(2-D)^2 \,, \tag{7.55}$$

and expanding everything provides:

$$\begin{aligned}\tilde{g}(D,r) = \mathcal{C}\; r^{d/2}\; \mathcal{S}_0(r) \;\times \\ \times \left(1 + (2-D)\frac{d}{2}\frac{\mathcal{S}_1(r)}{\mathcal{S}_0(r)} + (2-D)^2\frac{d}{2}\frac{\mathcal{S}_2(r)}{\mathcal{S}_0(r)} - \frac{\omega_n(2-D)^n d}{4} r \right. \\ \left. + \frac{(2-D)^2}{2!}\frac{d}{2}\left(\frac{d}{2}-1\right)\left(\frac{\mathcal{S}_1(r)}{\mathcal{S}_0(r)}\right)^2 + O(2-D)^3\right)\end{aligned} \tag{7.56}$$

Matching the coefficients of the expansion above with the result in (7.43) we set:

$$\begin{aligned}\mathcal{C} &= \frac{1}{\Gamma(\frac{d}{2}+1)} \\ \mathcal{S}_0(r) &= 1 \\ \mathcal{S}_1(r) &= \overline{\mathbb{C}}\;\left(1 - \frac{d}{2}\frac{1}{r} + O(1/r^2)\right) \\ \omega_n \equiv \omega_2 &= 2\,\overline{\mathbb{C}_c^2}\,,\end{aligned} \tag{7.57}$$

where we have skipped all higher order poles in the Laurent series of $\mathcal{S}_1(r)$
From the above considerations it follows that the correction to scaling exponent $\omega$ reads to lowest order in $2-D$:

$$\omega = \varepsilon\; 2\overline{\mathbb{C}_c^2}\;(2-D)^2 + O(2-D)^3 \,. \tag{7.58}$$

The result coincides with what we have found in the preceding section from the calculation within the scheme in the renormalized coupling.
Let us point out, however, that the scheme above is not unambiguous. Going to the next order it will turn out that the sum in (7.51) actually has to be extended to $j = 1$ in order to provide consistency with the expansion $(7.43)$. But then, it is not unambiguous, whether the term proportional to $r^{d/2+1}$ has to be attributed to $\omega_2$ or rather to $\mathcal{S}_2(r)$. From some simple general considerations one can easily see that it is in principle impossible to extract any information about the correction to scaling exponent from an expansion like (7.43) as long as one has no further information about the behavior of scaling functions like $\mathcal{S}(r)$ available. The only thing that we can conclude for sure is that the correction to scaling exponent in an ensemble of a manifold of toroidal topology and internal dimension close to $D = 2$, which interacts with a single short-range defect, is proportional to some power of $2-D$ and that this power is larger than 1:

$$\omega \sim (2-D)^n \,, \qquad n \geq 2 \,. \tag{7.59}$$

Actually, higher than linear powers of $r$ in the exponent (7.49) are fatal, because they destroy the scaling behavior for $z \to \infty$, which was intended to be encoded in the exponent $\omega/\varepsilon$.
Therefore, let us discuss another ansatz for $\tilde{g}(D,r)$ that does not show higher than linear powers of $r$ in the exponent as in (7.49):

$$\tilde{g}(D,r) = \mathcal{C}\left(\frac{1 - \mathcal{S}(2-D,r)\;\mathrm{e}^{-\frac{\omega}{\varepsilon}r}}{\omega/\varepsilon}\right)^{d/2} \,, \tag{7.60}$$

where $\mathcal{S}$ can be written as

$$\mathcal{S}(2-D,r) = 1 + \frac{\omega}{\varepsilon} r\ \tilde{\mathcal{S}}(2-D,r) \tag{7.61}$$

$\tilde{\mathcal{S}}$ being analytic in $D = 2$ such that

$$\tilde{\mathcal{S}}(2-D,r) = \sum_{n=1}^{\infty} \tilde{\mathcal{S}}_n(r)(2-D)^n \tag{7.62}$$

and to each order in $2 - D$, there is a Laurent series of the $\tilde{\mathcal{S}}_n(r)$ of the form

$$\tilde{\mathcal{S}}_n(r) = \sum_{j=-n_{\min}}^{n_{\max}} \tilde{s}_{n_j}\ r^j\ . \tag{7.63}$$

In contrast to (7.51) there is no restriction for positive powers in $r$, but we have to set

$$\mathcal{S}_0(r) \equiv 1 \tag{7.64}$$

from the beginning in order to obey to the properties (I) and (II).
Furthermore, $\omega/\varepsilon$ has some expansion in powers of $2 - D$:

$$\omega/\varepsilon = \omega_n(2-D)^n + O(2-D)^{n+1}\ . \tag{7.65}$$

Expanding first the expression in parenthesis of (7.60) taking only the lowest order of $\omega/\varepsilon$ into account leads to

$$\begin{aligned}\frac{1-\mathcal{S}(2-D,r)\,\mathrm{e}^{-\frac{\omega}{\varepsilon}r}}{\omega/\varepsilon} &= -r\ \left(\tilde{\mathcal{S}}_1(r)(2-D) + \tilde{\mathcal{S}}_2(r)(2-D)^2 + \tilde{S}_3(r)(2-D)^3\right) \\ &\quad + r\ \left(1 + \frac{\omega}{\varepsilon} r\ \tilde{\mathcal{S}}_1(r)(2-D)\right) - \frac{\omega}{\varepsilon}\frac{r^2}{2!} + \cdots\ ,\end{aligned} \tag{7.66}$$

where we have expanded $\mathcal{S}$ up to the third order in $2-D$. $\omega$ is at least of second order in $2-D$. Skipping all higher than third order terms and expanding everything in (7.54), we obtain:

$$\begin{aligned}\tilde{g}(D,r) &= \mathcal{C}\ r^{d/2}\left(1 - \tilde{\mathcal{S}}_1(r)(2-D) - \left(\frac{\omega_2}{2!}r + \tilde{\mathcal{S}}_2(r)\right)(2-D)^2\right. \\ &\qquad \left. - \left(-\frac{\omega_2}{2!} r\ \tilde{S}_1(r) + \frac{\omega_3}{2!}r + \tilde{S}_3(r)\right)(2-D)^3\right)^{d/2} \\ &= \mathcal{C}\ r^{d/2}\left(1 - \frac{d}{2}\left(\tilde{\mathcal{S}}_1(r)(2-D) + \left(\frac{\omega_2}{2!}r + \tilde{\mathcal{S}}_2(r)\right)(2-D)^2\right.\right. \\ &\quad \left. + \left(-\frac{\omega_2}{2!} r\ \tilde{S}_1(r) + \frac{\omega_3}{2!}r + \tilde{S}_3(r)\right)(2-D)^3\right) \\ &\quad + \frac{d}{4}\left(\frac{d}{2}-1\right)\left(\tilde{\mathcal{S}}_1^2(r)(2-D)^2 + 2\tilde{S}_1(r)\left(\tilde{S}_2(r) + \frac{\omega_2}{2!}\right)(2-D)^3\right) \\ &\quad \left. + \frac{d}{12}\left(\frac{d}{2}-1\right)\left(\frac{d}{2}-2\right)\left(\tilde{S}_1^3(r)(2-D)^3\right)\right)\end{aligned} \tag{7.67}$$

This time one may set

$$\begin{aligned} \mathcal{C} &= \frac{1}{\Gamma(\frac{d}{2}+1)} \\ \mathcal{S}_0(r) &= 1 \\ \tilde{\mathcal{S}}_1(r) &= -\overline{\mathbb{C}} \left(1 - \frac{d}{2}\frac{1}{r} + O(1/r^2)\right) \\ \omega_2 &= 2\,\overline{\mathbb{C}_c^2}\,, \end{aligned} \tag{7.68}$$

in order to match with the expansion in (7.43). Again, we recover the same result for $\omega$ as from the previous ansatz and the calculation within the renormalized coupling:

$$\omega = \varepsilon\; 2\overline{\mathbb{C}_c^2}\;(2-D)^2 + O(2-D)^3\;. \tag{7.69}$$

However, there still remains the ambiguity in attributing the second order terms either to $\omega_2$ or to $\tilde{\mathcal{S}}_2$ as it is obvious from (7.67). Nevertheless, making any choice for $\omega_2$ it is clear, that the third order term $\tilde{\mathcal{S}}_3(r)$ has sufficiently many parameters free to get the third order reconciliated with the second order a.s.f.. Of course, the behavior of $\mathcal{S}(r)$ for large values of $r$ is supposed to stay subexponential. This corresponds to the same demand on the scaling functions $C_i$ in (7.47). There is some additional information about the scaling function $\mathcal{S}(r)$ necessary, in order to enable an unambiguous analysis of the scaling behavior for dimensions D close to 2 . From the structure of the expansion (7.46), however, it is not possible to make a guess about the precise properties of $\mathcal{S}(r)$. A way out might be a complete solution of the problem in $D = 1$ within the $2 - D$ expansion.

# 8 Discussion and conclusion

In this work, we have discussed the perturbation expansion of a $D$-dimensional elastic manifold interacting via a $\delta$-interaction with a fixed point in embedding space. This calculation can be done exactly for $D = 1$, but becomes non-trivial for $D \neq 1$. Interestingly and quite surprisingly, it simplifies considerably in the limit of $D \to 2$, if one decides to work at finite $\varepsilon$. In that limit we were able to obtain an explicit expression for the renormalized coupling as function of the bare one, in terms of a non-trivial series. Analysis of this series shows that in the limit of large values of the bare coupling $z$, corresponding to strong repulsion or equivalently to large membrane sizes, the renormalized coupling $g$ diverges logarithmically as a function of $z$. This yields a vanishing correction-to-scaling exponent $\omega$ in the limit $D = 2$. Furthermore, dependent on the dimensionality $d$ of the embedding space the $\beta$-function shows up a zero at infinite bare coupling as $0 \leq d < 2$. Then, the renormalization flow tends to a fixed point, and the theory becomes scale invariant in this limit. Due to the logarithmic divergence of the renormalized coupling, however, the corresponding zero of the $\beta$-function in terms of the latter is, too, shifted to infinity. This is quite a remarkable result, because it reveals that the strong coupling behavior of a "phantom", polymerized membrane in a crumpled phase interacting with a $\delta$-like defect in embedding space is only accessible through a non-perturbative treatment and always largely deviates qualitatively from any finite loop expansion, be it within a minimal subtraction scheme or at finite $\varepsilon$.
Also, it is important to note that this result is completely independent of the regularization procedure. This does no longer hold true beyond the leading order, which should be accessible to an expansion in $2 - D$. We constructed its first order in a specific regularization scheme in [49]. While this reproduces qualitatively correctly the known result in $D = 1$ (and even exactly for $d = 0$), it suffers from its inconsistent renormalization scheme, which neglects the boundaries of a finite manifold. We used a hard cutoff in position space, while working with the infinite $D$-space correlator. It seems that only in an $\varepsilon$-expansion this procedure is systematic. Now, we have overcome this problem by constructing the $2 - D$-expansion on a manifold of toroidal shape of finite size, thus imposing periodic boundary conditions on the field. There is no further infrared cutoff necessary. We have carried out the expansion of the renormalized coupling up to the fourth order in $2 - D$. This reveals part of the general structure of the expansion. It is important to point out that in considering $g$ as a function of the bare coupling the limits $D \to 2$ and strong coupling ($z \to \infty$) can not be interchanged. While $g$ tends to infinity as $z$ does in $D = 2$, we expect finiteness of this limit as soon as $2 - D > 0$ and the existence of a strong coupling expansion as found for polymers ($D = 1$). We were able to guess an exact $g(D, z)$ as a function of $z$ and the internal dimension $D$, which satisfies these properties and which can be reconciliated with the available expansion in $2 - D$ by an appropriate matching of its free parameters. However, this matching is not unambiguous and therefore does not provide a decent determination of the prefactor in the relation

$$\omega \sim (2 - D)^2 \,. \tag{8.1}$$

The correction-to-scaling exponent $\omega$ is closely related to observables, which are accessible to Monte-Carlo simulations. This is for instance the monomer density at the potential of a membrane, which is pinned by one of its points close to the defect.

While results for the pinning problem are interesting in its own, the main motivation is certainly to obtain a better understanding of self-avoiding polymerized membranes. This model is well-behaved physically, since its fractal dimension $d_f$ is bounded by the dimension of the embedding space $d_f < d$. Preliminary studies [66] indicate that this problem can also be attacked by the methods developed in this work. This would be very welcome to check the 2-loop calculations [20,19] and the large-order behavior [67] on one side and numerical results (e.g. [34]) on the other.

# A Derivation of the kernel

Starting from the free theory with Hamiltonian

$$\mathcal{H}_0 = \frac{1}{2-D}\int_x \frac{1}{2}(\nabla r(x))^2 \tag{A.1}$$

yields the difference correlator

$$C^{kl}(x_1{-}x_2) := \left\langle \frac{1}{2}[r_k(x_1){-}r_l(x_2)]^2 \right\rangle_0 = \delta^{kl} C(x_1{-}x_2) \tag{A.2}$$

with

$$C(x_1{-}x_2) = |x_1{-}x_2|^{2-D}\ . \tag{A.3}$$

It can be shown as in [4] to be a solution in the sense of distributions of the Laplacian equation

$$\Delta C(x) = (2-D)S_D\delta^D(x)\ . \tag{A.4}$$

The difference correlator may be considered as the analytical continuation to values of $D<2$ of the usual two-point correlator. Let us shortly derive (A.3) starting from the well known form of the kernel in Fourier space

$$G(\vec{k}_1,\vec{k}_2) = \frac{\delta^D(\vec{k}_1{+}\vec{k}_2)}{(\vec{k}_1)^2}\ , \tag{A.5}$$

such that

$$G(x) = \frac{1}{(2\pi)^D}\int \mathrm{d}^D k\ \frac{\exp[i\vec{k}\vec{x}]}{k^2} \tag{A.6}$$

Introducing a Schwinger parametrization and splitting the integration over the momenta into a part integrating over the component, which is parallel to $\vec{x}$, and its complementary part leads to

$$\begin{aligned}
G(x) &= \frac{1}{(2\pi)^D}\int_0^\infty \mathrm{d}s \int_{-\infty}^{\infty} \mathrm{d}k_{\|} \int \mathrm{d}^{D-1}k_\perp\ \mathrm{e}^{ik_{\|}x - s(k_{\|}^2+k_\perp^2)} \\
&= \frac{1}{(2\pi)^D}\int_0^\infty \mathrm{d}s \int_{-\infty}^{\infty} \mathrm{d}k_{\|}\ \mathrm{e}^{-sk_{\|}^2+ik_{\|}x}\left(\int_{-\infty}^{\infty}\mathrm{d}k_\perp\ \mathrm{e}^{-sk_\perp^2}\right)^{D-1} \\
&= \frac{1}{(2\pi)^D}\int_0^\infty \mathrm{d}s\ \left(\frac{\pi}{s}\right)^{D/2}\mathrm{e}^{-\frac{x^2}{4s}} = \frac{1}{(2\sqrt{\pi})^D}\int_0^\infty \mathrm{d}s'\ s'^{D/2-2}\mathrm{e}^{-s'\frac{x^2}{4}} \\
&= \frac{1}{(2\sqrt{\pi})^D}\Gamma\left(\frac{D}{2}-1\right)\left(\frac{x^2}{4}\right)^{-(D/2-1)} = \frac{1}{S_D(2-D)}|x|^{2-D}
\end{aligned} \tag{A.7}$$

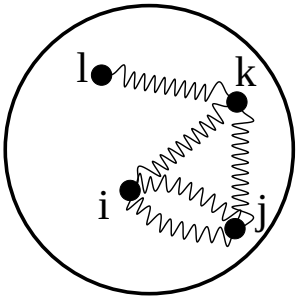


$$\equiv \qquad \overline{\mathbb{C}^2\,(x_i-x_j)\mathbb{C}(x_i-x_k)\mathbb{C}(x_j-x_k)\mathbb{C}(x_l-x_k)}$$

Figure B.1: Example of a fifth order diagram in the $2-D$-expansion.

# B *Mathematica*®–programs for the generation of the series contributions in the $2-D$-expansion

All terms to appear in the expansion in $2-D$ are of the form

$$\prod_{i=1}^{k}(\mathrm{Tr}M^{m_i})^{n_i}\ , m_i, n_i, k \in \mathbf{N} \tag{B.1}$$

as follows from (6.14). To $N$-loop order, $M$ is an $N \times N$-matrix as defined in (6.18). The diagrams to be evaluated at $n$th order in $2-D$ are positional averages of an ensemble of internal points on the manifold, which are connected through $n$ correlators as shown in the example of figure (B.1). The numerical value of the diagrams is determined through the topology of the graph, whose knots are given by the internal points and whose links correspond to the correlators joining them. It furthermore depends on the number of knots making up closed loops in the graph, but it does not depend on the loop order.
Then, the $N$-loop contribution at $n$th order in $2-D$ depends on the numerical value of the diagrams each coming up with a combinatorial factor involving the number of ways to form the corresponding graph from $N+1$ independent internal points. The combinatorial factor is a polynomial in $N$. Together with some power of the factor $(N+1)^{-1}$ from (6.17) the general form of the term (B.1) can be written as

$$\prod_{i=1}^{k}(\mathrm{Tr}M^{m_i})^{n_i} = \frac{P(N)}{(N+1)^{n_{\max}}}\ , n_{\max} \leq \sum_{i=1}^{k} m_i n_i\ , \tag{B.2}$$

and $P(N)$ is some polynomial in $N$. The degree of the polynomial is less than $2n$, if $n$ denotes the order in $2-D$.

In order to write down the term (B.1) as a function of $N$ we need know $P(N)$. Since its degree is bounded through $2n$, one can determine its coefficients through a fit-procedure to be applied on the values of (B.1) at the first $2n+1$ loop orders. This is done by the *Mathematica*®–modules, which are presented on the following pages. The module "Dreset" initializes the matrices $\mathfrak{D}^{(0)-1}$ and $\mathfrak{D}_{ik}$ (6.18) to obtain $M$. The "For" loop, which is individual for each

term (B.1) to be analyzed, recognizes the diagrams to appear and performs the evaluation to $N = 1, \ldots, N_{\max} \leq 2n + 1$ loops. Of course, the "values" are expressions involving finitely many diagrams.
The module "AnalyseListfkd" fits the $N_{\max}$ points through a polynomial being expanded in terms of the base given in (6.27).
Summing up all loop orders each term of the form (B.1) translates into some expression, which can be written in terms of the functions $f_k^d(z)$ as introduced in (6.39). This procedure is done by the module "Recognizefkd". Making several times use of the relation (6.45) all $f_k^{d\prime}s$ can be transformed into some $f_1^{d\prime}s$ making the leading behavior in the strong coupling limit obvious, which is then completely encoded in the upper index. This is done by "Reducefkd".
Finally, it might be convenient to express the diagrams in terms of positional averages of internal points, which are rather joint by the connected correlator as introduced in (7.6). The transcription of all expressions is performed by "Trans2Conn". The application of the discussed modules on the second order terms in the $2 - D$-expansion is also included in the sequel.

```
(* Initialization Cell *)
```

```
Dreset := Module[{},
  d[i_, j_] := c[n + 1, i] + c[n + 1, j] - c[i, j];
  c[i_, i_] := 0;
  SetAttributes[c, Orderless]; Dmat = Table[Table[d[j, i], {i, 1, n}], {j, 1, n}];
  D0 = IdentityMatrix[n] + Table[Table[1, {i, 1, n}], {j, 1, n}];
  D0m1 = IdentityMatrix[n] - 1 / (n + 1) Table[Table[1, {i, 1, n}], {j, 1, n}];
  ]; (* Module for the Inititialization of the matrices *)


listlen = 8  (* Global variables *)

8


AnalyseListfkd := Module[{ldl, wl, i, j, f1, res, h1, richtig},
  ldl = list[[listlen]] /. A_ * u_ /; NumberQ[u] → A;
  ldl = ldl /. ldl[[0]] → List;
  Print["Variables = ", ldl]; res = 0;
  For[i = 1, i ≤ Length[ldl], wl = (list /. {ldl[[i]] → 1});
   For[j = 1, j ≤ Length[ldl], wl = wl /. {ldl[[j]] → 0}; j++;];
   Print[i, ".) ", ldl[[i]], ": ", wl];
   f1 = Fit[wl, Prepend[Table[Product[x - i, {i, 0, n}], {n, 0, listlen - 2}], 1], x];
   f1 = f1 /. {u_ /; NumberQ[u] → Round[u]};
   res += f1 ldl[[i]];
   i++;];
  For[richtig = True; i = 1, i ≤ listlen, h1 = (res /. x → i) - list[[i]];
   If[h1 =!= 0, richtig = False; Print["Error: ", res, "/.x -> ", i, " != ", list[[i]]]]
   i++;];
  If[richtig, res, False]];


Recognizefkd := Module[{m, h},
  h = X //. x → 0;
  X = X - h - h f[1, d + max];
  Do[m = k;
   X = X //. Product[(-i + x), {i, 0, m}] → (-1)^(m) f[m + 2, d + max], {k, kmax, 0, -1}];
  X = X // Simplify;
  ];


Reducefkd := Module[{ma, mi, na, ni},
  Do[ma = l;
   Do[mi = k; X = X //. f[mi, d + ma] → (mi - 1) f[mi - 1, d + ma] - f[mi - 1, d + ma - 2];
    X = X // Simplify, {k, kmax, 2, -1}
    ], {l, max, -10, -2}
   ];
  X = X // Simplify;
  Do[na = o;
   Do[ni = n; X = Series[X, {f[na, d + ni], 0, 1}], {n, max, -10, -2}], {o, kmax, 1, -1}
   ];
  X = X // Simplify // Normal;
  Print[X];
  ];


Trans2Conn := Module[{na, ni},
  X = X //. C4 -> CC4 - 12 C2 C1^2 + 4 C3 C1 + 3 C1^4;
  X = X //. Csquare -> CCsquare - 5 C1^4;
  X = X //. Cblobtriangle -> CCblobtriangle + 2 Ctriangle C1 + C2 C1^2 - 2 C1^4;
  X = X //. C3 -> CC3 + 3 C2 C1 - 2 C1^3;
  X = X //. Ctriangle -> CCtriangle + C1^3;
  X = X //. C2 -> CC2 + C1^2;
  X = X // Simplify;
  Do[na = o;
   Do[ni = n; X = Series[X, {f[na, d + ni], 0, 1}], {n, max, 0, -2}], {o, kmax, 1, -1}
   ];
  X = X // Simplify // Normal;
  Print[X];
 ]
```

```
(* Here come the terms to be calculated *)
```

```
For[n = 0; list = {}, n < listlen, n++;
 Dreset;
 res1 = D0m1 . Dmat;
 res2 = res1 . res1;
 X = Sum[res2[[i, i]], {i, n}] // Expand;
 X = X //. c[__]^2 → C2;
 X = X //. c[__] → C1;
 X = X * (n + 1) // Expand;
 Print[n, ": ", X];
 list = Append[list, X];
 ]   (* The term Tr[(D0m1 D1)^2] *)
```

**AnalyseListfkd**

1: $2\,C2$

2: $-4\,C1^2 + 10\,C2$

3: $-18\,C1^2 + 30\,C2$

4: $-48\,C1^2 + 68\,C2$

5: $-100\,C1^2 + 130\,C2$

6: $-180\,C1^2 + 222\,C2$

7: $-294\,C1^2 + 350\,C2$

8: $-448\,C1^2 + 520\,C2$

Variables = $\{C1^2, C2\}$

1.) $C1^2$: $\{0, -4, -18, -48, -100, -180, -294, -448\}$

2.) $C2$: $\{2, 10, 30, 68, 130, 222, 350, 520\}$

$C1^2\,(-2\,(-1+x)\,x - (-2+x)\,(-1+x)\,x) + C2\,(2\,x + 3\,(-1+x)\,x + (-2+x)\,(-1+x)\,x)$

```
max = 4      (* First, adjust the global variables appropriately! *)
```

```
kmax = 9    (* f[kmax,d+max] *)
```

```
X = C1^2 (-2 (-1 + x) x - (-2 + x) (-1 + x) x) + C2 (2 x + 3 (-1 + x) x + (-2 + x) (-1 + x) x)
(* Tr (M^2) in terms of fkd's *)
```

**Recognizefkd**

**Reducefkd**

$(C1^2 - C2)\,f[1, -2+d] + (-4\,C1^2 + 3\,C2)\,f[1, d] + (5\,C1^2 - 4\,C2)\,f[1, 2+d] + (-2\,C1^2 + 2\,C2)\,f[1, 4+d]$

```
X = (C1^2 - C2) * f[1, -2 + d] + (-4 * C1^2 + 3 * C2) * f[1, d] +
 (5 * C1^2 - 4 * C2) * f[1, 2 + d] + (-2 * C1^2 + 2 * C2) * f[1, 4 + d]
```

**Trans2Conn**

$-CC2\,f[1, -2+d] + (-C1^2 + 3\,CC2)\,f[1, d] + (C1^2 - 4\,CC2)\,f[1, 2+d] + 2\,CC2\,f[1, 4+d]$

```
(* Here come the terms to be calculated *)
```

```
For[n = 0; list = {}, n < listlen, n++;
 Dreset;
 res1 = D0m1 . Dmat;
 X = (Sum[res1[[i, i]], {i, n}])^2 // Expand;
 X = X //. c[i_, j_] c[i_, j_] → C2;
 X = X //. c[__] → C1;
 X = X * (n + 1) // Expand;
 Print[n, ": ", X];
 list = Append[list, X];
 ]  (* The term Tr^2[D0m1 D1] *)
```

**AnalyseListfkd**

1: $2\,C2$

2: $8\,C1^2 + 4\,C2$

3: $30\,C1^2 + 6\,C2$

4: $72\,C1^2 + 8\,C2$

5: $140\,C1^2 + 10\,C2$

6: $240\,C1^2 + 12\,C2$

7: $378\,C1^2 + 14\,C2$

8: $560\,C1^2 + 16\,C2$

Variables = $\{C1^2, C2\}$

1.) $C1^2$: {0, 8, 30, 72, 140, 240, 378, 560}

2.) C2: {2, 4, 6, 8, 10, 12, 14, 16}

$2\,C2\,x + C1^2\,(4\,(-1+x)\,x + (-2+x)\,(-1+x)\,x)$

```
max = 4    (* First, adjust the global variables appropriately! *)
kmax = 9     (* f[kmax,d+max] *)
X = 2 C2 x + C1^2 (4 (-1 + x) x + (-2 + x) (-1 + x) x)    (* Tr^2 (M) in terms of fkd's *)
```

**Recognizefkd**

**Reducefkd**

$-C1^2\,f[1, -2+d] + 2\,C1^2\,f[1, d] + (C1^2 - 2\,C2)\,f[1, 2+d] + (-2\,C1^2 + 2\,C2)\,f[1, 4+d]$

```
X = -(C1^2 * f[1, -2 + d]) + 2 * C1^2 * f[1, d] +
  (C1^2 - 2 * C2) * f[1, 2 + d] + (-2 * C1^2 + 2 * C2) * f[1, 4 + d]
```

**Trans2Conn**

$-C1^2\,f[1, -2+d] + 2\,C1^2\,f[1, d] + (-C1^2 - 2\,CC2)\,f[1, 2+d] + 2\,CC2\,f[1, 4+d]$

# C Calculation of the diagrams in the $2-D$-expansion

In this section we will calculate the diagrams to appear in the $2-D$ expansion on the torus. It turns out that to obtain $\overline{\mathbb{C}}$ and $\overline{\mathbb{C}_c^2}$ we need evaluate two sums over discrete wavevectors obeying to periodic boundary conditions on the torus. Let us first derive the latter before turning to the explicit evaluation. Starting from the definition of the difference correlator $C(x)$,

$$C(x) := G(x) - G(0) \,, \tag{C.1}$$

where $G(x)$ is the usual two–point correlator, we obtain $C(x)$ through an inverse discrete Fourier–transformation from $G(k) = 1/\vec{k}^2$, which reads:

$$C(x) = \frac{1}{L^D} \sum_{\vec{k}\neq 0} \frac{1}{\vec{k}^2} \left(1 - \mathrm{e}^{i\vec{k}\vec{x}}\right) \,, \qquad \vec{k} = \frac{2\pi}{L}\vec{n} \,,\ \vec{n} \in \mathbf{Z}\times\mathbf{Z}\backslash\{\{0\}\times\mathbf{N}\} \,. \tag{C.2}$$

Performing the averaging procedure

$$\overline{C(x)} = \int_x C(x) \,, \tag{C.3}$$

where $1/L^D \int_x \mathrm{e}^{i\vec{k}\vec{x}} = \delta_{\vec{k}}^D$ is to be taken into account, the calculation of $\overline{C(x)}$ reduces to

$$\overline{C(x)} = I_1 := \sum_{k\neq 0} \frac{1}{\vec{k}^2} \,, \qquad \vec{k} = \frac{2\pi}{L}\vec{n} \,, \tag{C.4}$$

where $\vec{k}$ is $D$-dimensional, and the indices $n_i$ are running from $-\infty$ to $\infty$, $n_i = 0$ being excluded from the summation. Of course, in the expansion in powers of $2-D$ we need an analytic continuation to real values of D. Finally, to obtain $\overline{\mathbb{C}(x)}$ we have to subtract $\overline{\mathbb{C}^{(0)}(x)}$ from $\overline{C(x)}$. Due to our normalizations:

$$\overline{\mathbb{C}(x)} = S_D \left( \overline{C(x)} - \frac{\overline{\mathbb{C}^{(0)}(x)}}{2\pi(2-D)} \right) \,, \tag{C.5}$$

where $S_D$ denotes the volume of the unit sphere and $\overline{\mathbb{C}^{(0)}(x)} = 1$.
Turning to $\overline{\mathbb{C}_c^2(x)}$, we first note that within our normalizations we have

$$S_D^{-2}\overline{\mathbb{C}^2(x)} = \overline{(C(x) - \mathbb{C}^{(0)}(x)/(2\pi(2-D)))^2} = \overline{C(x)^2} - 2\frac{\overline{C(x)}}{2\pi(2-D)} + \frac{1}{(2\pi(2-D))^2} \tag{C.6}$$

and

$$S_D^{-2}\overline{\mathbb{C}(x)}^2 = \overline{C(x)}^2 - 2\frac{\overline{C(x)}}{2\pi(2-D)} + \frac{1}{(2\pi(2-D))^2} \tag{C.7}$$

according to (C.5), such that

$$\overline{\mathbb{C}_c^2(x)} \equiv \overline{\mathbb{C}^2(x)} - \overline{\mathbb{C}(x)}^2 = S_D^2 \left( \overline{C^2(x)} - \overline{C(x)}^2 \right) \,. \tag{C.8}$$

Knowing already the sum to be evaluated to obtain $\overline{C}$, (C.4), what is left to obtain is:

$$\overline{C^2(x)} = \int_y \int_x C^2(x) = \frac{1}{L^{2D}} \int_y \int_x \sum_{k_i \neq 0} \sum_{p_j \neq 0} \frac{1}{\vec{k}^2} \frac{1}{\vec{p}^2} \left( \mathrm{e}^{i\vec{k}\vec{x}} - 1 \right) \left( \mathrm{e}^{i\vec{p}\vec{x}} - 1 \right)$$

$$= \sum_{k_i \neq 0} \sum_{p_j \neq 0} \frac{1}{\vec{k}^2} \frac{1}{\vec{p}^2} \left( \delta^D_{\vec{k}+\vec{p}} - \delta^D_{\vec{k}} - \delta^D_{\vec{p}} + 1 \right) = \sum_{k_1 \neq 0} \frac{1}{\vec{k}^4} + \left[ \sum_{k_1 \neq 0} \frac{1}{\vec{k}^2} \right]^2 . \qquad \text{(C.9)}$$

Therefore,

$$S_D^{-2} \overline{\mathbb{C}_c^2(x)} = I_2 := \sum_{k \neq 0} \frac{1}{\vec{k}^4} , \qquad k_i = \frac{2\pi}{L} n_i . \qquad \text{(C.10)}$$

Let us first calculate $I_1$: Setting $L = 1$, renaming the indices $n_i$ into $k_i$ and introducing a Schwinger parametrization we have:

$$I_1 = \frac{1}{(2\pi)^2} \sum_{\substack{k_i = -\infty \\ k_i \neq 0}}^{\infty} \frac{1}{\vec{k}^2} = \frac{1}{(2\pi)^2} = \sum_{\substack{k_i = -\infty \\ k_i \neq 0}}^{\infty} \int_0^\infty \mathrm{d}s \, \mathrm{e}^{-s\vec{k}^2}$$

$$= \frac{1}{(2\pi)^2} \int_0^\infty \mathrm{d}s \left( \sum_{\substack{k=-\infty \\ k \neq 0}}^{\infty} \mathrm{e}^{-sk^2} \right)^D = \frac{1}{(2\pi)^2} \int_0^\infty \frac{\mathrm{d}s}{s^2} \left( \sum_{\substack{k=-\infty \\ k \neq 0}}^{\infty} \mathrm{e}^{-k^2/s} \right)^D , \qquad \text{(C.11)}$$

where it is to be noted that the sum in the last line is only one-dimensional. Furthermore, from now on it is clear, how $I_1$ is analytically continued to real values of $D$.
In order to evaluate this sum, we will make use of a Poisson-transformation, which reads:

$$\sum_{n=-\infty}^{\infty} \mathrm{e}^{-A(n-z/2)^2} = \sqrt{\frac{\pi}{A}} \sum_{l=-\infty}^{\infty} \mathrm{e}^{-\frac{\pi^2 l^2}{A} + i\pi l z} . \qquad \text{(C.12)}$$

The contribution from $l = 0$ is the approximation of the l.h.s. through a gaussian integral. Our aim is to calculate the coefficients of the $2 - D$ expansion of $I_1$ numerically using some algebraic manipulation program. Then, the integration interval in (C.11) has to be made finite. This is done as follows: For any $s_0 > 0$ we have

$$I_1 = \frac{1}{(2\pi)^2} \int_0^{s_0} \frac{\mathrm{d}s}{s^2} \left( \sum_{\substack{k=-\infty \\ k \neq 0}}^{\infty} \mathrm{e}^{-k^2/s} \right)^D + \frac{1}{(2\pi)^2} \int_{s_0}^\infty \frac{\mathrm{d}s}{s^2} \left( \sum_{\substack{k=-\infty \\ k \neq 0}}^{\infty} \mathrm{e}^{-k^2/s} \right)^D . \qquad \text{(C.13)}$$

For any finite $s_0 > 0$, the sum in the first integral can be truncated at some finite $k_{\max}$ for all $s \in [0, s_0]$. For the second integral (corresponding to large values of $s$) we make use of the poissonian formula (C.12) with $z = 0$ and choose $s_0$ in a way that terms $l \neq 0$ can be neglected:

$$\left( \sum_{\substack{k=-\infty \\ k \neq 0}}^{\infty} \mathrm{e}^{-k^2/s} \right)^D = \left( \sqrt{\pi s} - 1 + 2 \sum_{l=1}^{\infty} \mathrm{e}^{-\pi^2 l^2 s} \right)^D \approx (\sqrt{\pi s})^D (1 - (\sqrt{\pi s})^{-1})^D . \qquad \text{(C.14)}$$

Then, the second integral can be evaluated approximately through

$$\frac{1}{(2\pi)^2}\int_{s_0}^{\infty}\frac{\mathrm{d}s}{s^2}\left(\sum_{\substack{k=-\infty\\k\neq 0}}^{\infty}\mathrm{e}^{-k^2/s}\right)^D \approx \frac{1}{(2\pi)^2}\sum_{n=0}^{\infty}\frac{\Gamma(n-D)\pi^{(D-n)/2}}{\Gamma(n+1)\Gamma(-D)}\int_{s_0}^{\infty}\mathrm{d}s\; s^{\frac{D-n-4}{2}}$$
$$= \frac{1}{(2\pi)^2}\sum_{n=1}^{\infty}\frac{2\Gamma(n-D)\pi^{(D-n)/2}}{\Gamma(n+1)\Gamma(-D)(2-D+n)}s_0^{\frac{2-D+n}{2}} + 2\frac{s_0^{\frac{2-D}{2}}}{2\pi^{(2-D/2)}(2-D)}\,. \quad \text{(C.15)}$$

From (C.13) and (C.15) we then have:

$$I_1 \approx \frac{1}{(2\pi)^2}\left[\int_0^1\frac{\mathrm{d}s\; s_0}{s^2}\left(2\sum_{k=1}^{\infty}\mathrm{e}^{-k^2\frac{s_0}{s}}\right)^D + \sum_{n=1}^{\infty}\frac{2\Gamma(n-D)\pi^{(D-n)/2}}{\Gamma(n+1)\Gamma(-D)(2-D+n)}s_0^{\frac{2-D+n}{2}} + \frac{2\pi^{D/2}}{2-D}s_0^{\frac{2-D}{2}}\right]. \quad \text{(C.16)}$$

The third term above shows up a pole in $2-D$, which can be easily subtracted expanding the expression in powers of $2-D$. The pole is

$$I_1 = \frac{1}{2\pi(2-D)} + O((2-D)^0). \quad \text{(C.17)}$$

The precision of the machine that we used to evaluate (C.16) was sufficient in a way that we could select $s_0$ from an interval, such that the sum appearing in the integrand could be truncated at some finite $k_{\max}$ and the result was independent from the precise value of $s_0$ within the desired order of accuracy, therefore, justifying the approximation in (C.15). Of course, the other series can be safely truncated as well. Setting for instance $s_0 = 10$ and $k_{\max} = n_{\max} = 20$ we obtain with *Mathematica*®:

$$I_1 = \frac{1}{2\pi(2-D)} - 0.2382(1) + 0.3422(1)(2-D) + O((2-D)^2)\,. \quad \text{(C.18)}$$

On the torus we scaled the square root of the volume of the $D$-dimensional unitsphere into the field. Accordingly, comparing with (C.4) and (C.5) we then find:

$$\overline{\mathbb{C}} = -1.4967(6) + S_D\cdot 0.3422(1)(2-D) + O((2-D)^2)\,. \quad \text{(C.19)}$$

Let us turn to the evaluation of $I_2$ following the same strategy as above. Again, setting $L=1$ and introducing a Schwinger parametrization leads to:

$$I_2 = \frac{1}{(2\pi)^4}\int_0^{\infty}\mathrm{d}s\; s^{-3}\left(\sum_{\substack{k=-\infty\\k\neq 0}}^{\infty}\mathrm{e}^{-k^2/s}\right)^D$$
$$= \frac{1}{(2\pi)^4}\left[\int_0^1\frac{\mathrm{d}s}{s_0^2 s^3}\left(2\sum_{k=1}^{\infty}\mathrm{e}^{-k^2/(s_0 s)}\right)^D + \int_{s_0}^{\infty}\mathrm{d}s\; s^{-3}\left(\sum_{\substack{k=-\infty\\k\neq 0}}^{\infty}\mathrm{e}^{-k^2/s}\right)^D\right] \quad \text{(C.20)}$$

Once again applying the Poisson-transformation (C.12) with $z = 0$ on the second integral involving large values of $s$, we approximate

$$\int_{s_0}^{\infty} \mathrm{d}s\; s^{-3} \left( \sum_{\substack{k=-\infty \\ k\neq 0}}^{\infty} \mathrm{e}^{-k^2/s} \right)^D \approx \pi^{D/2} \int_{s_0}^{\infty} \mathrm{d}s\; s^{D/2-3} \left(1 - (\pi s)^{(-1/2)}\right)$$

$$\sum_{n=0}^{\infty} \frac{\Gamma(n-D)\pi^{(D-n)/2}}{\Gamma(n+1)\Gamma(-D)} \int_{s_0}^{\infty} \mathrm{d}s\; s^{\frac{D-n}{2}-3} = \sum_{n=0}^{\infty} \frac{2\Gamma(n-D)\pi^{(D-n)/2}}{\Gamma(n+1)\Gamma(-D)(4+n-D)} s_0^{\frac{D-n-4}{2}} , \tag{C.21}$$

such that we arrive at

$$I_2 \approx \frac{1}{(2\pi)^4} \left[ \int_0^1 \frac{\mathrm{d}s}{s_0^2 s^3} \left( 2\sum_{k=1}^{\infty} \mathrm{e}^{-k^2/(s_0 s)} \right)^D + \sum_{n=0}^{\infty} \frac{2\Gamma(n-D)\pi^{(D-n)/2}}{\Gamma(n+1)\Gamma(-D)(4+n-D)} s_0^{\frac{D-n-4}{2}} \right] . \tag{C.22}$$

There is no pole in $2-D$. Since $I_2$ appears at second order in $2-D$ we only need its value at $D = 2$. Again, it is safe to truncate both series appearing in (C.22) at some finite values $k_{\max}$ and $n_{\max}$, and $s_0$ has to be chosen from an appropriate interval. Setting $k_{\max} = n_{\max} = 20$ and $s_0 = 10$ we obtain with *Mathematica*®:

$$I_2 = 0.00109(1) + O((2-D)) , \tag{C.23}$$

or– due to the rescaling of the field by $S_D^{1/2}$–

$$\overline{\mathbb{C}_c^2} = 0.043(1) + O((2-D)) . \tag{C.24}$$

The implementation of the summations with *Mathematica*® is shown in the sequel.

```
kmax = 20

nmax = 20

ellipticThetas[s_, D_] :=
 (2*Pi)^(-2) *2^D*((Sum[Exp[-k^2/(su*s)], {k, 1, kmax}])^D) / (su*s^2)

ellipticTheta10n[D_] :=
 (2*Pi)^(-2) *(Sum[(2 Product[(-D+j), {j, 0, n-1}]) / ((n+2-D) Gamma[n+1]) *
     (Sqrt[Pi])^(D-n) *(su)^((D-2-n)/2),
    {n, 1, nmax}])

FullSimplify[Normal[
  Series[(Pi^(D/2-2)/2*su^((D-2)/2)/(2-D)-1/(2*Pi*(2-D))), {D, 2, 2}]]]

-1/(96 Pi) ((24 + 6 (-2 + D) Log[Pi] +
      (-2 + D)^2 Log[Pi]^2 + (-2 + D) Log[su] (6 + 2 (-2 + D) Log[Pi] + (-2 + D) Log[su]))
    Log[Pi su])

ellipticTheta00[D_] := -((24 + 6*(-2 + D)*Log[Pi] + (-2 + D)^2*Log[Pi]^2 +
    (-2 + D)*Log[su]*(6 + 2*(-2 + D)*Log[Pi] +
      (-2 + D)*Log[su]))*Log[Pi*su]) / (96*Pi)

I1[D_] := NIntegrate[els[s, D], {s, 0, 1}] + ell0n[D] + ell00[D]

su = 1
I1[2]

-0.238217

su = 2
I1[2]

-0.238216

su = 3
I1[2]

-0.238216

su = 4
I1[2]

-0.238216
```

```
kmax = 20

20

nmax = 20

20

els[s_, D_] :=
 (2^D/(16*Pi^4))*((Sum[Exp[-k^2/(su*s)], {k, 1, kmax}])^D) / (su^2*s^3)

ell0[D_] :=
 (Pi^(D/2-4)/16)*Sum[(2 Product[(-D+j), {j, 0, n-1}]) / ((n+4-D) Gamma[n+1]) *
     (1/Sqrt[Pi])^n*(su)^((D-4-n)/2),
    {n, 0, nmax}]

I2[D_] := NIntegrate[els[s, D], {s, 0, 1}] + ell0[D]

su = 1
I2[2]

1

0.00108915

su = 2
I2[2]

2

0.00108917

su = 3
I2[2]

3

0.00108917

su = 4
I2[2]

4

General::unfl : Underflow occurred in computation.

0.00108917
```

# D Exact results for polymers

In this section we would like to derive some results for gaussian polymer chains interacting with a $\delta$-like defect. The path integrals then turn out to be factorizable and thus exactly solvable.
Let us start from the (bulk) polymer propagator being defined as the conditional probability of finding the internal point $s'$ at the position $r_f$ when starting in $s$ at $r_i$. The propagator can be written as a functional integral for a restricted partition function of the free chain according to

$$\begin{aligned}\mathcal{Z}_{s,s'}(r_i|r_f) &= \int \mathcal{D}[r]\ \tilde{\delta}(r(s)-r_i)\tilde{\delta}(r(s')-r_f)\ e^{-\mathcal{H}[r]} \\ &= \int_k e^{-k^2|s'-s|+ik(r_f-r_i)} \ = \ |s'-s|^{-d/2}\ e^{-\frac{(r_f-r_i)^2}{4|s'-s|}}\ . \end{aligned} \tag{D.1}$$

The propagator (D.1) possesses the Markov property

$$\mathcal{Z}_{s,s''}(r_i|r_f) = \int \mathrm{d}^d r_m\ \mathcal{Z}_{s,s'}(r_i|r_m)\ \mathcal{Z}_{s',s''}(r_m|r_f)\ . \tag{D.2}$$

## D.1 Universal $1/r$ - repulsion law for polymers

We have shown in section 2.2 by a scaling argument that as long as $r \ll L^\nu$, the restricted partition function of a manifold pinned at one of its internal points scales as $\mathcal{Z}_\infty(r/L^\nu) \sim (r/L^\nu)^\theta$, with the contact-exponent given by (2.25). It is instructive to prove this for the special case of polymers in $d = 1$. According to (2.1) and (2.6) this corresponds to a polymer in $3d$-space interacting with a $\delta$-potential on a plane.
For this purpose we need the restricted partition function (D.1) in presence of a short-range interaction modeled through a $\delta$-potential, which is situated at the origin of the embedding space. The restricted partition function in the presence of the interaction will be denoted by $\mathcal{Z}^{g_0}_{s,s'}(r_i|r_f)$. We consider the case, where the chain is fixed at its ends, such that $s{=}0$ and $s'{=}L$. We furthermore switch to a grand-canonical ensemble and denote

$$\mathcal{Z}^{g_0}_\tau(r_i|r_f) := \int_0^\infty \mathrm{d}L\ \mathcal{Z}^{g_0}_{0,L}(r_i|r_f)\ e^{-\tau L}\ , \tag{D.3}$$

$\tau$ being some chemical potential. $\mathcal{Z}^{g_0}_\tau(r_i|r_f)$ can be expanded in a perturbation series in the coupling $g_0$ according to

$$\mathcal{Z}^{g_0}_\tau(r_i|r_f) \ = \ \sum_{n=0}^\infty (-g_0)^n \mathcal{Z}^{g_0,n}_\tau(r_i|r_f)\ . \tag{D.4}$$

The $\mathcal{Z}^{g_0,n}_\tau(r_i|r_f)$ are

$$\begin{aligned}\mathcal{Z}^{g_0,n}_\tau(r_i|r_f) := \int_0^\infty \mathrm{d}L \int_{0<x_1<\ldots<x_n<L} & \mathcal{Z}_{0,x_1}(r_i|0)\ \mathcal{Z}_{x_1,x_2}(0|0) \times \ldots \\ & \ldots \times \mathcal{Z}_{x_{n-1},x_n}(0|0)\ \mathcal{Z}_{x_n,L}(0|r_f)\ \mathrm{e}^{-\tau L} \\ = \left[\int_0^\infty \mathrm{d}x\ \mathrm{e}^{-x\tau}\mathcal{Z}_{0,x}(r_i,0)\right] & \left[\int_0^\infty \mathrm{d}x\ \mathrm{e}^{-x\tau}\mathcal{Z}_{0,x}(0,0)\right]^{n-1}\left[\int_0^\infty \mathrm{d}x\ \mathrm{e}^{-x\tau}\mathcal{Z}_{0,x}(0,r_f)\right] \\ = \ \mathcal{Z}^0_\tau(r_i|0)\ \mathcal{Z}^0_\tau(0|0)^{n-1}\ \mathcal{Z}^0_\tau(0|r_f)\ , \end{aligned} \tag{D.5}$$

where we have used that after integration over $L$, the integrals factorize; we further have defined

$$\begin{aligned}\mathcal{Z}_\tau(r_i|r_f) &= \int_0^\infty \mathrm{d}s \mathcal{Z}_{0,s}(r_i|r_f)\mathrm{e}^{-\tau s} \\ &= \int_0^\infty \mathrm{d}s \int_k \mathrm{e}^{-(k^2+\tau)s+ik(r_f-r_i)} = \int_k \frac{\mathrm{e}^{ik(r_f-r_i)}}{k^2+\tau} \,. \end{aligned} \tag{D.6}$$

In $d{=}1$ the integration over the momenta $k$ in (D.6) leads to

$$\mathcal{Z}_\tau(r_i|r_f)_{|d=1} \;=\; \sqrt{\frac{\pi}{\tau}}\, e^{-\sqrt{\tau}|r_f-r_i|} \,. \tag{D.7}$$

Let us now lock at what terms appear in the $n$-th order coefficient in (D.5): From the initial point of the chain a factor $\mathcal{Z}_\tau(r_i|0)$ is contributed, while the final point is coming up with $\mathcal{Z}_\tau(0|r_f)$. Furthermore, the internal points give $n{-}1$ powers of $\mathcal{Z}_\tau(0|0)$, where

$$\mathcal{Z}_\tau(0|0) = \sqrt{\frac{\pi}{\tau}} \,. \tag{D.8}$$

The $(n{=}0)$-coefficient is special: Clearly, one has

$$\mathcal{Z}_\tau^{g_0,0}(r_i|r_f) = \mathcal{Z}_\tau(r_i|r_f) \,. \tag{D.9}$$

Inserting (D.8)-(D.9) into (D.5) we obtain for (D.4):

$$\begin{aligned}\mathcal{Z}_\tau^{g_0}(r_i|r_f) &= \sqrt{\frac{\pi}{\tau}} \left[\mathrm{e}^{-\sqrt{\tau}|r_f-r_i|} + \mathrm{e}^{-\sqrt{\tau}(|r_f|+|r_i|)} \sum_{n=1}^\infty \left(-g_0\sqrt{\frac{\pi}{\tau}}\right)^n\right] \\ &= \sqrt{\frac{\pi}{\tau}} \left[\mathrm{e}^{-\sqrt{\tau}|r_f-r_i|} - \mathrm{e}^{-\sqrt{\tau}(|r_f|+|r_i|)} \frac{1}{1+\frac{1}{g_0}\sqrt{\frac{\tau}{\pi}}}\right] \,. \end{aligned} \tag{D.10}$$

The limit of $g_0 \to \infty$ can be taken and leaves us with the beautiful result

$$\mathcal{Z}_\tau^\infty(r_i|r_f) = \sqrt{\frac{\pi}{\tau}} \left(\mathrm{e}^{-\sqrt{\tau}|r_f-r_i|} - \mathrm{e}^{-\sqrt{\tau}(|r_f|+|r_i|)}\right) \,. \tag{D.11}$$

This is the propagator of a scalar field with Dirichlet boundary conditions. It has applications when studying critical phenomena of e.g. an Ising magnet in half-space [68,69]. Performing the inverse Laplace-transformation of (D.11) we arrive at

$$\mathcal{Z}_L^\infty(r_i|r_f) = \frac{1}{L^{1/2}} \left(\mathrm{e}^{-\frac{(r_f-r_i)^2}{4|L|}} - \mathrm{e}^{-\frac{(|r_f|+|r_i|)^2}{4|L|}}\right) \,. \tag{D.12}$$

We conclude that a $\delta$- potential acting in a hyper-plane suppresses all configurations which penetrate or touch it, when taking its amplitude to infinity.
Finally, in order to prove the universal repulsion law, we start from (D.12) and integrate over all final positions $r_f$:

$$\mathcal{Z}_L^\infty(r_i) = \int_{-\infty}^{\infty} \mathrm{d}r_f \;\mathcal{Z}_L^\infty(r_i|r_f) = 2\sqrt{\pi}\left(1 - \mathrm{erf}\frac{|r_i|}{2\sqrt{L}}\right) \,, \tag{D.13}$$

erf denoting the error function. For small arguments we have

$$1 - \mathrm{erf}(x) \;\sim\; x \;. \tag{D.14}$$

Furthermore, $\mathcal{Z}_L^\infty(r_i)$ denotes the restricted partition function of a chain pinned at one of its ends in $r_i$. To obtain $\mathcal{Z}_\infty(r/L^\nu)$ in (2.23) we have to evaluate:

$$\mathcal{Z}_\infty(r/L^\nu) = \frac{1}{L}\int_0^L \mathrm{d}s\; \mathcal{Z}_s^\infty(r)\mathcal{Z}_{L-s}^\infty(r) \;\sim\; \left(\frac{r}{\sqrt{L}}\right)^2 \tag{D.15}$$

according to (D.14) in the scaling regime $r \ll L^{1/2}$. We thus find that $\theta = 2$, which confirms (2.25) for $D = 1$ and $d = 1$. The above proof can be extended to arbitrary dimensions $0<d<2$, where $\varepsilon>0$ for polymers. Then, $\theta = 4 - 2d$.

It would be nice to make the same arguments for membranes. However, the proof is based on a drastic simplification, which only occurs in $D=1$ and shows up in the factorizability of loop diagrams as in (D.5). This has no extension to manifolds of internal dimension $D>1$.

## D.2 Strong coupling expansion for the renormalized coupling $g$

In the following we want to derive an expression for the renormalized coupling $g$ as defined in (2.10) in terms of a strong coupling expansion in powers of the bare coupling. This is needed in the fixed membrane size ensemble as it is also considered in the $2 - D$-expansion. In order to make matching our strong coupling series about $D = 2$ with the known exact result for polymers, we shortly derive the latter both for an open as well as a closed chain.
Starting from the definition of the polymer-propagator let us point out that the full partition function then is defined as

$$\mathcal{Z}^O = \int_{r_f}\int_{r_i} \mathcal{Z}_{s,s'}(r_i|r_f) \quad \text{, open end polymer} \tag{D.16}$$

$$\mathcal{Z}^C = \int_{r} \mathcal{Z}_{s,s'}(r|r) \quad \text{, closed polymer} \tag{D.17}$$

In both cases the integrand is expanded in powers of the bare coupling according to (D.4). Generally, the $n$th order coefficient in (D.5) is coming up with $n-1$ powers of $\mathcal{Z}_\tau(0|0)$ to be here calculated for arbitrary $d < 2$. Accordingly,

$$\mathcal{Z}_\tau(0|0) = \int_k \frac{1}{k^2+\tau} = \pi^{-d/2}\frac{S_d\frac{\pi}{2}\tau^{-\varepsilon}}{\sin(\frac{d\pi}{2})} = \Gamma(\varepsilon)\tau^{-\varepsilon} \;, \tag{D.18}$$

where we have used the normalization of the integral according to (3.6) and

$$\Gamma(\varepsilon)\Gamma(1-\varepsilon) = \frac{\pi}{\sin(\pi\varepsilon)} \qquad \text{and} \qquad S_d = 2\frac{\pi^{d/2}}{\Gamma(\frac{d}{2})} \;.$$

Note that here $\varepsilon = 1 - d/2$. Furthermore, there is a $\mathcal{Z}_\tau(r_i|0)\mathcal{Z}_\tau(0|r_f)$ from the end-points contributing according to (D.16) in the case of an open end chain

$$\int_{r_i}\int_{r_f} \mathcal{Z}_\tau(r_i|0)\mathcal{Z}_\tau(0|r_f) = \left(\int_r\int_k \frac{\mathrm{e}^{-ikr}}{k^2+\tau}\right)^2 = \tau^{-2} \;, \tag{D.19}$$

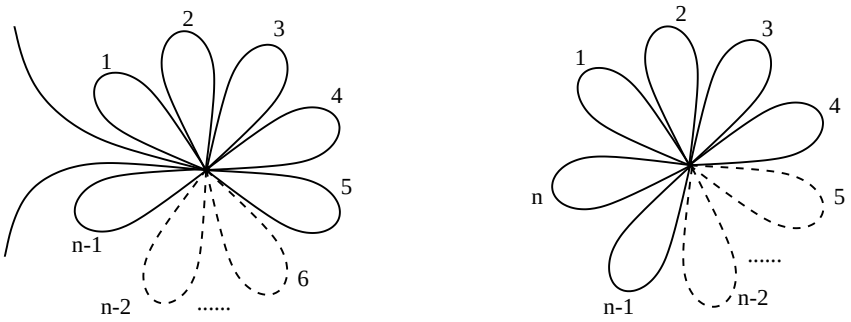


Figure D.1: "Daisy"-diagrams contributing to $\mathcal{Z}^O$ (left) and $\mathcal{Z}^C$ (right), (D.16), each leaf representing the integration over an internal distance.

while for a closed chain one is obtaining:

$$\int_r \mathcal{Z}_\tau(r|0)\mathcal{Z}_\tau(0|r) = \int_r \int_{k_i} \int_{k_f} \frac{\mathrm{e}^{ir(k_f-k_i)}}{(k_i^2+\tau)(k_f^2+\tau)} = \int_k \frac{1}{(k^2+\tau)^2} = \varepsilon\Gamma(\varepsilon)\tau^{-\varepsilon-1} \qquad \text{(D.20)}$$

The case $n$=0 is special. For an open polymer we have to evaluate

$$\int_{r_i}\int_{r_f} \mathcal{Z}_\tau^{g_0,0}(r_i|r_f) = \int_{r_i}\int_{r_f}\int_k \frac{\mathrm{e}^{ik(r_f-r_i)}}{k^2+\tau} = \mathcal{V}_{\mathbb{R}^d}\tau^{-1}\,, \qquad \text{(D.21)}$$

while a closed chain is yielding

$$\int_r \mathcal{Z}_\tau^{g_0,0}(r|r) = \mathcal{V}_{\mathbb{R}^d}\int_k \frac{1}{k^2+\tau} = \mathcal{V}_{\mathbb{R}^d}\Gamma(\varepsilon)\tau^{-\varepsilon} \qquad \text{(D.22)}$$

Diagrammatically, the $n$th order contribution to the partition function (D.16) can be written according to (D.18-D.22) as shown in fig. (D.1).

Let us now calculate $\mathcal{Z}^0 - \mathcal{Z}^{g_0}$ for a closed chain:

$$\mathcal{Z}^0 - \mathcal{Z}^{g_0} = -\varepsilon\tau^{-1}\sum_{n=1}^{\infty}(-\Gamma(\varepsilon)(g_0\tau^{-\varepsilon})^n = \varepsilon\tau^{-1}\frac{\Gamma(\varepsilon)g_0\tau^{-\varepsilon}}{1+\Gamma(\varepsilon)g_0\tau^{-\varepsilon}}$$

$$= \varepsilon\tau^{-1}\frac{1}{1+\tau^\varepsilon(\Gamma(\varepsilon)g_0)^{-1}} = \varepsilon\tau^{-1}\sum_{n=0}^{\infty}\left(-\frac{\tau^\varepsilon}{\Gamma(\varepsilon)g_0}\right)^n = \varepsilon\sum_{n=0}^{\infty}\left(-\frac{1}{\Gamma(\varepsilon)g_0}\right)^n\tau^{n\varepsilon-1}\,. \qquad \text{(D.23)}$$

Performing an inverse Laplace-transformation, we arrive at

$$g_C := (\mathcal{Z}^0 - \mathcal{Z}^{g_0})(L) = \frac{1}{2\pi i}\int_{\gamma-i\infty}^{\gamma+i\infty}\mathrm{d}\tau\ \mathrm{e}^{\tau L}(\mathcal{Z}^0 - \mathcal{Z}^{g_0})$$

$$= \varepsilon\left[1+\sum_{n=1}^{\infty}\left(-\frac{1}{\Gamma(\varepsilon)g_0L^\varepsilon}\right)^n\frac{\Gamma(n\varepsilon)\sin(\pi n\varepsilon)}{\pi}\right] = \varepsilon\left[1+\sum_{n=1}^{\infty}\left(-\frac{1}{\Gamma(\varepsilon)g_0L^\varepsilon}\right)^n\frac{1}{\Gamma(1-n\varepsilon)}\right]\,, \qquad \text{(D.24)}$$

where we have used that for any $\mu > 0$

$$\frac{1}{2\pi i}\int\limits_{\gamma-i\infty}^{\gamma+i\infty} \mathrm{d}\tau\ \tau^{\mu-1}\mathrm{e}^{\tau L} = \frac{\Gamma(\mu)\sin(\pi\mu)}{\pi} L^{-\mu}\ . \tag{D.25}$$

$\mathcal{Z}^0 - \mathcal{Z}^{g_0}$ as given in (D.24) is the dimensionless renormalized coupling $g$ in the case of a closed chain. Note that in the calculation of the partition function of an open end chain there has to be performed one more integration over the field $r$, such that only $(\mathcal{Z}^0 - \mathcal{Z}^{g_0})L^{(\varepsilon-1)} =: g$, $1-\varepsilon$ being the dimension of the field, becomes dimensionless.
Before we proceed let us shortly consider how to treat the limit of vanishing bulk space dimension $d$ in this framework: Setting $d = 0$ and equivalently $\varepsilon = 1$ for polymers, then, the renormalized coupling is obtained from (D.23) and (D.24) as

$$g_C(d{=}0) = \frac{1}{2\pi i}\int\limits_{\gamma-i\infty}^{\gamma+i\infty} \frac{\mathrm{d}\tau}{\tau}\ \mathrm{e}^{\tau L}\frac{g_0}{g_0+\tau}\ . \tag{D.26}$$

This time, the inverse Laplace-transformation can be immediately evaluated in terms of residues. First order poles of the integrand are located at $\tau = 0$ and $\tau = -g_0$, therefore providing

$$g_C(d{=}0) = 1 - \mathrm{e}^{-g_0 L}\ , \tag{D.27}$$

which is consistent with what we have found within the expansion in $2 - D$ (6.76). Let us calculate the inverse Laplace-transformation of $\mathcal{Z}^0 - \mathcal{Z}^{g_0}$ for an open end chain:

$$\begin{aligned}\mathcal{Z}^0 - \mathcal{Z}^{g_0} &= \tau^{-2} g_0 \sum_{n=1}^{\infty}(-(g_0\Gamma(\varepsilon)\tau^{-\varepsilon})^{n-1} = \frac{g_0\tau^{-2}}{1+(g_0\Gamma(\varepsilon)\tau^{-\varepsilon})} \\ = \frac{\tau^{\varepsilon-2}}{\Gamma(\varepsilon)}\frac{g_0\Gamma(\varepsilon)\tau^{-\varepsilon}}{1+g_0\Gamma(\varepsilon)\tau^{-\varepsilon}} &= \frac{\tau^{\varepsilon-2}}{\Gamma(\varepsilon)}\frac{1}{1+(g_0\Gamma(\varepsilon))^{-1}\tau^{\varepsilon}} = \frac{\tau^{\varepsilon-2}}{\Gamma(\varepsilon)}\sum_{n=0}^{\infty}\left(-\frac{1}{g_0\Gamma(\varepsilon)}\right)^n \tau^{n\varepsilon}\ ,\end{aligned} \tag{D.28}$$

leading to

$$\begin{aligned}(\mathcal{Z}^0 - \mathcal{Z}^{g_0})(L) &= \frac{1}{2\pi i}\int\limits_{\gamma-i\infty}^{\gamma+i\infty} \mathrm{d}\tau\ \mathrm{e}^{\tau L}(\mathcal{Z}^0 - \mathcal{Z}^{g_0}) \\ &= -\frac{1}{\Gamma(\varepsilon)}\sum_{n=0}^{\infty}\left(-\frac{1}{g_0\Gamma(\varepsilon)}\right)^n \int\limits_{\gamma-i\infty}^{\gamma+i\infty} \mathrm{d}\tau\ \frac{L\,\tau^{(n+1)\varepsilon-1}}{(n+1)\varepsilon-1}\ \mathrm{e}^{\tau L} \\ = -\frac{1}{\Gamma(\varepsilon)}\sum_{n=0}^{\infty}\left(-\frac{1}{g_0\Gamma(\varepsilon)}\right)^n & L^{1-(n+1)\varepsilon}\frac{\Gamma((n+1)\varepsilon)}{(n+1)\varepsilon-1}\frac{\sin(\pi(n+1)\varepsilon)}{\pi} \\ &= L^{1-\varepsilon}\left[\frac{\sin(\pi\varepsilon)}{(1-\varepsilon)\pi} + \sum_{n=1}^{\infty}\left(-\frac{1}{L^{\varepsilon}g_0\Gamma(\varepsilon)}\right)^n \frac{1}{\Gamma(2-n\varepsilon)}\right]\ ,\end{aligned} \tag{D.29}$$

where we have used that for $0 < \mu < 1$

$$\int\limits_{\gamma-i\infty}^{\gamma+i\infty} \mathrm{d}\tau\ \tau^{\mu-2}\ \mathrm{e}^{\tau L} = \frac{\tau^{\mu-1}}{\mu-1}\ \mathrm{e}^{\tau L}\Big|_{\gamma-i\infty}^{\gamma+i\infty} - L \int\limits_{\gamma-i\infty}^{\gamma+i\infty} \mathrm{d}\tau\ \frac{\tau^{\mu-1}}{\mu-1}\ \mathrm{e}^{\tau L}\ , \tag{D.30}$$

and the boundary term vanishes. The dimensionless renormalized coupling then is defined as in (2.10), such that

$$g_O := (\mathcal{Z}^0 - \mathcal{Z}^{g_0})(L) L^{\varepsilon-1} = \frac{\sin(\pi\varepsilon)}{(1-\varepsilon)\pi} + \sum_{n=1}^{\infty} \left(-\frac{1}{L^\varepsilon g_0 \Gamma(\varepsilon)}\right)^n \frac{1}{\Gamma(2-n\varepsilon)}\ . \tag{D.31}$$

From the strong coupling expansions (D.24) and (D.31) one easily obtains the fixed point values of $g$. For the closed chain we find

$$g_C^* = \varepsilon\ , \tag{D.32}$$

while for the open end chain we have

$$g_O^* = \frac{\sin(\pi\varepsilon)}{(1-\varepsilon)\pi}\ . \tag{D.33}$$

### D.3 Weak coupling expansion

In order to be complete let us turn the expansions (D.24) and (D.31) into weak coupling expansions. This can be easily done starting for instance from the expansion in the Laplace-transformed picture for the closed chain as given in the top line in (D.23). Then,

$$\begin{aligned} g_C := (\mathcal{Z}^0 - \mathcal{Z}^{g_0})(L) &= \frac{1}{2\pi i} \int\limits_{\gamma-i\infty}^{\gamma+i\infty} \mathrm{d}\tau\ \mathrm{e}^{\tau L}(\mathcal{Z}^0 - \mathcal{Z}^{g_0}) = \frac{-\varepsilon}{2\pi i} \sum_{n=1}^{\infty} (-g_0\Gamma(\varepsilon))^n \int\limits_{\gamma-i\infty}^{\gamma+i\infty} \mathrm{d}\tau\ \tau^{-n\varepsilon-1}\ \mathrm{e}^{\tau L} \\ &= -\varepsilon \sum_{n=0}^{\infty} \frac{(-g_0\Gamma(\varepsilon)L^\varepsilon)^n}{\Gamma(1+n\varepsilon)}\ , \end{aligned} \tag{D.34}$$

where we have simply used the analytical continuation of (D.25) to arbitrary values of $\mu$. (D.25) can be obtained from integrating along a branch cut, which makes it necessary to have $\mu > 0$. But $\mu$ can be always rendered positive through a sufficient number $m$ of partial integrations according to (D.30). Having chosen $m$ appropriately, it drops out after the inverse Laplace transformation has been performed.

Let us apply the same procedure to the weak coupling expansion of the renormalized coupling of the open chain in the top line in (D.28):

$$\begin{aligned} (\mathcal{Z}^0 - \mathcal{Z}^{g_0})(L) = \frac{1}{2\pi i} \int\limits_{\gamma-i\infty}^{\gamma+i\infty} \mathrm{d}\tau\ \mathrm{e}^{\tau L}(\mathcal{Z}^0 - \mathcal{Z}^{g_0}) &= \frac{g_0}{2\pi i} \sum_{n=1}^{\infty} (-(g_0\Gamma(\varepsilon))^{n-1} \int\limits_{\gamma-i\infty}^{\gamma+i\infty} \mathrm{d}\tau\ \tau^{-(n-1)\varepsilon-2}\ \mathrm{e}^{\tau L} \\ &= L g_0 \sum_{n=1}^{\infty} \frac{(-g_0\Gamma(\varepsilon)L^\varepsilon)^{n-1}}{\Gamma(2+(n-1)\varepsilon)}\ , \end{aligned} \tag{D.35}$$

from what follows that

$$g_O := L^{\varepsilon-1}(\mathcal{Z}^0 - \mathcal{Z}^{g_0}) = g_0 L^\varepsilon \sum_{n=0}^{\infty} \frac{(-g_0\Gamma(\varepsilon)L^\varepsilon)^n}{\Gamma(2+n\varepsilon)} \; . \tag{D.36}$$

## D.4 Semi-flexible polymers

Theories consisting in some one-dimensional manifold interacting with a single defect turn out to be always one-loop exact. This is due to the factorizability of the path-integrals like (D.5) to appear in the perturbation theory. Let us now discuss another model taking once again advantage of this property. Consider so-called semi-flexible polymers, whose configurations are controlled by bending elasticity. For low temperatures or equivalently on short scales their configurational space can be parametrized by some $d$-dimensional field $\vec{r}$, being defined through the displacement of the individual mass points with respect to some flat background, therefore allowing for no overlaps or even self-intersections of the polymer. Then, the curvature along the manifold can be approximated through the usual Laplacian $\partial_{tt}\vec{r}(t)$ and the free Hamiltonian reads:

$$\mathcal{H}_0[\vec{r}] = \int_0^L \mathrm{d}t \; \frac{1}{2}(\Delta\vec{r}(t))^2 \; . \tag{D.37}$$

Let us now consider the interaction with some short-range, $\delta$-like defect, acting in the displacement space and being located at the origin: A short distance analysis shows that any two nearby intersections of the polymer with the defect appear like a single, parallel intersection [70]. This is due to the bending stiffness of the manifold suppressing short-wavelength fluctuations. Taking the most relevant, orientational dependent interaction into account, which is

$$\mathcal{H}_{int}[\vec{r}] = v_0 \int_0^L \mathrm{d}t \; \delta^d(\vec{r}(t))\delta^d(\nabla\vec{r}(t)) \; , \tag{D.38}$$

let us shortly sketch, how to completely sum up the perturbation theory in this case following the same lines as in the preceding sections. Once again, we need to find the propagator of the corresponding Schrödinger-type equation, which is defined through the path-integral:

$$\mathcal{G}_{t,t'}(r_i, v_i|r_f, v_f) = \int \mathcal{D}[\vec{r}] \; \delta^d(r(t)-r_i)\delta^d(\nabla r(t)-v_i)\delta^d(r(t')-r_f)\delta^d(\nabla r(t')-v_f) \; \mathrm{e}^{-\mathcal{H}_0[\vec{r}]} \; , \tag{D.39}$$

where $r_i, v_i$ and $r_f, v_f$ denote position and slope of the initial and final point, respectively. Be $\mathcal{G}^{v_0}_{t,t'}$ the corresponding propagator in presence of the interaction (D.38). Switching to a grand-canonical ensemble,

$$\mathcal{G}^{v_0}_\tau(r_i, v_i|r_f, v_f) = \int_0^\infty \mathrm{d}L \; \mathcal{G}_{0,L}(r_i, v_i|r_f, v_f) \; \mathrm{e}^{-\tau L} \; , \tag{D.40}$$

the perturbation series of $\mathcal{G}^{v_0}_\tau(r_i, v_i|r_f, v_f)$ can then be written as

$$\mathcal{G}^{v_0}_\tau(r_i, v_i|r_f, v_f) = \sum_{n=0}^{\infty} (-v_0)^n \mathcal{G}^{v_0,n}_\tau(r_i, v_i|r_f, v_f) \; . \tag{D.41}$$

However, solving the path-integral of the free problem (D.39) poses considerable problems, when treating the energyless tilt mode. The solution has been obtained from the equivalent problem of the corresponding Schrödinger-type equation [71–73]. It reads:

$$\mathcal{G}_{t,t'}(r_i, v_i|r_f, v_f) = \left(\frac{\sqrt{3}}{\pi(t'-t)^2}\right)^d \mathrm{e}^{-\frac{6}{(t'-t)^3}S_{t,t'}(r_i,v_i|r_f,v_f)} , \tag{D.42}$$

where

$$S_{t,t'}(r_i, v_i|r_f, v_f) = (r_f-r_i - v_i(t'-t))^2 + \frac{(t'-t)^2}{3}(v_f-v_i)^2 - (t'-t)(r_f-r_i-v_i(t'-t))(v_f-v_i) \tag{D.43}$$

is the action of the minimal energy path.
In analogy to (D.5) the path-integral to be calculated to obtain $\mathcal{G}_\tau^{v_0,n}(r_i, v_i|r_f, v_f)$ factorizes after "time-ordering" the distances:

$$\mathcal{G}_\tau^{v_0,n}(r_i, v_i|r_f, v_f) = \left[\int_0^L \mathrm{d}L\ \mathrm{e}^{-\tau L}\mathcal{G}_{0,L}(r_i, v_i|0, 0)\right]\left[\int_0^L \mathrm{d}L\ \mathrm{e}^{-\tau L}\mathcal{G}_{0,L}(0, 0|0, 0)\right]^{n-1} \times$$
$$\times \left[\int_0^L \mathrm{d}L\ \mathrm{e}^{-\tau L}\mathcal{G}_{0,L}(0, 0|r_f, v_f)\right] , \qquad n \geq 1 . \tag{D.44}$$

The $n = 0$ contribution is obtained from

$$\mathcal{G}_\tau^{v_0,0}(r_i, v_i|r_f, v_f) = \int_0^L \mathrm{d}L\ \mathrm{e}^{-\tau L}\mathcal{G}_{0,L}(r_i, v_i|r_f, v_f) . \tag{D.45}$$

It is hard to calculate the Laplace-transform of the propagator (D.42), but the renormalized coupling $v$ can be easily obtained from $\mathcal{Z}^0 - \mathcal{Z}^{v_0}$, $\mathcal{Z}^{v_0}$ being the full partition function given by

$$\mathcal{Z}^{v_0}(\tau) = \int \mathrm{d}^d r_i\ \mathrm{d}^d v_i\ \mathrm{d}^d r_f\ \mathrm{d}^d v_f\ \mathcal{G}_\tau^{v_0}(r_i, v_i|r_f, v_f) \tag{D.46}$$

in the Laplace-transformed picture. Since

$$\int_0^\infty \mathrm{d}L\ \mathrm{e}^{-\tau L}\int \mathrm{d}^d r_i\ \mathrm{d}^d v_i\ \mathcal{G}_{0,L}(r_i, v_i|0, 0) = 3^{-d/2}\frac{\Gamma(1-2d)}{\tau^{1-2d}} \tag{D.47}$$

and

$$\int_0^\infty \mathrm{d}L\ \mathrm{e}^{-\tau L}\mathcal{G}_{0,L}(0, 0|0, 0) = \left(\frac{\sqrt{3}}{\pi}\right)^d \frac{\Gamma(1-2d)}{\tau^{1-2d}} , \tag{D.48}$$

we find:

$$(\mathcal{Z}^0 - \mathcal{Z}^{v_0})(\tau) = -\Gamma(1-2d)\,\tau^{-(1-2d)}\left(\frac{3\sqrt{3}}{\pi}\right)^{-d}\sum_{n=1}^\infty (-v_0)^n\left(\frac{3^{d/2}\Gamma(1-2d)}{\pi^d}\tau^{-(1-2d)}\right)^n$$
$$= \frac{3^{-d}\Gamma^2(1-2d)\ v_0\tau^{-2(1-2d)}}{1 + v_0\tau^{-(1-2d)}\frac{3^{d/2}\Gamma(1-2d)}{\pi^d}} = \left(\frac{3\sqrt{3}}{\pi}\right)^{-d}\Gamma(1-2d)\tau^{-(1-2d)}\sum_{n=0}^\infty\left(-v_0\tau^{-(1-2d)}\frac{3^{d/2}\Gamma(1-2d)}{\pi^d}\right)^{-n} , \tag{D.49}$$

where we have turned the series into a strong coupling expansion. Performing an inverse Laplace transformation,

$$\begin{aligned}&\frac{1}{2\pi i}\int\limits_{\gamma-i\infty}^{\gamma+i\infty} \mathrm{d}\tau\ \mathrm{e}^{\tau L}(\mathcal{Z}^0-\mathcal{Z}^{v_0})(\tau)\\ &=\left(\frac{3\sqrt{3}}{\pi}\right)^{-d}\Gamma(1-2d)L^{1-2d}\sum_{n=0}^{\infty}\left(\frac{3^{d/2}\Gamma(1-2d)}{\pi^d}\right)^{-n}\frac{(-v_0L^{1-2d})^{-n}}{\Gamma(1+(n-1)(1-2d))}\,,\end{aligned} \tag{D.50}$$

the dimensionless renormalized coupling $v$ reads:

$$v:=(\mathcal{Z}^0-\mathcal{Z}^{v_0})(L)L^{-(1-2d)}=\left(\frac{3\sqrt{3}}{\pi}\right)^{-d}\Gamma(1-2d)\sum_{n=0}^{\infty}\left(\frac{3^{d/2}\Gamma(1-2d)}{\pi^d}\right)^{-n}\frac{(-v_0L^{1-2d})^{-n}}{\Gamma(1+(n-1)(1-2d))}\,. \tag{D.51}$$

The fixed point is obtained sending the dimensionless bare coupling $z:=v_0L^{1-2d}$ to $\infty$:

$$v^*:=\lim_{z\to\infty}v(z)=\left(\frac{3\sqrt{3}}{\pi}\right)^{-d}\frac{\Gamma(1-2d)}{\Gamma(2d)}\,. \tag{D.52}$$

From the strong coupling expansion (D.51) one may immediately read off the value of the correction to scaling exponent $\omega$ at the fixed point:

$$\omega(v^*)=1-2d\,. \tag{D.53}$$

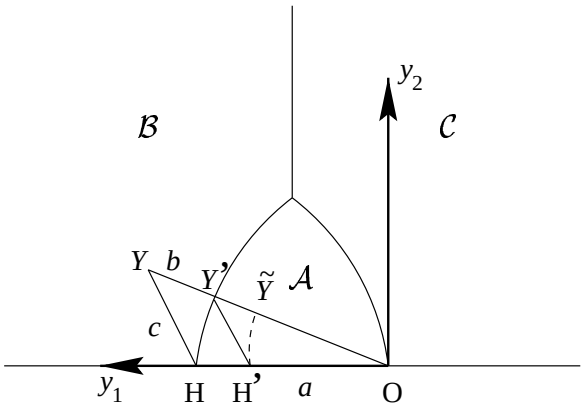


Figure E.1: The sectors $\mathcal{A}, \mathcal{B}$ and $\mathcal{C}$

# E Conformal mapping of the sectors

In order to calculate the two-loop diagram efficiently, one wants to write it as an integral over a finite domain only. To do so we need the technique of conformal mapping of the sectors, which also serves for analytically continuing the measure of integration to internal dimensions $D < 1$. This technique has been extensively used and well documented in the context of self-avoiding tethered membranes [26,20,4], but we repeat the presentation here for completeness.
Generally, in evaluating the three-point divergences we need to integrate over some domain in the upper half-plane (see 4.11). The measure of integration reads

$$\int_y \;=\; \frac{S_{D-1}}{S_D} \int_{-\infty}^{\infty} \mathrm{d}y_1 \int_0^{\infty} \mathrm{d}y_2 \; (y_2)^{D-2} \tag{E.1}$$

and the integrand is a function $f$ of the three distances $a, b$ and $c$ between the points $O = (0,0)$, $H = (-L, 0)$ and $Y = (y_1, y_2)$, given explicitly by (see fig. E.1)

$$a = L = \text{fixed}, \quad b = \sqrt{(y_1)^2 + (y_2)^2}\,, \quad c = \sqrt{(L-y_1)^2 + (y_2)^2}\,. \tag{E.2}$$

In our problem $f$ is homogeneous, of degree $\lambda$, but not necessarily symmetric:

$$f(\kappa a, \kappa b, \kappa c) \;=\; \kappa^{-\lambda} f(a,b,c)\,. \tag{E.3}$$

Let us now explicitly show, how sectors can be mapped onto each other. Specializing to the mapping $\mathcal{B} \to \mathcal{A}$ we choose a coordinate system as given in figure (E.1). The mapping $\mathcal{B} \to \mathcal{A}$ is mediated by a special conformal transformation, the inversion with respect to the circle around $O$ and radius $L$. In complex coordinates this is ($\bar{Y}$ is the complex conjugate of $Y$)

$$Y \longrightarrow \tilde{Y} = \frac{L^2}{\bar{Y}} = Y\,\frac{L^2}{b^2} \;\Leftrightarrow\; Y = \tilde{Y}\,\frac{L^2}{\tilde{b}^2} \tag{E.4}$$

such that

$$\begin{pmatrix} y_1 \\ y_2 \end{pmatrix} \;\longrightarrow\; \begin{pmatrix} \tilde{y}_1 \\ \tilde{y}_2 \end{pmatrix} \;=\; \begin{pmatrix} \frac{y_1 L^2}{b^2} \\ \frac{y_2 L^2}{b^2} \end{pmatrix} \;\Leftrightarrow\; \begin{pmatrix} y_1 \\ y_2 \end{pmatrix} \;=\; \begin{pmatrix} \frac{\tilde{y}_1 L^2}{\tilde{b}^2} \\ \frac{\tilde{y}_2 L^2}{\tilde{b}^2} \end{pmatrix}\,. \tag{E.5}$$

This change of coordinates gives a Jacobian for the measure (E.1)

$$\left(\frac{L^2}{\tilde{b}^2}\right)^D \quad . \tag{E.6}$$

It can easily be seen that the mapping $\mathcal{B} \to \mathcal{A}$ is one to one: First, be $Y=(y_1, y_2) \in \mathcal{B}$, that is $b > L$ and $b > c$. Then,

$$\tilde{c}^2 \;=\; ((\tilde{y}_1 - L)^2 + (\tilde{y}_2)^2) \;=\; \frac{L^4 - 2y_1L^3 + b^2L^2}{b^2} \;=\; L^2\frac{c^2}{b^2} < L^2 \tag{E.7}$$

and

$$\tilde{b}^2 \;=\; L^2\frac{L^2}{b^2} < L^2 \; . \tag{E.8}$$

Since $\tilde{b}^2, \tilde{c}^2 < L^2$, $\tilde{Y} \in \mathcal{A}$. Second, for the inverse mapping, $Y(\tilde{Y} \in \mathcal{A}) \in \mathcal{B}$ is checked as follows:

$$c^2 \;=\; b^2 + L^2 - 2y_1L \;=\; b^2 + L^2 - 2\tilde{y}_1\frac{L^3}{\tilde{b}^2} < b^2 \; , \tag{E.9}$$

since

$$\tilde{c}^2 = \tilde{b}^2 - 2\tilde{y}_1L + L^2 < L^2 \Leftrightarrow L^2 - 2\tilde{y}_1\frac{L^3}{\tilde{b}^2} < 0$$

and

$$b^2 = L^2\frac{L^2}{\tilde{b}^2} > L^2 \; . \tag{E.10}$$

Since $b > L$ and $b > c$, $Y \in \mathcal{B}$. Finally, let us look at how the whole integral transforms. First inserting the transformed variables including the Jacobian (E.6) and second using the homogeneity (E.3), we arrive at

$$\int\limits_{Y\in\mathcal{B}} f(a=L,b,c) = \int\limits_{\tilde{Y}\in\mathcal{A}} \left(\frac{L}{\tilde{b}}\right)^{2D} f\left(L, \frac{L^2}{\tilde{b}}, \frac{\tilde{c}L}{\tilde{b}}\right) = \int\limits_{\tilde{Y}\in\mathcal{A}} \left(\frac{L}{\tilde{b}}\right)^{2D-\lambda} f(\tilde{b}, \tilde{a}=L, \tilde{c}) \; . \tag{E.11}$$

Let us restate the above calculation in a completely geometric interpretation as sketched in the figure. The mapping consists of two steps:

- The rescaling with respect to $O$ by a factor $L/b$ which maps $Y$ onto $Y'$ and $H$ onto $H'$. (E.3) implies that $f$ is changed by a factor $\left(\frac{L}{b}\right)^{-\lambda}$.
- A mirror operation, which maps $Y'$ onto $H$ and $H'$ onto $\tilde{Y}$, leaving invariant the origin $O$. This operation is a permutation of the first two arguments of $f$.

The mapping $Y \to \tilde{Y}$ corresponds to the special conformal transformation (E.4).
Analogously, we find that

$$\int\limits_{Y\in\mathcal{C}} f(a=L,b,c) \;=\; \int\limits_{\tilde{Y}\in\mathcal{A}} \left(\frac{L}{\tilde{c}}\right)^{2D-\lambda} f(\tilde{c}, \tilde{b}, \tilde{a}=L) \; . \tag{E.12}$$

## Acknowledgements

Allen, die zum Gelingen dieser Arbeit beigetragen haben, möchte ich herzlich danken: Hans Werner Diehl, der mir die Mitarbeit in seiner Arbeitsgruppe ermöglicht hat und mit zahlreichen Anregungen und Kritik beigetragen hat. Kay J. Wiese, der auch nach seinem Fortgang an die Strände Kaliforniens (ITP, Santa Barbara) die Arbeit stets engagiert betreut hat und bei dem meine zahlreichen Fragen fast immer Gehör fanden. Mein zweiwöchiger Aufenthalt in Santa Barbara bleibt in guter Erinnerung. Insbesondere auch eine lange Diskussion mit Andreas Ludwig, der sich eingehend für den Limes $D \to 2$ und die Entwicklung in $2 - D$ interessiert hat.
Für anregende Diskussionen oder Tips danke ich weiterhin besonders Lothar Schäfer und Ralf Blossey.
Darüber hinaus danke ich allen weiteren Mitarbeitern der Arbeitsgruppe und des Fachbereichs Physik, die den Aufenthalt in Essen interessant oder angenehm gemacht haben, sei es wissenschaftlich gesehen oder sei es aufgrund anderer Ablenkungen. Insbesondere Andrea Ostendorff, Anja Gerwinski, Alexandra Apel, Boris Shalaev, Frau Thälker, Florian Jasch, Hannes Hager, Hans Werner Diehl, Harald Karl, Ira Terwyen, Jens Eggers, Jouni Kallounki, Kay Wiese, Knut Elsner, Lothar Schäfer, Martin Smock, Mykola Sphot, Philipp Kuhn, Ralf Blossey, Reinhard Leidl, Rona Rangsch, Rüdiger Oberhage, Sutapa Mukherij und Ulla Lensen.
Diese Arbeit ist von der DFG im Rahmen des Leibniz Programms Di 378/2-1 unterstützt worden.

# R References

[1] L. Schäfer, *Excluded Volume Effects in Polymer Solutions*, Springer Verlag, Berlin, Heidelberg, 1999.

[2] G. Blatter, M.V. Feigel'man, V.B. Geshkenbein, A.I. Larkin and V.M. Vinokur, *Vortices in high-temperature superconductors*, Rev. Mod. Phys. **66** (1994) 1125.

[3] M. Kardar, G. Parisi and Y.-C. Zhang, *Dynamic scaling of growing interfaces*, Phys. Rev. Lett. **56** (1986) 889–892.

[4] K.J. Wiese, *Polymerized membranes, a review*. volume *19* of *Phase Transitions and Critical Phenomena*, Acadamic Press, London, 1999.

[5] J. des Cloizeaux and G. Jannink, *Polymers in Solution, Their Modelling and Structure*, Clarendon Press, Oxford, 1990.

[6] P.-G. de Gennes, *Scaling concepts in polymer physics*, Cornell University Press, Ithaca and London, 1979.

[7] E. Eisenriegler, *Polymers near surfaces*, World Scientific, 1993.

[8] M. Fixman, *Excluded volume in polymer chains*, J. Chem. Phys. **23** (1955) 1656–1659.

[9] L. Schafer and T.A. Witten, *Renormalized field theory of polymer solutions*.

[10] J. des Cloizeaux, *Polymers in solutions: Principles and applications of a direct renormalization method*, J. de Physique **42** (1981) 635–652.

[11] S.F. Edwards, *The statistical mechanics of polymers with excluded volume*, Proc. Phys. Soc. **85** (1965) 613.

[12] P.-G. De Gennes, *Exponents for the excluded volume problem as derived by the Wilson method*, Phys. Lett. **A 38** (1972) 339–340.

[13] Y. Kantor and D.R. Nelson, *Crumpling transition in polymerized membranes*, Phys. Rev. Lett. **58** (1987) 2774–2777.

[14] Y. Kantor and D.R. Nelson, *Phase transitions in flexible polymeric surfaces*, Phys. Rev. **A 36** (1987) 4020–4032.

[15] Y. Kantor, M. Kardar and D.R. Nelson, *Statistical mechanics of tethered surfaces*, Phys. Rev. Lett. **57** (1986) 791–795.

[16] Y. Kantor, M. Kardar and D.R. Nelson, *Tethered surfaces: Statics and dynamics*, Phys. Rev. **A 35** (1987) 3056–3071.

[17] M. Paczuski, M. Kardar and D.R. Nelson, *Landau theory of the crumpling transition*, Phys. Rev. Lett. **60** (1988) 2638.

[18] M. Paczuski and M. Kardar, *Renormalization-group analysis of the crumpling transition in large $d$,* Phys. Rev. **A 39** (1989) 6086–6089.

[19] F. David and K.J. Wiese, *Scaling of self-avoiding tethered membranes: 2-loop renormalization group results*, Phys. Rev. Lett. **76** (1996) 4564.

[20] K.J. Wiese and F. David, *New renormalization group results for scaling of self-avoiding tethered membranes*, Nucl. Phys. **B 487** (1997) 529–632.

[21] M. Kardar and D.R. Nelson, *$\varepsilon$ expansions for crumpled manifolds*, Phys. Rev. Lett. **58** (1987) 1289 and 2280 E.

[22] J.A. Aronovitz and T.C. Lubensky, *Fluctuations of solid membranes*, Phys. Rev. Lett. **60** (1988) 2634–2637.

[23] F. David, B. Duplantier and E. Guitter, *Renormalization and hyperscaling for self-avoiding manifold models*, Phys. Rev. Lett. **72** (1994) 311.

[24] F. David, B. Duplantier and E. Guitter, *Renormalization theory for the self-avoiding polymerized membranes*, cond-mat/**9702136** (1997).

[25] T. Hwa, *Generalized $\varepsilon$ expansion for self-avoiding tethered manifolds*, Phys. Rev. **A 41** (1990) 1751–1756.

[26] K.J. Wiese and F. David, *Self-avoiding tethered membranes at the tricritical point*, Nucl. Phys. **B 450** (1995) 495–557.

[27] R.R. Chianelli, E.B. Prestridge, T.A. Pecorado and J.P. de Neufville, *Molybdenum disulfide in the poorly crystalline "rag" structure*, Science **203** (1979) 1105.

[28] T. Hwa, E. Kokufuta and T. Tanaka, *Conformation of graphite oxide membranes in solution*, Phys. Rev. **A 44** (1991) 2235.

[29] X. Wen, C.W. Garland, T. Hwa, M. Kardar, E. Kokufuta, Y. Li, M. Orkisz and T. Tanaka, *Crumpled and collapsed conformations in graphite oxide membranes*, Nature **355** (1992) 426.

[30] M.S. Spector, E. Naranjo, S. Chiruvolu and J.A. Zasadzinski, *Conformations of a tethered membrane: Crumpling in graphitic oxide?*, Phys. Rev. Lett. **73** (1994) 2867–2870.

[31] A. Baumgärtner, *Does a polymerized membrane crumple?*, J. Phys. I France **1** (1991) 1549–1556.

[32] A. Baumgärtner and W. Renz, *Crumpled self-avoiding tethered surfaces*, Europhys. Lett. **17** (1992) 381–386.

[33] D.M. Kroll and G. Gompper, *Floppy tethered networks*, J. Phys. I France **3** (1993) 1131.

[34] G. Thorleifsson M. Bowick, A. Cacciuto and A. Travesset, *Universality classes of self-avoiding fixed-connectivity membranes*, Eur. Phys. J. **E 5** (2001) 149.

[35] D.B. Abraham, *Solvable model with a roughening transition for a planar ising ferromagnet,* Phys. Rev. Lett. **44** (1980) 1165–1168.

[36] M.E. Fisher, *Walks, walls, wetting and melting,* J. Stat. Phys. **34** (1984) 665–729.

[37] P.J. Upton, *Exact interface model for wetting in the planar ising model,* Phys. Rev. E **60** (1999) 3475–3478.

[38] H. Nakanishi and M.E. Fisher, *Multicriticality of wetting, prewetting, and surface transition,* Phys. Rev. Lett. **49** (1982) 1565–1568.

[39] E. Brézin, B.I. Halperin and S. Leibler, *Critical wetting in three dimensions,* Phys. Rev. Lett. **50** (1983) 1387.

[40] R. Lipowsky, D.M. Kroll and R.K.P. Zia, *Effective field theory for interface delocalization transitions,* Phys. Rev. B **27** (1983) 4499–4502.

[41] D.M. Kroll, R. Lipowsky and R.K.P. Zia, *Universality classes for critical wetting,* Phys. Rev. B **32** (1985) 1862.

[42] D.S. Fisher and D.A. Huse, *Wetting transitions: a functional renormalization-group approach,* Phys. Rev. B **32** (1985) 247–56.

[43] R. Lipowsky and M.E. Fisher, *Scaling regimes and functional renormalization for wetting transitions,* Phys. Rev. B **36** (1987) 2126–2241.

[44] F. David and S. Leibler, *Multicritical unbinding phenomena and nonlinear functional renormalization group,* Phys. Rev. B **41** (1990) 12926–9.

[45] G. Forgas, R. Lipowsky and T.M. Nieuwenhuizen, *The behaviour of interfaces in ordered and disordered systems*. volume *14* of *Phase Transitions and Critical Phenomena*, pages 136–376, Academic Press London, 1991.

[46] B. Duplantier, *Interaction of crumpled manifolds with euclidean elements,* Phys. Rev. Lett. **62** (1989) 2337.

[47] F. David, B. Duplantier and E. Guitter, *Renormalization of crumpled manifolds,* Phys. Rev. Lett. **70** (1993) 2205.

[48] F. David, B. Duplantier and E. Guitter, *Renormalization theory for interacting crumpled manifolds,* Nucl. Phys. **B 394** (1993) 555–664.

[49] H.A. Pinnow and K.J. Wiese, *Interacting crumpled manifolds,* J. Phys. A: Math. Gen. **35** (2002) 1195–1229.

[50] D.R. Nelson, T. Piran and S. Weinberg Eds., *Statistical Mechanics of Membranes and Surfaces,* Proceedings of the Fifth Jerusalem Winter School for Theoretical Physics, World Scientific, Singapore, 1989.

[51] W. Helfrich, *Elastic properties of lipid bilayers: theory and possible experiments,* Z. Naturforschung **C 28** (1973) 693–703.

[52] W. Helfrich, *Effect of thermal undulations on the rigidity of fluid membranes and interfacs*, J. Phys. (Paris) **46** (1985) 1263.

[53] L. Peliti and S. Leibler, *Effects of thermal fluctuations on systems with small surface tension*, Phys. Rev. Lett. **54** (1985) 1690–1693.

[54] H.A. Pinnow and W. Helfrich, *Effect of thermal undulations on the bending elasticity and spontaneous curvature of fluid membranes*, Eur. Phys. J. E **3** (2000) 149–157.

[55] G. Gompper and D.M. Kroll, J. Phys. I France **6** (1996) 1305.

[56] L.H. Liu, S.-C. Derick and J. Palek, *Visualization of the hexagonal lattice in the erythrocyte membrane skeleton*, J. Cell Biol. **104** (1987) 527–536.

[57] H. Falk and V. Speth, in [74].

[58] L.D. Landau and I.M. Lifshitz, *Elastizitätstheorie*, volume *7* of *Lehrbuch der theoretischen Physik*, Akademie-Verlag Berlin, 1983.

[59] M.J. Bowick, S.M. Catterall, M. Falcioni, G. Thorleifsson and K. Anagnostopoulos, *The flat phase of fixed-connectivity membranes*, Nucl. Phys. B Proc. Suppl. **53** (1997) 746–752.

[60] D.R. Nelson and L. Peliti, *Fluctuations in membranes with crystalline and hexatic order*, J. Physique **48** (1987) 1085–1092.

[61] M. Doi, *Introduction to polymer physics*, Clarendon Press, Oxford, 1996.

[62] M. Lassig and R. Lipowsky, *Critical roughening of interfaces: a new class of renormalizable field theories*, Phys. Rev. Lett. **70** (1993) 1131–4.

[63] M. Goulian, *The gaussian approximation for self-avoiding tethered surfaces*, J. Phys. II France **1** (1991) 1327–1330.

[64] P. Le Doussal, *Tethered membranes with long-range self-avoidance: large dimension limit*, J. Phys. **A 25** (1992) 469–476.

[65] E. Guitter and J. Palmeri, *Tethered membranes with long-range interaction*, Phys. Rev. **A 45** (1992) 734–744.

[66] H. Pinnow and K.J. Wiese, work in progress.

[67] F. David and K.J. Wiese, *Large orders for self-avoiding membranes*, Nucl. Phys. **B 535** (1998) 555–595.

[68] H.W. Diehl, *Field-theoretical approach to critical behaviour of surfaces*. volume *10* of *Phase Transitions and Critical Phenomena*, pages 76–267, Academic Press London, 1986.

[69] E. Eisenriegler, K. Kremer and K. Binder, *Adsorption of polymer chains at surfaces: scaling and monte-carlo analysis*, J. of Chem. Phys. **77** (1982) 6296.

[70] R. Bundschuh and M. Lässig, *Delocalization transitions of semi-flexible manifolds*, cond-mat/9902233 (1999) 1–4.

[71] D.A. Huse A.C. Maggs and S. Leibler, Europhys. Lett. **8** (1989) 615.

[72] G. Gompper and T.W. Burkhardt, *Unbinding transition of semiflexible membranes in* $(1+1)$ *dimensions*, Phys. Rev. A **40** (1989) 6124–6127.

[73] T.W. Burkhardt, *Semiflexible polymer in the half plane and statistics of the integral of a brownian curve*, J. Phys. A: Math. Gen. **26** (1993) L1157–L1162.

[74] H. Kleinig and P. Sitte, *Zellbiologie*, Gustav Fischer, 4th edition, 1999.